Bureau of Safety and Environmental Enforcement
Oil Spill Preparedness Division

Improved Oil Recovery Efficiency Sensor – Phase 2

Final Report

December 2023

Slawomir Winecki, Ph.D.

US Department of the Interior
Bureau of Safety and Environmental Enforcement
Oil Spill Preparedness Division

Improved Oil Recovery Efficiency Sensor – Phase 2

Final Report

OSRR # 1119

December 2023

Author:
Slawomir Winecki, Ph.D.

Prepared under Contract Number
140E0119C0012
By
Battelle Memorial Institute

US Department of the Interior
Bureau of Safety and Environmental Enforcement
Oil Spill Preparedness Division

DISCLAIMER

Contracts:
Study concept, oversight, and funding were provided by the US Department of the Interior (DOI), Bureau of Safety and Environmental Enforcement (BSEE), Oil Spill Preparedness Division (OSPD), Sterling, Virginia, under Contract Number 140E0119C0012. This report has been technically reviewed by BSEE, and it has been approved for publication. The views and conclusions contained in this document are those of the authors and should not be interpreted as representing the opinions or policies of the US Government, nor does mention of trade names or commercial products constitute endorsement or recommendation for use.

REPORT AVAILABILITY

The PDF file for this report is available through the following sources. Click on the URL and enter the appropriate search term to locate the PDF:

Document Source	Search Term	URL
Bureau of Safety and Environmental Enforcement (BSEE)	Project Number – 1128	Development of a Recovery Efficiency Sensor - Phase II | Bureau of Safety and Environmental Enforcement (bsee.gov)
U.S. Department of the Interior Library	Emerging Pollution Response Technology Evaluation: Adsorbents	https://library.doi.gov
National Technical Reports Library	Emerging Pollution Response Technology Evaluation: Adsorbents	https://ntrl.ntis.gov/NTRL/

Sources: a) BSEE (2019), b) DOI [2021], c) National Technical Information Service (2021)

CITATION

Winecki, Slawomir. 2023. Improved Oil Recovery Efficiency Sensor – Phase 2. U.S. Department of the Interior, Bureau of Safety and Environmental Enforcement. Report No.: 1119. Contract No: E0119C0012.

Bureau of Safety and Environmental Enforcement Oil Spill Preparedness Division

Improved Oil Recovery Efficiency Sensor – Phase 2 Final Report

Prepared by:
Battelle Memorial Institute
505 King Avenue
Columbus, Ohio 43201-2696

Technical POC:
Slawomir Winecki, Ph.D.
E-mail: wineckis@battelle.org
Phone: (614) 424-4154

Submitted to:
U.S. Department of the Interior
Bureau of Safety and Environmental Enforcement
Acquisition Operations Branch
45600 Woodland Road, Mailstop VAE-AMD
Sterling, VA 20166
Attn: Caroline Laikin-Credno, CPCM
Phone: 703-787-1828
Email: caroline.laikin-credno@bsee.gov
December 31, 2023

BAA Solicitation 140E0119R0007

.

Table of Contents

List of Tables

List of Figures

Page

1. Executive Summary

Since 2018, Battelle Memorial Institute (Battelle) has developed technologies to measure the percentage of oil and water in oil-water mixtures. This technology was implemented in the form of a flowthrough sensor, called a Recovery Efficiency (RE) sensor. The first version of the RE sensor was developed under Bureau of Safety and Environmental Enforcement (BSEE) contract E17PC00011 and tested at the Ohmsett Facility in June 2018. This version of the sensor had a few significant limitations: (1) the sensor required an air-free stream, (2) there was no wireless communication with the user, and (3) the sensor case was not shock proof since it was made as a three-dimensional (3-D) printed plastic enclosure. The second version of the RE sensor, which was developed under BSEE contract 140E0119C0012, eliminated these limitations. First, the second version uses an improved measurement principle that can account for oil-water streams that contain air and/or are separated by gravity. Second, it includes both wired and wireless communication capability between the sensor unit and a tablet PC providing a user interface. Third, the current version of the sensor has an aluminum enclosure, which is designed for demanding marine environments. Figure 1 shows the RE sensor being tested at Ohmsett in June of 2022.

Figure 1: Battelle's RE sensor during tests at Ohmsett, June 2022.

The RE sensor is constructed as an open section of a 3-inch diameter pipe, 30.5 inches long, weighing 35 lbs. The sensor uses two aluminum quick hose connectors, one male and one female. A set of adaptors allowing for connections with 2-, 3-, or 4-inch size hoses is provided. The sensor uses two Texas Instruments FD2214 integrated circuits (ICs) each providing four channels of high sensitivity admittance measurement at a rate of approximately 10 measurements per second. These measurements were used in an algorithm to calculate a real time oil fraction in the oil-seawater passing through the sensor. A MSP432 microcontroller is used for sensor control and algorithm implementation. This selection of components and the overall design of the sensor allow for operations at a broad temperature range of -25°F to

120°F. The sensor can operate using an external power supply or a rechargeable lithium-ion battery providing over 48 hours of operations at the low temperature range (-25-20°F) and over 150 hours at room temperature (60-80°F).

The user interface is implemented as a software app running on a ruggedized tablet PC ALGIZ 8X. Figure 2 shows this tablet with one of the software tabs open. The tablet can be connected with the sensor via a cable connection or radio link operating in the 915 MHz band. This band was selected due to its compatibility with a marine environment and its broad unrestricted usability through multiple continents.

Figure 2: The ruggedized tablet ALGIZ 8X with the sensor software running.

The BSEE requirement for RE sensor accuracy was set at +/- 6% oil fraction defined as average error observed during Ohmsett testing under realistic oil recovery conditions. This accuracy target included all oil fraction ranges, all oil types, and water salinities in the 1-5 wt% range. This accuracy target was the main challenge of the project since it pushes the limits of existing technologies. During the June 2022 Ohmsett testing, the RE sensor did not meet this accuracy target although it came relatively close. In the July 2023 Ohmsett campaign, the RE sensor did not work properly due to a software error. The sensor output was erratic and poorly correlated with the oil fraction of tested oil-water streams. However, the raw data were recorded successfully and were used for subsequent data analysis. Table 1 presents the accuracy levels observed during different stages of the Phase 2 project.

Table 1: Accuracy of RE sensor achieved during different stages of the project.

Project Stage	Observed Accuracy and Sensor Performance (algorithm version used)
July 2022 Ohmsett testing	• Hydrocal 300 oil, average error **9.39%,** maximum error 21.8% • Diesel, average error **7.72%**, maximum error 18.3% (1st version of the algorithm)
MATLAB algorithm simulation carried out post Ohmsett 2022 testing and using raw data collected during Ohmsett 2022 testing	• Hydrocal 300 oil, average error **4.07%**, maximum error 10.9% • Diesel, average error **4.20%,** maximum error 10.4% (2nd version of the algorithm)
July 2023 Ohmsett testing	• Sensor output was erratic due to software error. Only raw data were collected
MATLAB algorithm simulation carried out post Ohmsett 2023 testing and using raw data collected during Ohmsett 2022 and 2023 testing	• Hydrocal 300 oil (2023 data), average error **6.37%**, maximum error 17.1% • Calsol oil (2023 data), average error **8.84%**, maximum error 24.7% • Hydrocal 300 oil (2022 data), average error **3.57%,** maximum error 10.1% • Diesel (2022 data), average error **4.86%**, maximum error 12.7% • Overall average error for all tests **6.38%** (3rd version of the algorithm)

The RE sensor already can be used to help responders more efficiently recover oil during a response operation. Currently, responders do not have a method for knowing in real time how much water they are collecting with their oil. Collecting a large amount of water means that temporary storage will be more quickly consumed and require the responder to halt recovery to offload recovered fluids. This sensor will provide information to allow responders to make informed decisions during recovery. For example, if a responder has collected oil within a boom but is recovering mostly water while skimming, the responder may decide to stop the skimmer, continue to collect in the boom, and begin recovery again when more oil is contained within the boomed area.

More generally, the sensor can be applied to any application where oil-water mixtures need to be evaluated for oil content or, equivalently, for water cut, and where high-water salinity prevents use of traditional sensors. Possible applications include oil and gas industrial settings where highly saline brines are used, and oil content needs to be measured. Battelle holds three issued U.S. patents related to this technology [1-3].

2. Phase 2 Activities

The Phase 2 effort was divided into seven tasks. The sections below describe each task in detail.

Task 1. Selection of Electronic Components and Limited Sensor Modeling

The goal of this task was selection of electrode geometry and electronic components needed for the sensor's operation.

Selection of electrode geometry and the principles of oil fraction measurement were the key parts of this task and of the overall Phase 2 effort. The sensor developed in Phase 1 used a combination of two types of measurements: (1) a dielectric measurement for oil-rich mixtures, and (2) an eddy current measurement for water-rich mixtures. During the first few months of Phase 2 (Fall 2019 - Spring 2020) it became clear that the eddy current measurement could not be used due to unavailability of a commercial components realizing this type of measurement. Particularly, implementation of the eddy current measurement which is reliable at a broad temperature range and allows for multiple measurements per second could not be realized using existing integrated circuits. Construction of an eddy current measurement circuit using discrete components would be prohibitively costly, thereby not possible within the available Phase 2 budget. Instead, Battelle decided to base the sensor design on two Texas Instruments FD2214 ICs each providing four channels of high sensitivity admittance measurements with a resolution of approximately 0.001 pF and at a rate of approximately 10 measurements per second.

Although the FD2214 IC is usually used to performs a dielectric measurement, tests carried out at Battelle demonstrated that this circuit can also be used to measure electrical conductivity of oil-water mixtures with a properly selected electrode geometry which minimizes the capacitive coupling but emphasizes the conductivity component of admittance [4]. Specifically, a set of two metal collar electrodes placed around a sensor cavity pipe at a significant distance exceeding a few pipe diameters, if used with the FD2214 IC, provides reliable conductivity measurements. The two yellow electrodes shown schematically in Figure 3 were adopted for this purpose. The ability to measure electric conductivity using this type of electrode geometry was a new finding based on modeling and tests carried out in this project. In addition, two channels of the FD2214 IC were used for a traditional dielectric type of measurement. The first dielectric measurement was carried out using electrodes placed at the top and bottom of the sensor cavity pipe. This set of electrodes and the signal generated were labeled top/bottom (T/B). The second dielectric measurement was carried out using electrodes mounted on opposite sides of the sensor cavity; this set of electrodes was labeled right/left (R/L). In addition, five FD2214 IC channels were used for five pairs of level electrodes. The bottom pair was labeled L1, the top pair named L5, and electrode pairs L2-L4 were placed in between as shown in Figure 3.

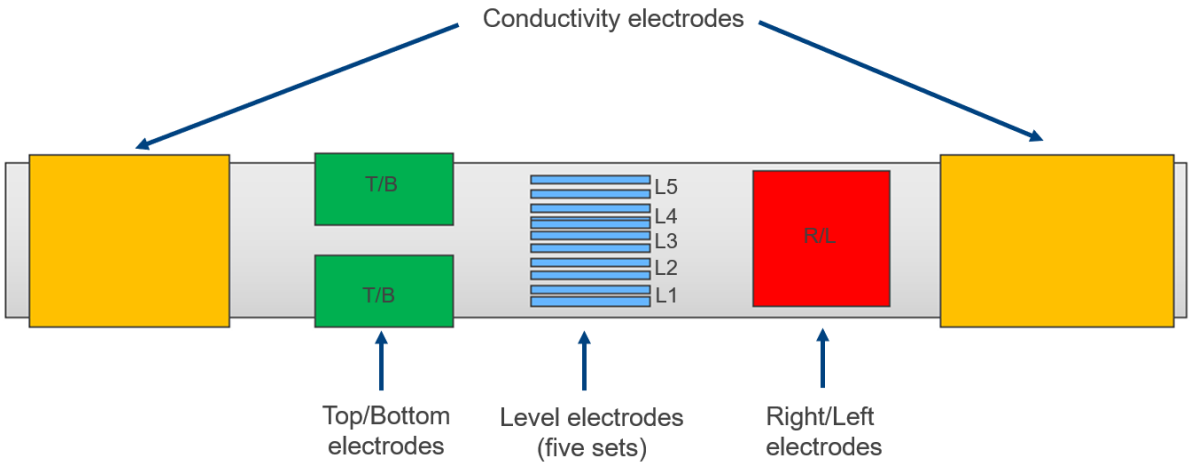

Figure 3: Schematic of electrode arrangement adopted for the RE sensor.

The second key decision defining the sensor hardware was the selection of a suitable microcontroller. Battelle decided to use the MSP432 microcontroller for all algorithm calculations and for the overall control of the sensor system. The key factor in this selection was the

expectation that the MSP432 platform will continue to be available for at least the next 5 to 10 years, and its support available even longer. Computational power was not a factor since the RE sensor algorithm is relatively simple and uses only about 1% of the available processing capability of the MSP432.

The user interface was implemented as a software app running on a ruggedized tablet PC ALGIZ 8X. Figure 2 shows this tablet with one of the software tabs open. The ALGIZ 8X tablet allows for easy connections with peripherals via an external “backpack” mounted on its back. This capability was used to mount a radio transmitter communicating with the RE sensor. The 915 MHz band was selected for wireless communications due to its compatibility with a marine environment and its broad unrestricted usability through multiple continents.

Battery-based operation for a period of 48 hours, especially at low temperatures, requires proper selection of battery type and size. Battelle evaluated capabilities of two rechargeable battery types, nickel-metal-hydrate and lithium ion, in the entire temperature range, -25°F to 120°F, and compared them with expected power requirements of electronic components. The rechargeable lithium ion battery pack ALG8X-08B with a 76.6 Watt hour capacity was selected as the optimal solution since it allowed for about 150 hr of battery operation at normal temperatures and about 48 hr of operations at -20 to -25°F. Note that all lithium ion batteries stop working below these temperatures. It is recommended that for such low temperature operations, use of an external power supply provided with the sensor is considered. Figure 4 shows the ALG8X-08B battery installed in the sensor’s sealed battery compartment.

Figure 4: The sensor’s Li-ion battery pack ALG8X-08B installed in the sensor.

Task 2. Construction of Experimental Setup

The goal of this task was construction of an experimental setup capable of generating mixed oil-water-air streams and to test the sensor’s performance at different oil types, oil-water ratios, flows, and flow regimes. These tests allowed the development of a sensor algorithm.

The setup, shown in Figures 5 and 6, consisted of a 50-gallon plastic drum, two variable speed pumps, an air injection port, as well as all required connections and valves. The drum was filled with approximately a 50/50% mixture of oil and water. Due to the relatively slow pumping speed of the pumps (up to 10-12 gallons per minute [gpm] for total flow), both liquids separated in the

drum allowing for their independent feeding into the pumps. This allowed for easy control of oil/water ratio by speed adjustments of the two variable speed pumps. Both liquids were combined prior to entering the sensor cavity. Selected tests were carried out using controlled air injection into the liquid streams. The setup was capable of working with the four types of oils used in the first phase of the project: Hydrocal 300, Calsol 8240, Hoops, and Pacific Energy A-38; however, most of the tests were carried out with Hydrocal 300. Table 2 presents viscosities of these oils.

Table 2: Oils used in testing.

Oil	Type	Viscosity at 20°C (poise)
Hydrocal 300	refined	1.54
Calsol 8240	refined	16.8
Hoops	crude	0.1
Pacific Energy A-38	crude	28.6

Use of Calsol 8240 and Pacific Energy A-38 oils was challenging due to the high viscosity of these oils. The major challenge affecting Battelle tests was formation of relatively stable emulsions under some flow conditions and oil types. On numerous occasions, the tests had to be separated by a few days to ensure emulsion separation.

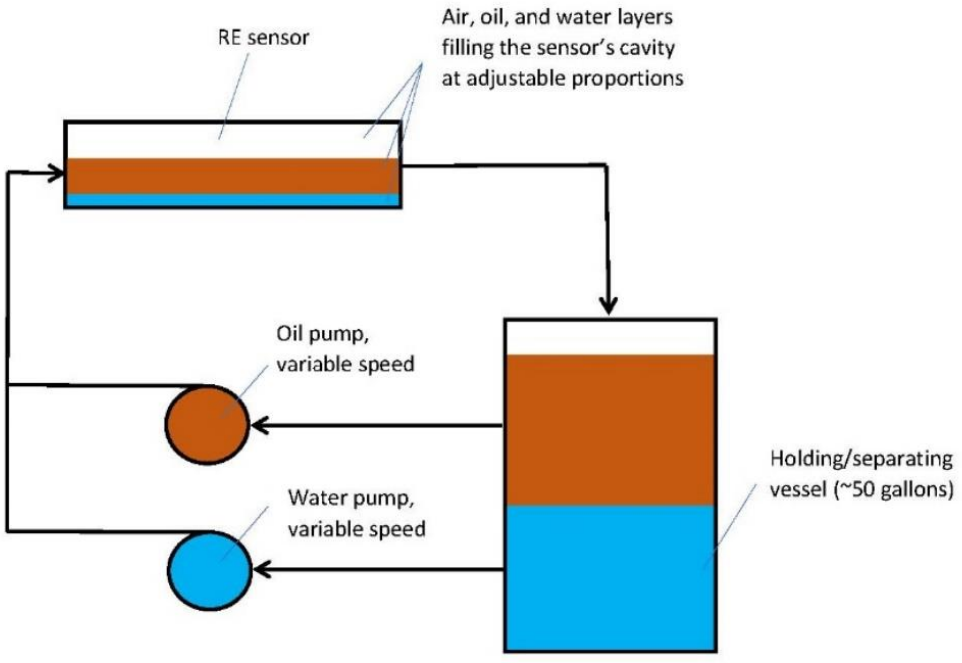

Figure 5: Schematic of the experimental setup for dynamic flow testing.

Figure 6: Battelle's experimental setup.

The part of the algorithm handling the partially empty sensor cavity required testing with precisely controlled water, oil, and air fractions. This could not be realized in the setup shown in Figures 5 and 6. Instead, a simple setup was used where a sensor cavity was filled manually with the desired volume of water and oil. A small pump (~2 gpm) was used to facilitate liquid handling. Figure 7 shows one of the versions of this apparatus used during the project.

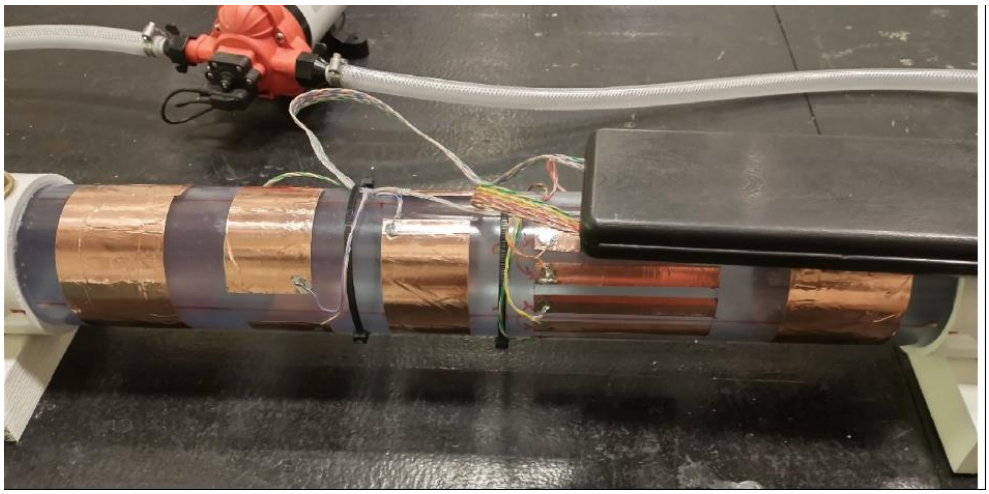

Figure 7: Experimental setup for static testing (one of the several versions used).

Task 3. Construction of Sensor Prototypes

The goal of this task was construction of four sensor prototypes.

This task constituted a major part of the project since it included design and construction of the mechanical parts of the sensor as well as electronic components. Figure 8 presents the RE sensor with its major components. The sensor can be connected with hoses used for oil recovery via the standard 3-inch cam-and-groove fittings, one female and one male. The flow direction is not important, as the sensor can be connected both ways. The sensor must operate horizontally with its legs placed on a level solid surface. Other orientations may produce inaccurate sensor readings.

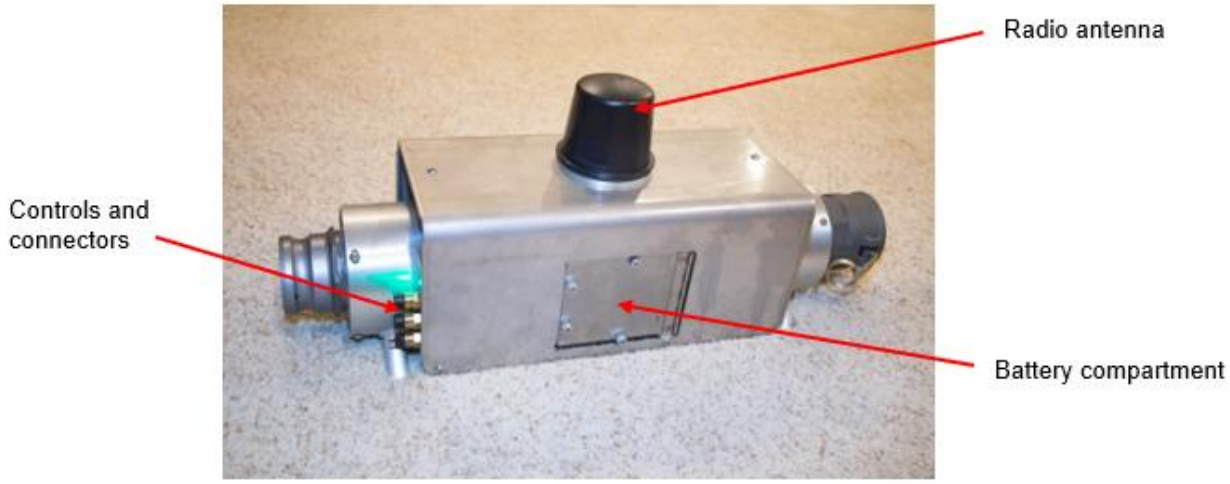

Figure 8: The oil recovery sensor.

The sensor is equipped with the ON/OFF switch, a green light emitting diode (LED) indicating the sensor is ON, and the three electrical connectors. Figure 9 shows the location of these components on the sensor.

Figure 9: The sensor's controls and connectors.

Figure 10 shows the sensor during assembly. Two sealed compartments are visible on the outside of the sensor enclosure; one of these compartments is used to host electronic components, and the other is designed for the battery. The sensor's electrodes were constructed as flexible circuit boards attached to the fiber glass sensor cavity. The electrode assembly was mounted in a larger (5 inch diameter) aluminum pipe providing mechanical strength and water-tight seal. The sensor enclosure was constructed using anodized aluminum and stainless steel, as both materials provide appropriate protection against marine environment conditions.

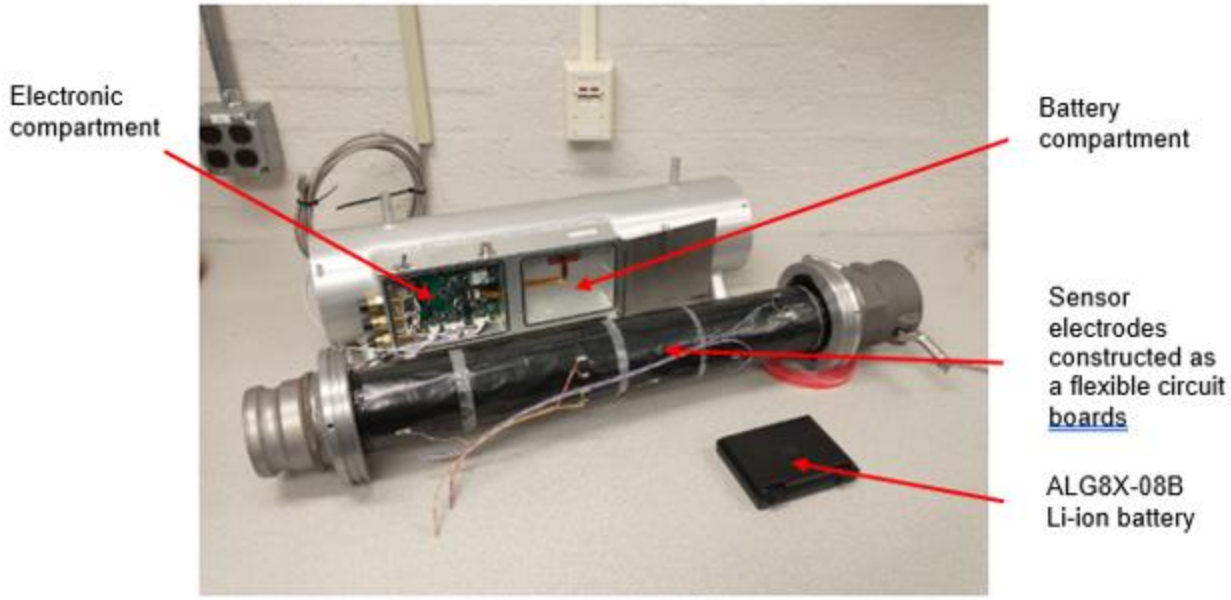

Figure 10: Sensor during assembly at Battelle.

Figure 11 shows the tablet's "backpack" hosting a 915 MHz, two-way transceiver and antenna. The radio communication mode starts once the sensor and the tablet are turned on, are within range of each other, and the communication cable is not connected to the sensor.

Figure 11: The radio transmitter and the antenna attached to the back of tablet PC.

The four sensor prototypes were constructed as four identical systems packaged in ruggedized portable Pelican cases containing all parts required for sensor operations. The cases prevent

ingress of water when exposed to dripping, splashing, and spraying of fresh or saline water. Each prototype contains the following components:

- The sensor unit.
- The sensor tablet computer, with its own power supply.
- Handheld salinity meter.
- Two sets of rechargeable batteries: one for sensor operations and another to be charged.
- Battery charger operating on standard alternating current (AC) power outlet.
- Adaptor fittings required for quick connection with 2- or 4-inch external hoses.
- Three custom cables providing:
    - Data communication between the sensor and the tablet
    - Charging of the sensor's battery
    - Connection with an external flow meter
- Sensor manual, both in printed and electronic forms.

One of the prototype sensor kits was used during Ohmsett testing campaigns in 2022 and 2023.

Task 4. Sensor Algorithm Development, Testing and Calibration at Battelle

The goal of this task was development of the sensor algorithm based on tests carried out with different oil-water mixtures.

This task was another major effort of the project since the algorithm development proved to be more challenging than expected. The original proposal outlined about 240 tests with different oil-water combinations. This plan proved to be inadequate due to several factors:

- The sensor's electronics were affected by shielding effects that overshadowed the measured signals. This forced repeated testing of several sensor prototypes including the final all-metal enclosure.
- The conductivity measurement was particularly challenging. Multiple electrode geometries and electronic configurations had to be tested.
- The COVID-19 pandemic delayed the testing. One of the unexpected challenges caused by this delay was decomposition of several oils used for testing. For this reason, Battelle carried out the majority of testing using the Hydrocal 300 oil.
- Due to repeated testing of the same oils, oil properties changed. Particularly, a dramatic increase in tendency to form stable emulsions was observed, which by the end of the testing campaign caused tests to be frequently interrupted with 1-2 day breaks to allow for emulsion separation.

Overall, Battelle carried out about 300 dynamic flow tests (using the setup shown in Figure 6) and about 500 static tests. These tests were used not only to develop the sensor algorithm but also to optimize the electrode geometry and troubleshoot different electronic issues. A significant effort was made to select components of the resonance circuits used by the FD2214 IC, including optimal selection of resonance frequency range for different measurement

channels. As mentioned above, a major effort was needed to develop effective electromagnetic shielding configuration and the electrode wiring arrangement.

All results presented in this report specify which version of the algorithm was used to generate them. In addition, Table 2 lists electronic files that provide details of each algorithm version. Battelle developed the algorithm using MATLAB simulations that, once finalized, were implemented in the MSP432 microcontroller program. Table 3 lists examples of MATLAB scripts as well as data files used by these scripts.

Table 3: Evolution of the sensor's algorithm.

Algorithm Version	Data Used for Development	Comments	Electronic Files with Data and MATLAB Implementation
1st version used during Ohmsett 2022 tests	Dynamic and static data collected at Battelle prior to July 2022 Ohmsett testing	2022 Ohmset tests demonstrated that the Battelle's testing is not representative for the oil recovery application due to the limited flow capability. The part of this algorithm handling a partially empty sensor was implemented without changes in 2nd and 3rd versions.	MATLAB script: Phase_2_Algorithm_ver7.m Data: Normalized_Response.xlsx
2nd version used during Ohmsett 2023 tests	Data collected during the Ohmsett 2022 testing	Software error issues prevented testing of this algorithm during the Ohmset 2023 campaign	MATLAB script: Phase_2_Algorithm_Calibration_2.m Data: Unit4_Ohmsett_Response.xlsx
3rd version developed after Ohmsett 2023 test	Data collected during both Ohmsett campaigns, 2022 and 2023	This version has not been tested at Ohmsett but is uploaded into the sensor prototype sent to BSEE.	MATLAB script: Phase_2_Algorithm_Calibration_12.m Data: Unit4_Ohmsett_Temp_Response.xlsx

Task 5. Sensor Testing at Ohmsett

The goal of this task was verification of the RE sensor performance, specifically the first version of the algorithm, under conditions that realistically simulate real offshore oil recovery operations.

The Ohmsett tests were carried out during the last week of June 2022. A total of 22 tests were carried out using Hydrocal- and diesel-seawater mixtures at two flow rates, 30 and 60 gpm. All tests were carried out with water at 2.7 wt% salinity which was the salinity of water available at the Ohmsett testing tank. Figure 12 presents a diagram of the setup used; Figure 13 shows the actual testing.

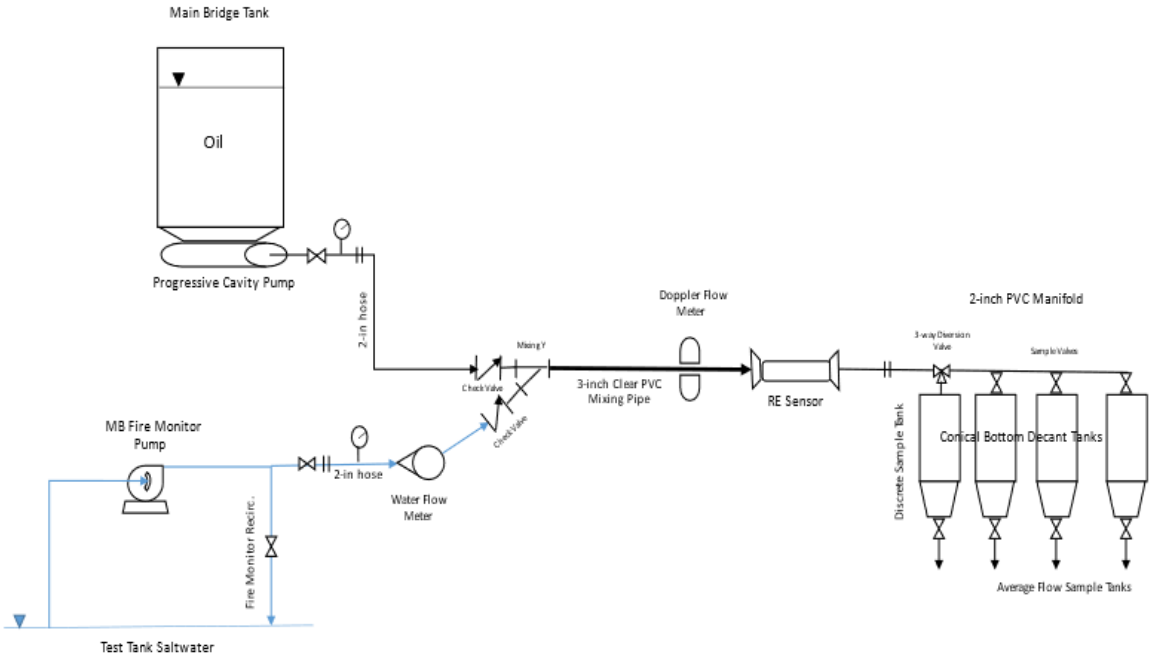

Figure 12: Diagram of the Ohmsett testing setup.

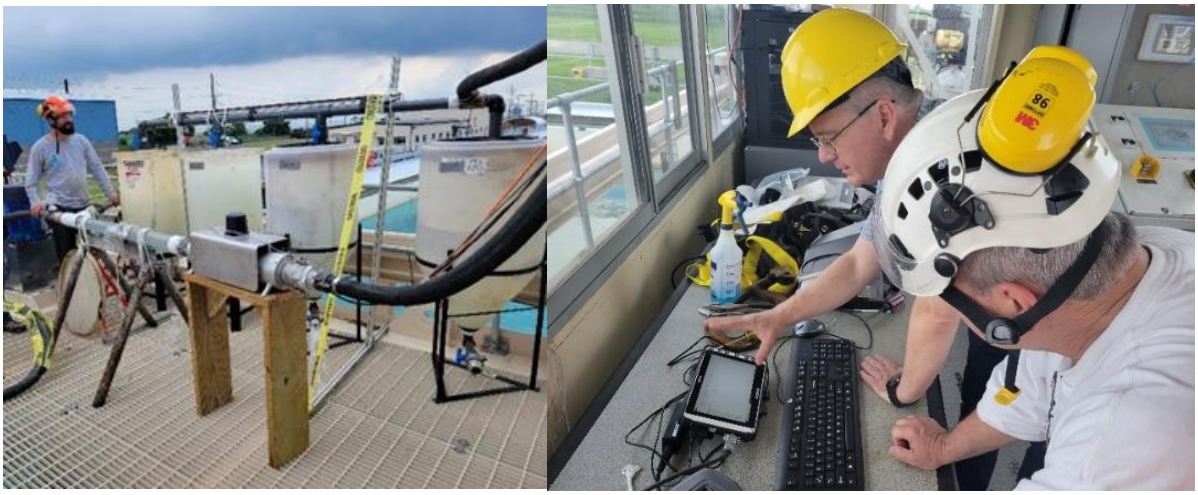

Figure 13. June 2022 Phase 2 RE sensor measuring oil and water percentage in fluid (left) and viewing of real time results on the ruggedized tablet (right)

Figure 14 shows the correlation between the oil fraction measured by the sensor (vertical axis) and the true oil fraction (horizontal axis). The shown oil fraction measured by the sensor is an arithmetic average of about 30 to 40 values recorded during each test. The true oil fraction was determined based on the volumes of collected oil and water, which includes the correction for water droplets suspended in oil.

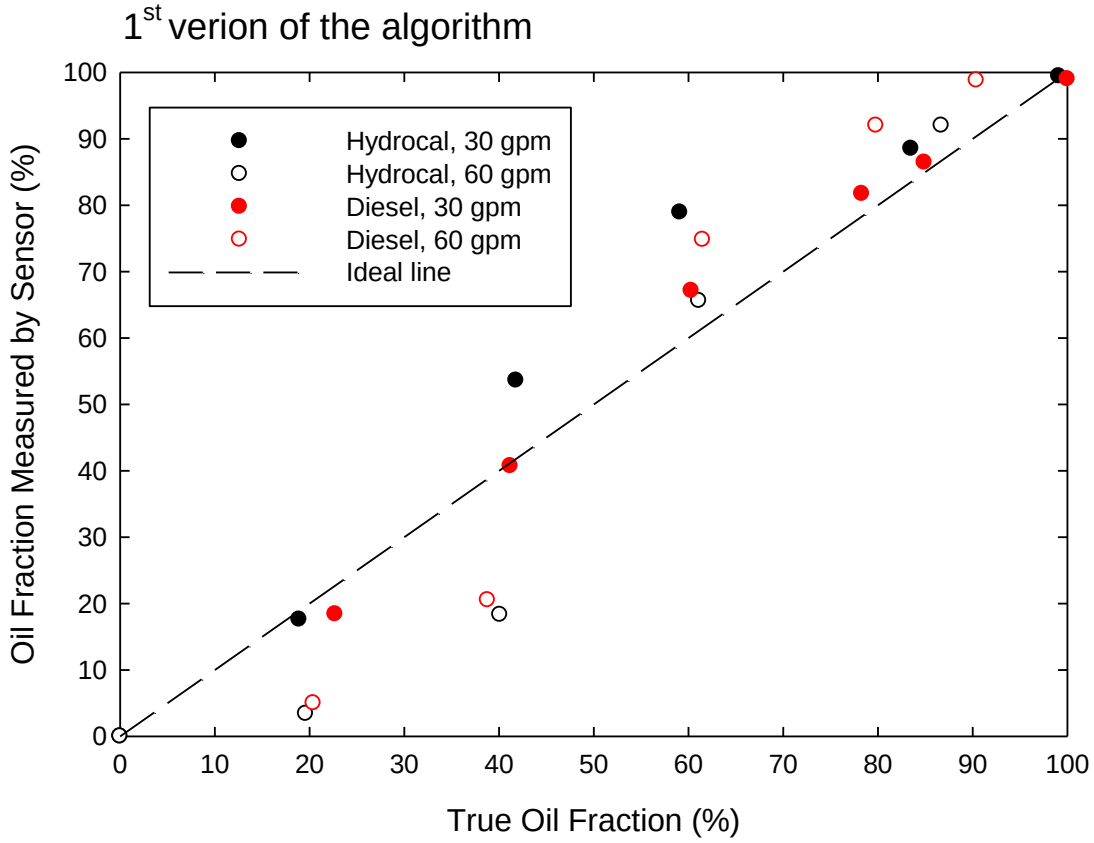

Figure 14: Performance of the Battelle's RE sensor with the algorithm used during Ohmsett tests in June 2022. The sensor operated with the 1st version of the algorithm.

Although the overall correlation between the true oil fraction and the sensor output is apparent, the oil fraction measurement error clearly exceeds the acceptable limits in about half of the tests. Specifically, at the 60-gpm flow rate, oil fraction of water-rich mixtures (oil fraction less than ~ 50%) is significantly underestimated for both oils. The oil fraction for the great majority of oil-rich mixtures (oil fraction more than ~ 50%) is overestimated. The average error for the tests carried out with Hydrocal 300 oil was 9.39%, while the maximum error for this oil was 21.8%. In the case of diesel, the average error was 7.72%, with a maximum error of 18.3%. Appendix B presents the raw data presented in Figure 14.

The source of errors was tracked to the difference in flow patterns of oil-water mixtures, specifically differences caused by much smaller flows used in Battelle's experimental setup. The Battelle setup consisted of a 50-gallon vessel (a drum) and pumps capable of delivering no more than 10 to 12 gpm total flow. Such low flows cause significant separation of oil and water, especially for the water-rich mixtures that readily separate due to gravity. The RE sensor algorithm was developed based on tests carried out under these flow restrictions. In contrast, the tests carried out at Ohmsett used much larger flows, 30 and 60 gpm, that are more representative for the actual oil recovery operations. Visual observation of oil-water mixing patterns, possible on both systems due to use of transparent sections, indicated that the oil-water streams tested at Ohmsett were more dispersed, in particular, at 60 gpm. The experimental setup used at Battelle was simply not capable of generating these levels of dispersion.

Task 6. Final Algorithm Refinement and Prototype Delivery

The goal of this task was to analyze lessons learned during the 2022 Ohmsett testing and to develop of an improved version of the algorithm.

The second version of the algorithm was developed using the raw signal data recorded by the sensor software during the Ohmsett July 2022 testing campaign. The RE sensor records all raw data from eight pairs of electrodes plus temperatures, every second the sensor is turned on. These raw data are recorded as Excel-readable files on the tablet PC. These features allowed for off-line testing of different algorithms using the data collected at Ohmsett.

The main improvement introduced in the second version of the algorithm was the flow pattern and dispersion sensing using the set of five electrode pairs attached to the sides of the sensor cavity. The first algorithm version used during Ohmsett tests contained only two of these pairs. The bottom pair was used to detect a “sensor empty” condition, while the top pair detected the sensor being full of liquid, free of air.

Figure 15 shows the performance of the RE sensor with a modified algorithm, which uses dispersion detection in addition to the regular dielectric and conductivity measurements. Clearly shown is the accuracy of the sensor is improved over the performance observed during the Ohmsett tests, presented in Figure 14. For the Hydrocal 300 oil, average error is reduced to 4.07%, maximum error reduced to 10.9%. For the diesel, average error is reduced to 4.20%, with a maximum error of 10.4%. Appendix C presents the raw data presented in Figure 15.

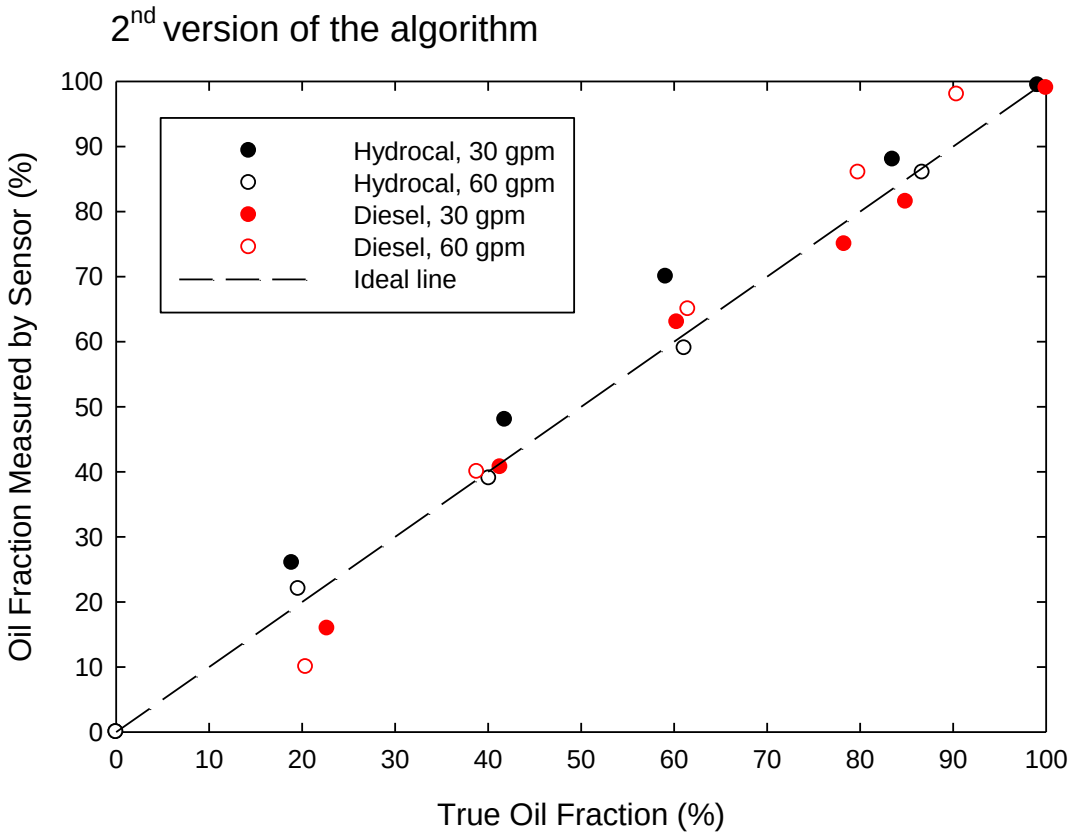

Figure 15: MATLAB- simulated performance of the Battelle’s RE sensor with the 2nd version of algorithm developed following the July 2022 Ohmsett tests.

Task 7. Development of Sensor Production and Commercialization Plan

The goal of this task was development of a sensor manufacturing plan including identification of a potential manufacturing partner. In agreement with BSEE, this task was abandoned.

3. Phase 2 Extension Activities

The main objective of this additional effort was to verify the second version of the algorithm. This verification required an additional round of Ohmsett testing, carried out in June 2023, and confirmation of the new temperature correction terms. The secondary goal was implementation of the timestamp feature into the sensor's software. This Phase 2 extension effort was divided into three tasks described below.

Task 1. Validation of the Modified Algorithm at Broad Temperature Range

The RE sensor algorithm uses temperature to correct for effects of changing electrical conductivity with temperature. This part of the algorithm used a known expression for seawater conductivity as a function of salinity and temperature. Since the Battelle setup as well as the Ohmsett setup do not allow for control of temperature, testing at different temperatures was not a part of the Phase 2 work plan. This introduced an unnecessary risk for the sensor**,** which is intended to be used at a very broad temperature range. To mitigate this risk, in this task the RE sensor's response was tested at different temperatures.

All four sensor prototypes were tested; however, all units produced essentially identical results. The tests were carried out with simulated seawater at three salinities: 1 wt%, 3 wt%, and 5 wt%. For each salinity, the sensor cavity was filled with seawater chilled with water ice to about 12°C and then allowed to slowly warm up to ambient temperature. The sensor software recorded the eight raw sensor signals and values of temperature.

The temperature effects observed in this task were used in the second and third versions of the algorithm.

Appendix D presents the temperature response results obtained for one of the prototypes.

Task 2. Addition of a Timestamp Feature

This task involved a small modification of the tablet software. The "Settings" tab shown in Figure 16 was amended with the "Add Note" button. Pressing this button opens a window enabling addition of a short note into the current row in the Excel recording sensor's output. This feature can be used at any time the sensor software operates and records sensor data. The notes can be used as time markers that simplify interpretation of the recorded data.

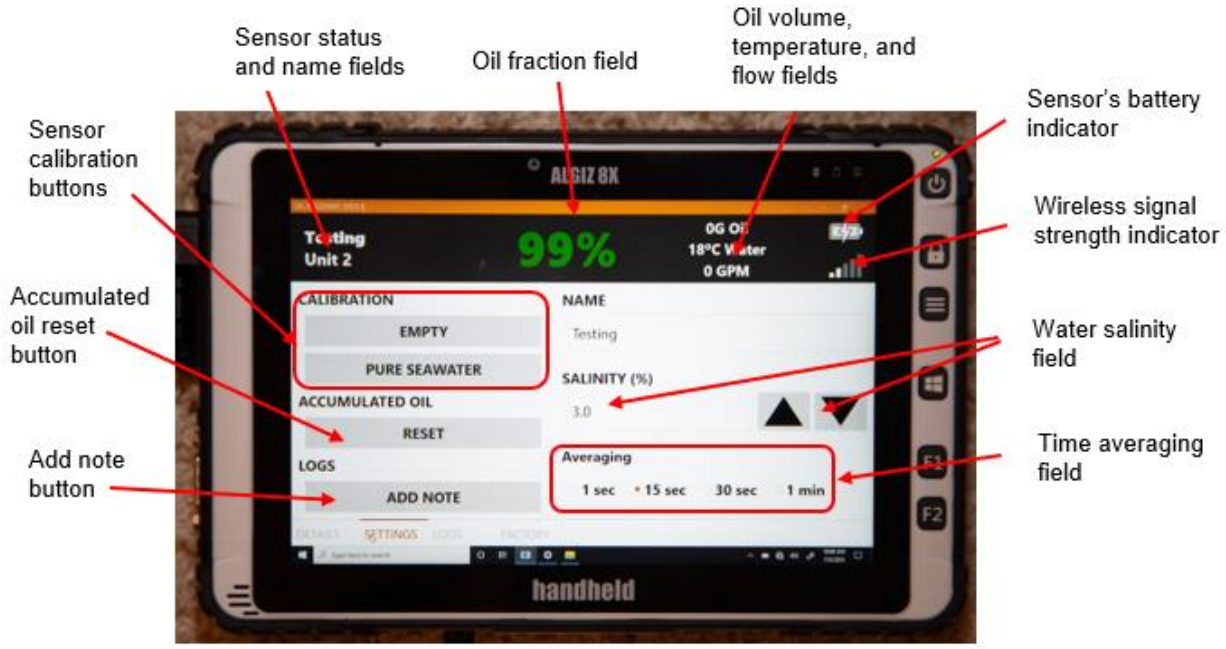

Figure 16: The "Settings" tab implementation the time stamp (add note) feature.

Task 3. Validation of the Modified Algorithm at Ohmsett

The goal of this task was verification of the RE sensor performance, specifically the second version of the algorithm, under conditions that realistically simulate real offshore oil recovery operations.

The Ohmsett tests were carried out over two weeks in July 2023. A total of 40 tests were carried out using Hydrocal- and Calsol-seawater mixtures at two flow rates, 30 and 60 gpm. The tests were carried out with two water salinities, 1 wt% and 3 wt%.

Unfortunately, the RE sensor's algorithm behaved erratically, producing output values that were poorly correlated with the true oil fraction of tested oil-water streams. This behavior was attributed to a software error which could not be corrected during the Ohmsett campaign. Despite this challenge, Battelle and BSEE decided to go ahead and perform the testing with the goal of collecting the raw sensor data for future analysis. The collected data were analyzed and used for development of the third version of the algorithm. Appendices E and F present results of both 2022 and 2023 data when analyzed using the third version of the algorithm.

The third version of the algorithm produced the following accuracy:

- Overall average error (all 2022 and 2023 tests): 6.38%
- For Calsol oil (2023 tests): average error 8.84%, maximum error 24.7%
- For Hydrocal 300 oil (2023 tests): average error 6.37%, maximum error 17.1%
- For Hydrocal 300 oil (2022 tests): average error 3.57%, maximum error 10.1%
- For Diesel oil (2022 tests): average error 4.86%, maximum error 12.7%

4. Conclusions

Conclusions of this project can be summarized as follows:

- Measurement of oil fractions during offshore oil recovery operations is a challenging technical problem which was recognized by BSEE prior to issuing both the Phase 1 and 2 solicitations. Battelle attempted, and made great progress, in solving this challenge in both Phase 1 and 2 projects.
- Battelle's RE sensor did not meet the accuracy of 6% requested by BSEE. Instead, accuracy around 7-9% was observed during the June 2022 Ohmsett testing. Better accuracies were achieved using MATLAB simulations; however, this was not confirmed during the 2023 Ohmset tests due to the software error. Values of maximum errors, reaching up to about 20% in some cases, further impeded BSEE assessment of this technology.
- The sensor's hardware met all requirements set by BSEE and includes modern design architecture based on off-the-shelf electronic components. The sensor offers a long-term battery operation due to its very low power consumption (~500 mW, most of it consumed by radio communications). The sensor can operate in a very broad temperature range from -25°F up to 120°F. The sensor construction is shock resistant and fully compatible with a marine environment.
- Although BSEE decided not to continue development of the sensor, Battelle may do so. Specifically, the applications in the oil and gas industry appear very attractive.

5. Recommendations

Development of the sensor algorithm is not complete. Battelle believes an additional engineering would produce a more robust algorithm providing consistent sensor accuracy of about 7-8% (average error) and eliminate excessive maximum error values. All sensor algorithms developed to date use the two-measurement approach which alternates between the dielectric measurement for oil-rich mixtures and conductivity measurement for water rich streams. The main drawback of this approach is the discontinuity which causes the sensor readings to be erratic for intermediate values of oil fraction. Elimination of this effect would require a more granular algorithm that classifies the electrical conductivity of oil-water mixtures into multiple, likely three or four, groups that are representative of the expected two-phase flow patterns. The algorithm should be further simplified with the elimination of the "empty" and "pure water" calibrations. Such calibrations are confusing for the user and as demonstrated by the 3rd version of the algorithm, not necessary. The sensor algorithm could be finalized using the raw data collected during the Ohmsett 2022 and 2023 testing campaigns; however, additional Ohmset tests would be needed to formally validate the algorithm.

It is very likely the sensor accuracy could be improved by its use in a vertical orientation. This orientation eliminates the effect of oil-water stratification and makes the sensor algorithm much simpler. Also, with the vertical sensor orientation, the complication of air pockets within the

sensor inside of the sensor cavity is eliminated. The use of the sensor in a vertical orientation would require collection of raw data at Ohmsett and development of a new algorithm. The experimental setup constructed at Battelle cannot be used for such tests due to its flow limitations. Note that during testing at Ohmsett both orientations can be tested simultaneously using two sensors connected in series.

The use of the sensor in a vertical orientation should be implemented as an addition to the current horizontal mode, as the sensor's users would be able use the sensor in either orientation depending on the required measurement accuracy.

The sensor is capable of using signals from an external flowmeter. Battelle implemented this capability in the sensor hardware and software. A significant effort was made at Battelle to test an ultrasonic type of flowmeter (provided by BSEE) with different oil-water mixtures and with several flowmeter's mounting configurations, but the flowmeter accuracy was very poor. Clearly, the two-phase streams pose a challenge for the ultrasonic flowmeter. Further work is needed to determine what flowmeter type would be compatible with the oil-water streams encountered in offshore recovery operations.

6. Appendices

A. Sensor Performance Requirements

At the beginning of the Phase 2 project, BSEE set the following requirements for the RE sensor:

- The RE sensor shall have the ability to measure the percentage of oil and water in recovered fluid across the entire range of oil fractions and water salinities of 1-5% on a continuous basis and transmit this data in real time to the user.
- The RE sensor shall be able to measure multiple types of crude and refined oils and oil emulsions without requiring calibration for oil type.
- The RE sensor shall have an average measurement accuracy of +/- 6% for all oil fractions, oil types, and water tests conducted, including oil types, oil fractions, and salinities. For example, if the test fluid contains 50% oil, the RE Sensor shall indicate that the fluid contains from 44% to 56 oil.
- The RE sensor shall measure the oil content in oil-seawater mixtures regardless of air content contained in the recovery hose and passing through the RE sensor. This will be a significant improvement over the 1st version of the sensor, which worked only with a transfer hose filled with a liquid mixture. Practical oil recovery operations usually involve partially empty hoses containing rapidly changing oil, water, and air fractions. The proposed sensor will use a modified detection principle, developed at Battelle after the first phase of the project.
- The RE sensor shall be constructed as an open section of a pipe without any internal flow restrictions. The sensor cavity will be 3-inch diameter. The RE sensor's length will be no greater than 36 inches. The RE Sensor's overall outer diameter will be no greater than 12 inches and will be minimized as much as practical.

- The sensor shall use two aluminum quick hose connectors, one male and one female. Each prototype will be provided with a set of end-adapters allowing for connections with 2-, 3-, or 4-inch size hoses.
- The sensor enclosure shall be made of metal to provide sufficient mechanical strength.
- The RE sensor output signal shall be transmitted through wireless signal (type to be determined) capable of working in a marine environment over 200-400 ft distance.
- The sensor will have the capability to be powered by two methods:
    - By an internal rechargeable battery (see the two bullet points below)
    - By an external, low voltage (ex 5-24 VDC) power supply connected through a cable.
- The RE sensor shall be powered by batteries, most likely a set of D-size cells. Both alkaline and rechargeable battery options will be available. The rechargeable batteries will be able to be recharged while in the RE Sensor via the cable connection if desired. The alkaline or rechargeable batteries will also be easily accessible for replacement with fresh batteries. The RE sensor will be able to operate continuously for an agreed-on number of hours between battery charge or replacement. Battelle will conduct a study that specifies number and type of batteries required versus operational time and temperature. The RE sensor shall be able to operate at a minimum of 48 hours between battery charge or replacement.
- Required battery pack capacity for low temperature operations, including -25°F will be identified during Task 1. The goal will be to enable the 48 hours operation at these temperatures; however, Battelle reserves the right to provide this with an additional battery pack, which is attached to the sensor in a way that maintains the overall sensor autonomy and convenient use. The battery size will be finalized in collaboration with BSEE during Task 1.
- The RE sensor UI/control will be provided using a display such as a rugged tablet. The RE sensor UI/control will be able to operate as intended in a marine environment. It should operate as intended in humidity levels up to 90% relative humidity, when exposed to dripping or splashing with fresh or salt water, exposure to rain or blowing rain, after being dropped from a height of 3 feet onto a hard surface, and after surface exposure to oil droplets or smears. The RE Sensor UI/control should be operational in a temperature range of -20°F to 120°F. The user will be able to read the display in bright sunlight and in low light conditions.
- The RE sensor will be able to operate as intended in environmental conditions that would be typically be present during a marine oil spill response operation. This includes exposure to salt water, immersion in salt water down to 1 meter, humidity levels up to 90% relative humidity, and UV exposure. The RE Sensor will be able to operate as intended when subjected to mechanical vibrations that would be typically experienced by shipboard equipment (ref. Mil-Std 810, method 528). The RE sensor will be able to operate as intended after being dropped from a height of 3 feet onto a hard surface. The RE sensor will operate as intended in temperature range of -25°F to 120°F.
- The RE sensor will need to be calibrated for water salinity due to the use of eddy current measurements. The RE Sensor calibration will be able to be accomplished in two ways. The RE sensor can be calibrated by filling the cavity with saline water and selecting a

calibration mode on the UI/control. The water salinity can also be input into the UI/control. A submersible salinity meter that can measure the water salinity will be included with each RE Sensor System. This salinity meter could then be lowered below the water surface to avoid any surface oil and record salinity in the field.

- The system, including the RE sensor, the sensor control/user interface, user's manual, quick start instructions, spare batteries, battery charger, handheld salinity meter, and other components necessary to operate the sensor shall be delivered in a lightweight, watertight, ruggedized case. The user should be able to open the case and have everything required to operate the system. The case shall prevent ingress of water when exposed to dripping, splashing, and spraying of fresh or saline water. Battelle will discuss with BSEE whether the end adaptors will be included in this case or will be packaged separately.
- The RE sensor shall meet the requirements for an International Protection Marking of IP67.
- The RE sensor UI/control shall provide the user with an ongoing readout of the oil/water percentage. Battelle and BSEE will discuss and agree on the specific readout and what modes of operation shall be included. For example, one mode may be a red light, yellow light, green light display that simply indicates that the oil/water percentage is good, average, or poor. Another mode may provide a numerical readout, averaged over a selected time period. The user should have the option to select the time period for data averaging, and choice of data display.
- The RE sensor system shall record and save measurement data, ideally within the RE Sensor (rather than in the UI/control). If required by the system design and/or power consumption requirements, Battelle reserves the right to save the measured data on the tablet UI/control. Battelle will discuss with BSEE tradeoffs between the two data storage locations.
- The RE sensor shall have the capability to use an external flow meter signal to calculate the overall volumes of oil and water collected. Battelle will discuss with BSEE possible options for providing flow information into the RE sensor system.
- The TRL of this system when delivered shall be 8 as defined in the BSEE specifications for definition of TRLs associated with Oil Spill Response Technologies and Equipment [5].

B. Results of Ohmsett Tests in June 2022

The June 2022 Ohmsett tests of the Battelle's RE sensor used two oils, Hydrocal-300 and Diesel, and two flow rates, 30 and 60 gpm. During these tests, the sensor used the first version of the algorithm. Table 4 shows the values of true oil fraction and the values measured by the sensor. The oil fraction measured by the sensor is an arithmetic average of about 30-40 values recorded during each test. The true oil fraction was determined based on the volumes of collected oil and water, which includes the correction for water droplets suspended in oil. Note that Figure 14 shows these data in a graphical form.

Table 4: Results of Ohmsett tests carried out in June 2022.

Test #	Oil Type	Salinity (wt%)	Flow (gpm)	Target Oil Fraction (vol%)	Grab Sample Oil Fraction (vol%)	Oil Fraction Indicated by Sensor (vol%)
1	Pure water	2.7	30	0	0	0
2	Hydrocal	2.7	30	20	19.0	17.6
3	Hydrocal	2.7	30	40	41.7	53.6
4	Hydrocal	2.7	30	60	59.1	78.9
5	Hydrocal	2.7	30	80	83.6	88.5
6	Hydrocal	2.7	30	100	99.1	99.4
7	Pure water	2.7	60	0	0	0
8	Hydrocal	2.7	60	20	19.6	3.4
9	Hydrocal	2.7	60	40	40.1	18.3
10	Hydrocal	2.7	60	60	62.7	65.6
11	Hydrocal	2.7	60	80	86.7	92
12	Diesel	2.7	30	20	22.7	18.4
13	Diesel	2.7	30	40	41.3	40.7
14	Diesel	2.7	30	60	60.3	67.1
15	Diesel	2.7	30	80	78.3	81.7
16	Diesel	2.7	30	100	100	99
17	Diesel	2.7	60	20	20.4	5
18	Diesel	2.7	60	40	38.8	20.5
19	Diesel	2.7	60	60	61.5	74.8
20	Diesel	2.7	60	80	79.8	92
21	Diesel	2.7	60	90	90.3	98.8
22	Diesel	2.7	30	85	85.3	86.4

Accuracy for Hydrocal oil:

- Average error (average for tests 2-6, 8-11): 9.39%
- Maximum error (test 9): 21.8%

Accuracy for Diesel:

- Average error (average for tests 12-22): 7.72%
- Maximum error (test 18): 18.3%

C. Results of MATLAB Simulation following Ohmsett Tests in July 2022

Following the June 2022 Ohmsett tests, Battelle developed a second version of sensor algorithm which was implemented as a MATLAB simulation applied to the raw data collected in July 2022. Table 5 shows the results of this simulation. Note that Figure 15 shows these data in a graphical form. Unfortunately, this level of accuracy was not confirmed during the 2023 Ohmsett tests.

Table 5: Results of version 2 algorithm MATLAB simulation following Ohmsett tests carried out in July 2022.

Test #	Oil Type	Salinity (wt%)	Flow (gpm)	Target Oil Fraction (vol%)	Grab Sample Oil Fraction (vol%)	Oil Fraction from new algorithm (vol%)
1	Pure water	2.7	30	0	0	0
2	Hydrocal	2.7	30	20	19.0	26
3	Hydrocal	2.7	30	40	41.7	48
4	Hydrocal	2.7	30	60	59.1	70
5	Hydrocal	2.7	30	80	83.6	88
6	Hydrocal	2.7	30	100	99.1	99
7	Pure water	2.7	60	0	0	0
8	Hydrocal	2.7	60	20	19.6	22
9	Hydrocal	2.7	60	40	40.1	39
10	Hydrocal	2.7	60	60	62.7	59
11	Hydrocal	2.7	60	80	86.7	86
12	Diesel	2.7	30	20	22.7	16
13	Diesel	2.7	30	40	41.3	41
14	Diesel	2.7	30	60	60.3	63
15	Diesel	2.7	30	80	78.3	75
16	Diesel	2.7	30	100	100	99
17	Diesel	2.7	60	20	20.4	10
18	Diesel	2.7	60	40	38.8	40
19	Diesel	2.7	60	60	61.5	65
20	Diesel	2.7	60	80	79.8	86
21	Diesel	2.7	60	90	90.3	98
22	Diesel	2.7	30	85	85.3	82

Accuracy for Hydrocal oil:

- Average error (average for tests 2-6, 8-11): 4.07%
- Maximum error (test 4): 10.9%

Accuracy for Diesel:

- Average error (average for tests 12-22): 4.20%
- Maximum error (test 17): 10.4%

D. Results of Temperature Tests

The temperature response tests were carried out with water at three salinity levels: 1 wt%, 3 wt%, and 5 wt%. The tests were performed simultaneously for all four prototypes, the sensors were connected in series and filled with one common water stream that was warmed up or chilled during the tests. Essentially identical data were collected for all four prototypes. Results obtained for unit #4 are presented below. These results were used to develop temperature correction equations that were implemented in the second and third version of the algorithm.

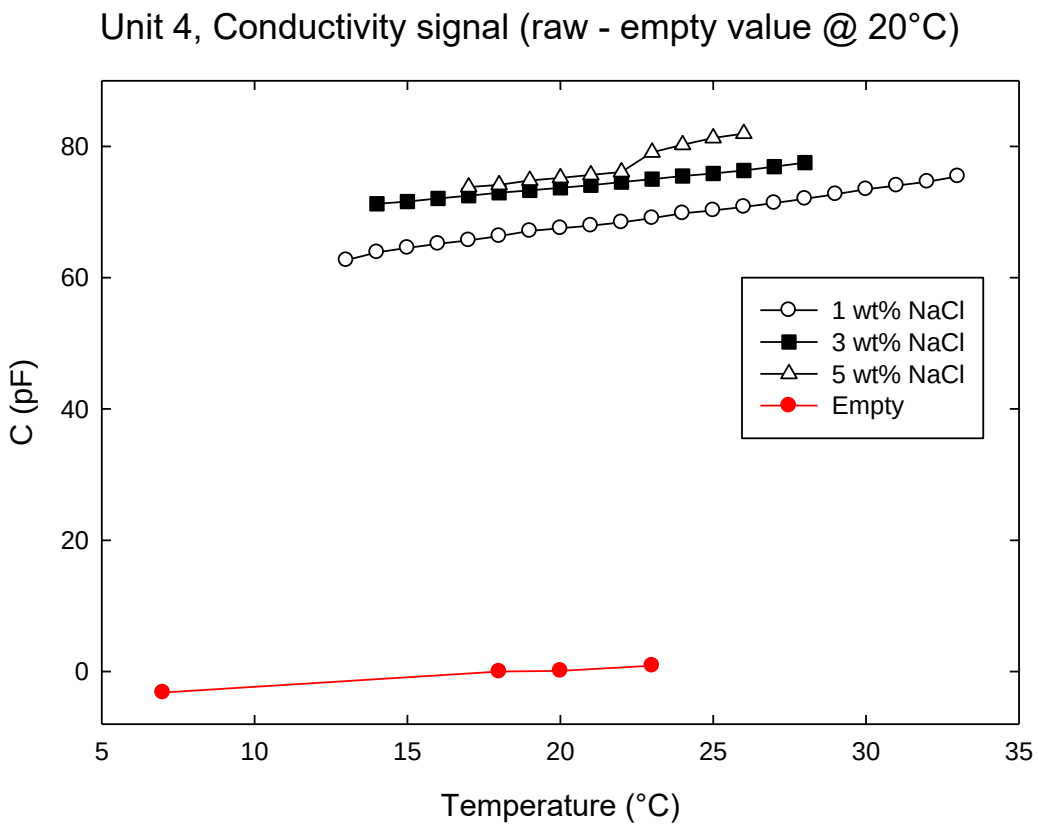

Figure 17: Temperature response of the conductivity signal.

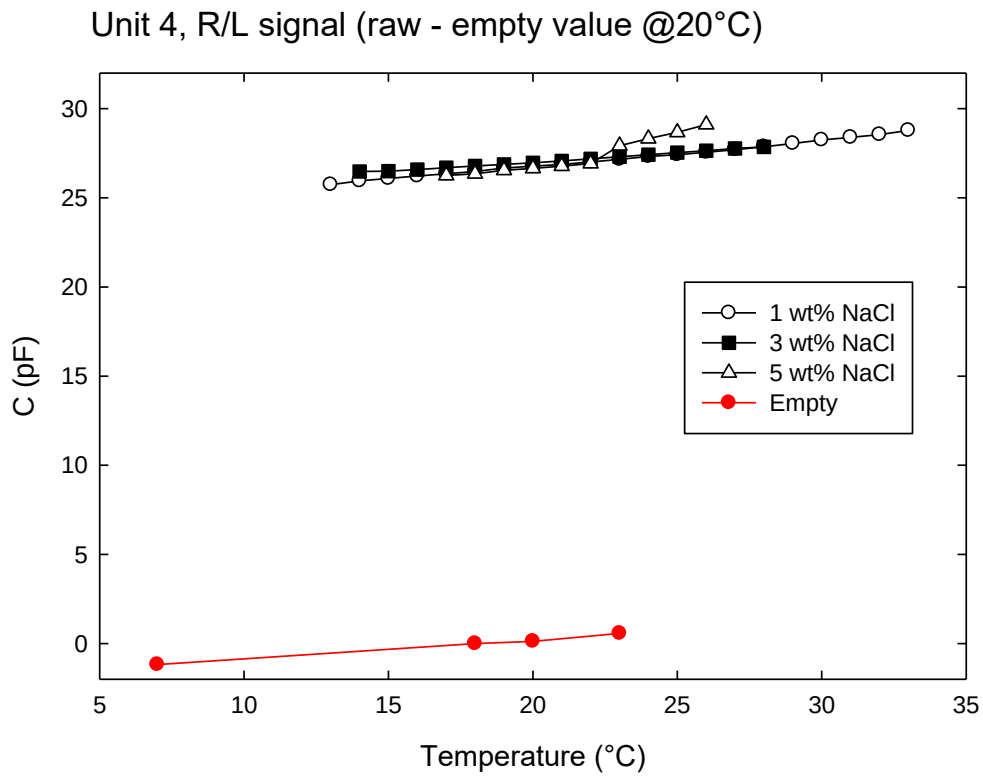

Figure 18: Temperature response of the R/L signal.

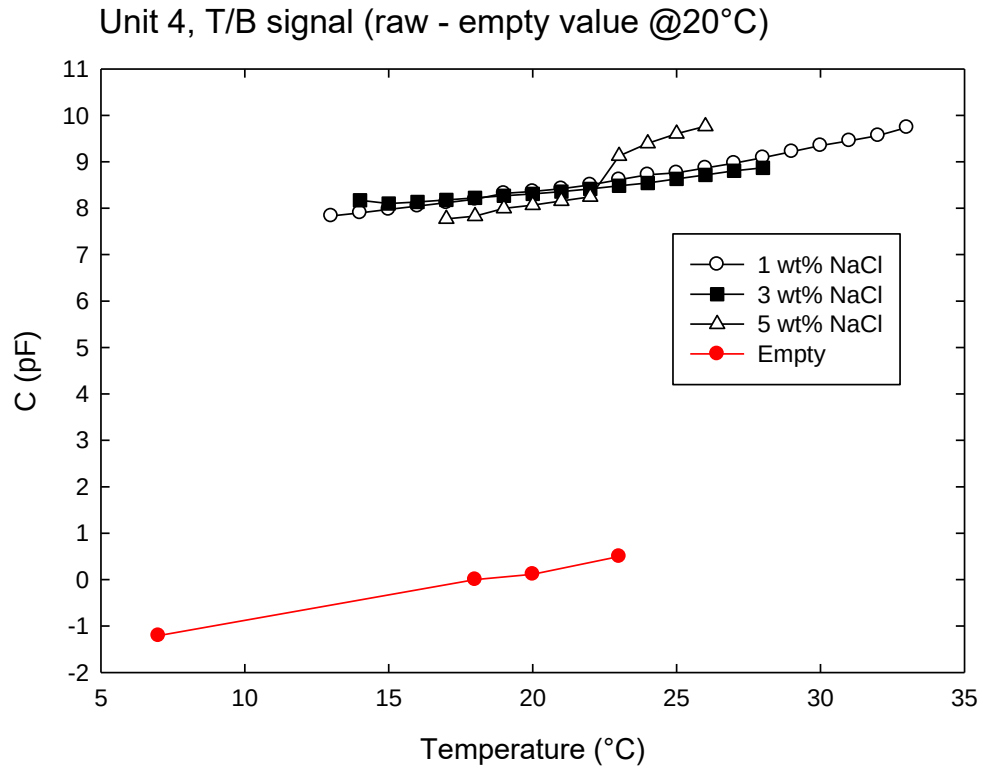

Figure 19: Temperature response of the T/B signal.

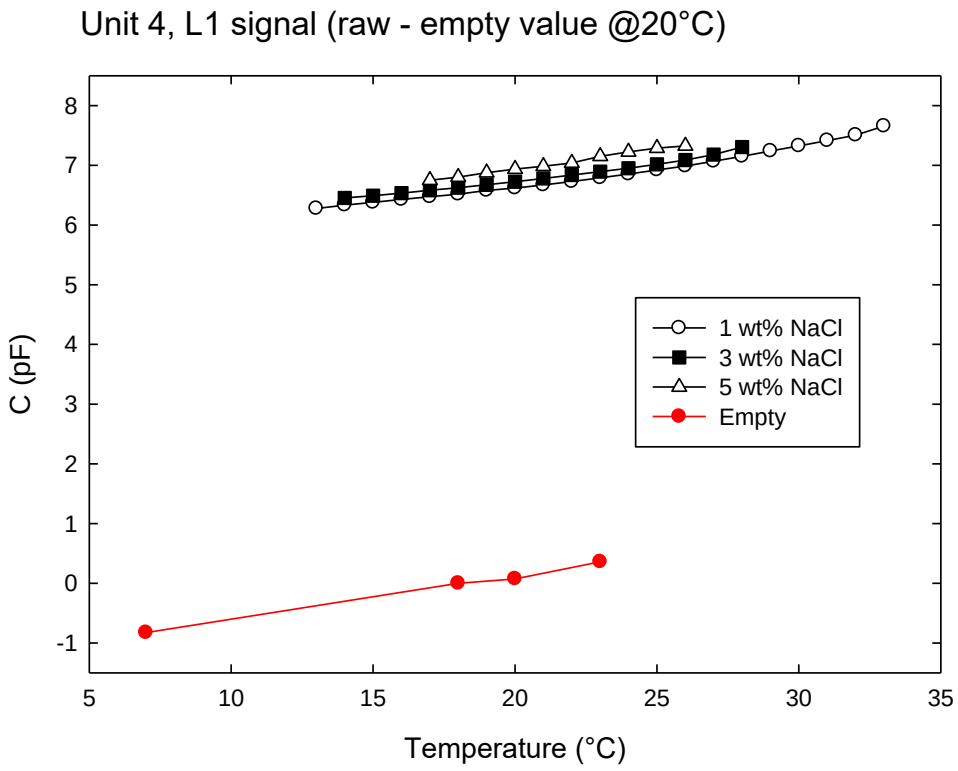

Figure 20: Temperature response of the L1 signal.

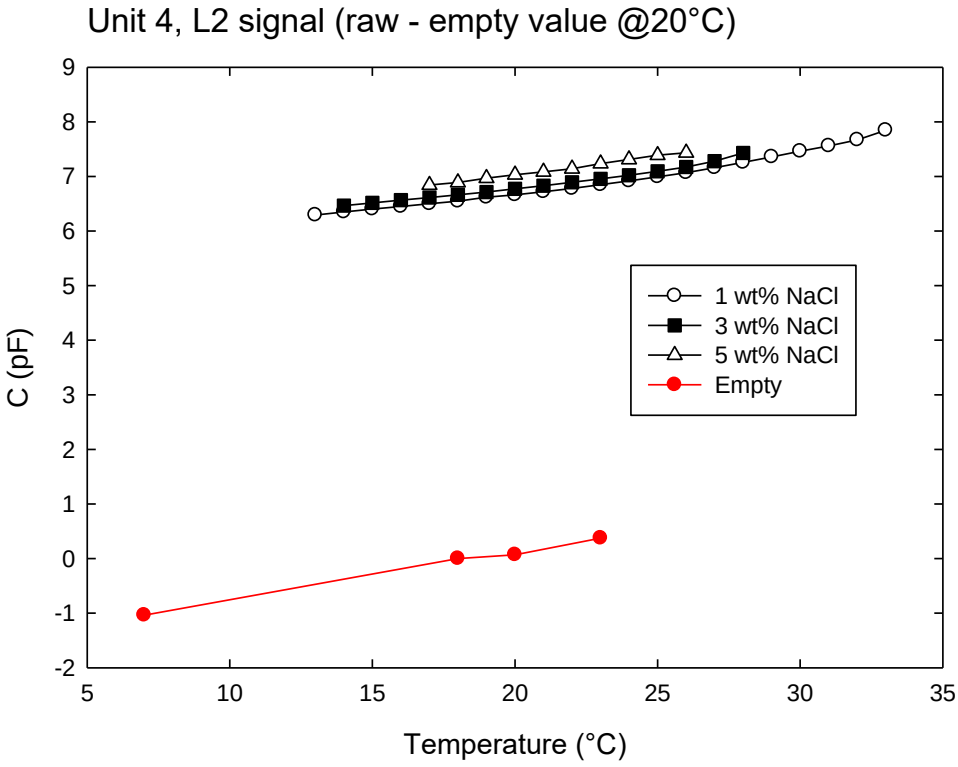

Figure 21: Temperature response of the L2 signal.

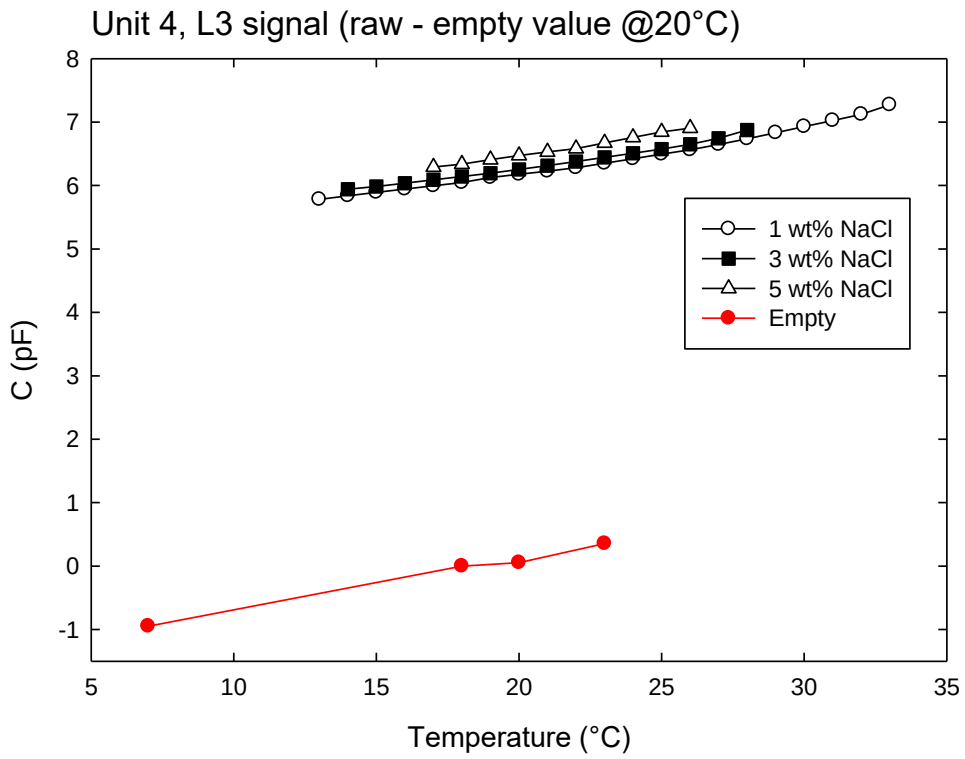

Figure 22: Temperature response of the L3 signal.

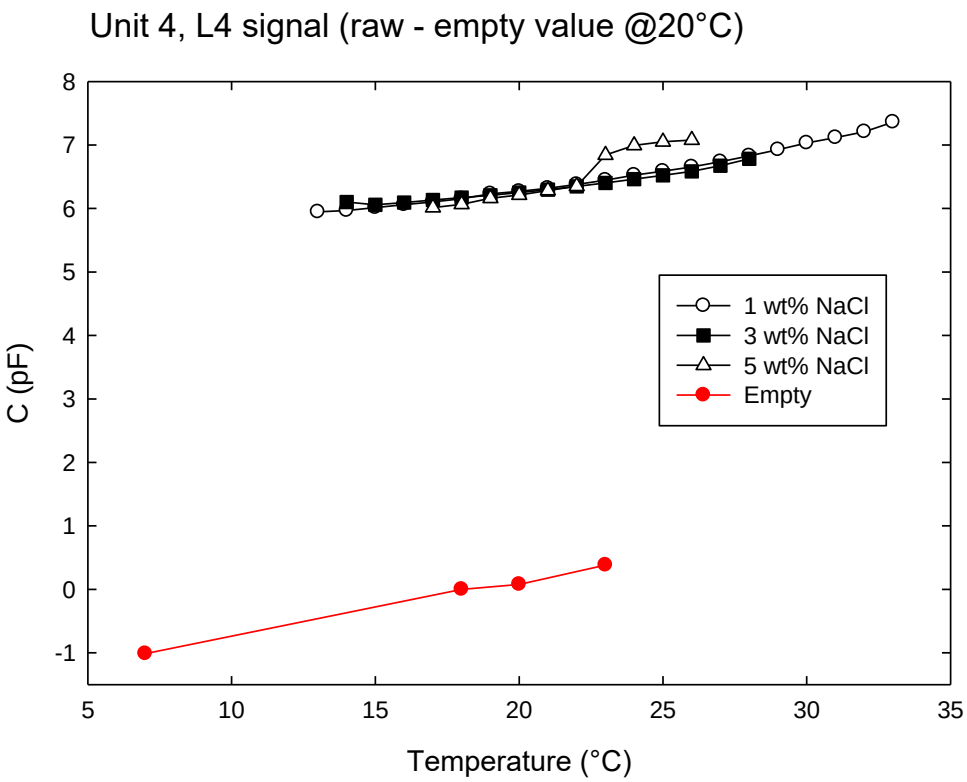

Figure 23: Temperature response of the L4 signal.

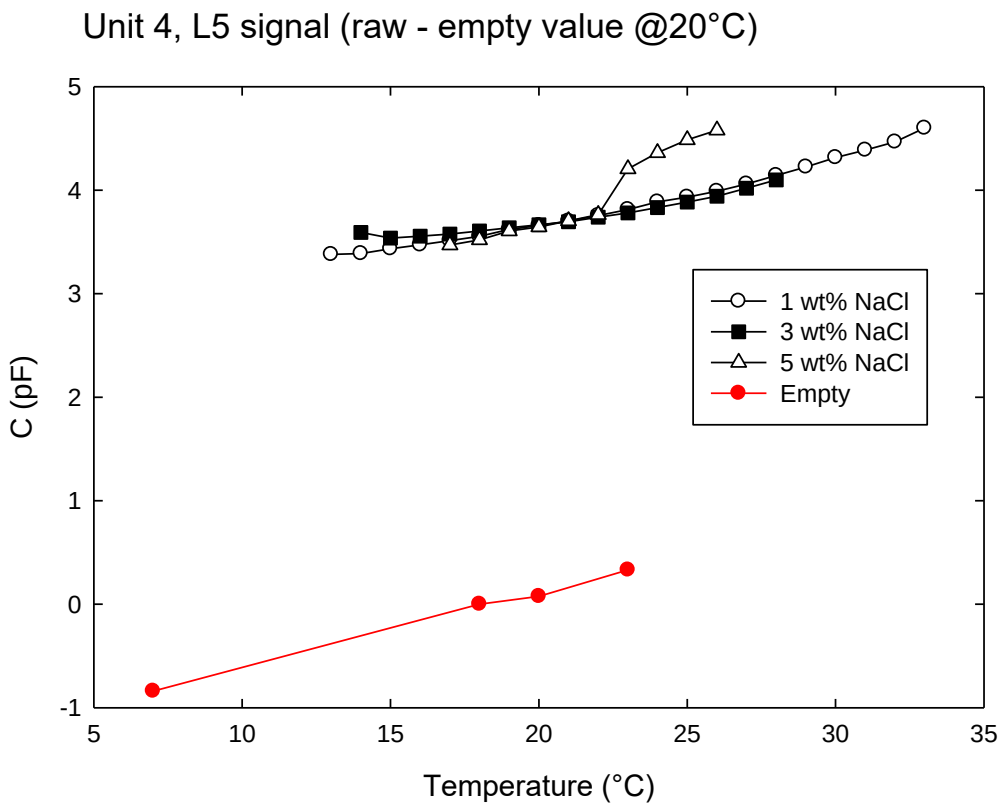

Figure 24: Temperature response of the L5 signal.

E. Results of MATLAB Simulation following Ohmsett Tests in July 2023

Following the June 2023 Ohmsett tests, Battelle developed a third version of sensor algorithm which was implemented as a MATLAB simulation applied to the raw data collected in July 2022. Table 6 shows the results of this simulation, Figure 25 presents this data in a graphical form. Note that several tests (test 30-34) were carried out using a static mixer installed in front of the sensor. The goal of these tests was to assess the effect of vigorous mixing on flow patterns. These tests are reported for completeness in Table 6 but were not included in algorithm simulations.

Table 6: Results of version 3 algorithm MATLAB simulation using data from both Ohmsett campaigns (2022 and 2023).

Test # (year)	Oil Type	Salinity (wt%)	Flow (gpm)	Target Oil Fraction (vol%)	Grab Sample Oil Fraction (vol%)	Oil Fraction from new algorithm (vol%)
1 (2023)	Pure water	3	30	0	0.0	2.8
2 (2023)	Calsol	3	30	20	6.4	28.5
3 (2023)	Calsol	3	30	40	32.4	28.9
4 (2023)	Calsol	3	30	60	Not available (60% used in analysis)	59.2
5 (2023)	Calsol	3	30	80	68.0	78.2
6 (2023)	Calsol	3	30	100	87.9	97.4
7 (2023)	Pure water	3	60	0	0.0	22.9
8 (2023)	Calsol	3	60	20	17.3	15.8
9 (2023)	Calsol	3	60	40	36.4	30.6
10 (2023)	Calsol	3	60	60	52.4	38.9
11 (2023)	Calsol	3	60	80	67.8	77.8
12 (2023)	Calsol	3	60	100	94.5	97.2
13 (2023)	Calsol	3	30	20	18.1	33.6
14 (2023)	Hydrocal	3	30	20	20.3	33.1
15 (2023)	Hydrocal	3	30	40	39.6	50.7
16 (2023)	Hydrocal	3	30	60	61.2	70.6
17 (2023)	Hydrocal	3	30	80	82.0	83.2
18 (2023)	Hydrocal	3	30	100	99.7	98.2
19 (2023)	Hydrocal	3	60	20	19.6	16.9
20 (2023)	Hydrocal	3	60	40	38.8	41.5
21(2023)	Hydrocal	3	60	40	39.8	38.4
22(2023)	Hydrocal	3	60	60	59.1	51.6
23(2023)	Hydrocal	3	60	80	80.2	79.8
24(2023)	Pure water	1	30	0	0.0	15.1
25(2023)	Hydrocal	1	30	20	19.3	36.4
26(2023)	Hydrocal	1	30	40	37.8	41.9
27(2023)	Hydrocal	1	30	60	57.0	70.0
28(2023)	Hydrocal	1	60	40	40.2	33.5
29(2023)	Hydrocal	1	60	60	59.5	55.5
30 (2023)	Calsol	3	30 (static mixer)	40	35.6	18.1
31 (2023)	Calsol	3	30 (static mixer)	60	56.9	48.5
32 (2023)	Calsol	3	30 (static mixer)	20	19.6	19.2
33 (2023)	Calsol	3	60 (static mixer)	40	36.7	15.4
34 (2023)	Calsol	3	60 (static mixer)	20	18.7	2.0
35 (2023)	Calsol	3	60	20	18.5	43.2

Test # (year)	Oil Type	Salinity (wt%)	Flow (gpm)	Target Oil Fraction (vol%)	Grab Sample Oil Fraction (vol%)	Oil Fraction from new algorithm (vol%)
36 (2023)	Calsol	3	60	40	36.7	46.2
37 (2023)	Calsol	3	60	60	56.3	50.1
38 (2023)	Calsol	3	30	20	19.5	29.1
39 (2023)	Calsol	3	30	40	36.7	36.4
40 (2023)	Calsol	3	30	60	56.9	61.8
1 (2022)	Pure water	2.7	30	0	0	1.1
2 (2022)	Hydrocal	2.7	30	20	19.0	21.2
3 (2022)	Hydrocal	2.7	30	40	41.7	46.8
4 (2022)	Hydrocal	2.7	30	60	59.1	69.2
5 (2022)	Hydrocal	2.7	30	80	83.6	85.0
6 (2022)	Hydrocal	2.7	30	100	99.1	99.0
7 (2022)	Pure water	2.7	60	0	0	8.6
8 (2022)	Hydrocal	2.7	60	20	19.6	19.2
9 (2022)	Hydrocal	2.7	60	40	40.1	34.1
10 (2022)	Hydrocal	2.7	60	60	62.7	56.6
11 (2022)	Hydrocal	2.7	60	80	86.7	87.4
12 (2022)	Diesel	2.7	30	20	22.7	31.7
13 (2022)	Diesel	2.7	30	40	41.3	45.7
14 (2022)	Diesel	2.7	30	60	60.3	56.6
15 (2022)	Diesel	2.7	30	80	78.3	67.2
16 (2022)	Diesel	2.7	30	100	100	99.0
17 (2022)	Diesel	2.7	60	20	20.4	12.9
18 (2022)	Diesel	2.7	60	40	38.8	39.1
19 (2022)	Diesel	2.7	60	60	61.5	60.5
20 (2022)	Diesel	2.7	60	80	79.8	79.6
21 (2022)	Diesel	2.7	60	90	90.3	92.9
22 (2022)	Diesel	2.7	30	85	85.3	72.6

Overall average error (all 2022 and 2023 tests): 6.38%

Accuracy for Calsol oil (2023 data):

- Average error (average for tests 2-6, 8-13, 35-40): 8.84%
- Maximum error (test 35): 24.7%

Accuracy for Hydrocal 300 oil (2023 data):

- Average error (average for tests 14-23, 25-29): 6.37%
- Maximum error (test 25): 17.1%

Accuracy for Hydrocal 300 oil (2022 data):

- Average error (average for tests 2-6, 8-11): 3.57%
- Maximum error (test 4): 10.1%

Accuracy for Diesel oil (2022 data):

- Average error (average for tests 12-22): 4.86%
- Maximum error (test 22): 12.7%

F. Time-Dependent Output of the Third Version of the Algorithm Generated via MATLAB Simulation – 2022 & 2023 Ohmsett Tests

Correlation plot for 2022 & 2023 campaigns

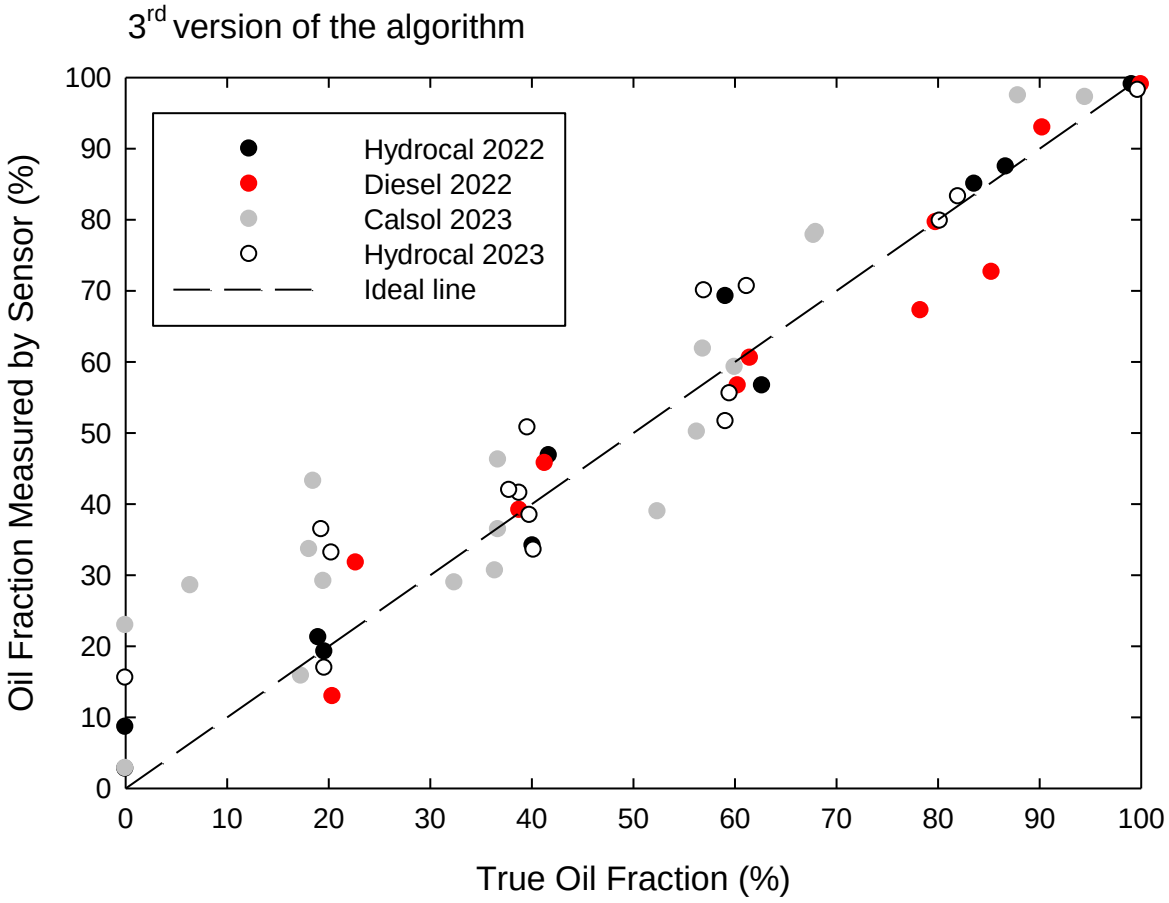

Figure 25: Correlation plot for 3rd version algorithm, Ohmsett 2022 & 2023 campaigns.

Ohmsett 2023 campaign

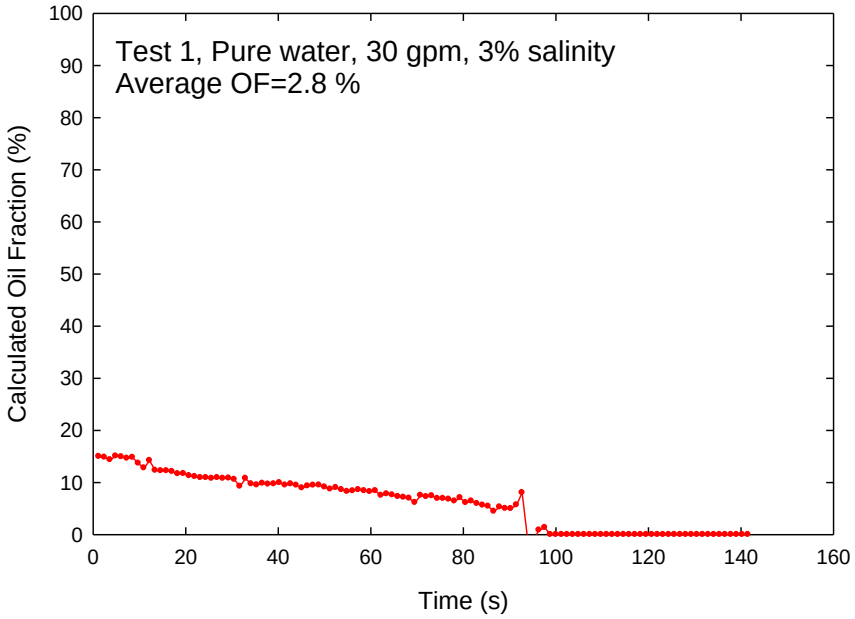

Figure 26: Test 1 (July 12, 2023) measured oil fraction as a function of time.

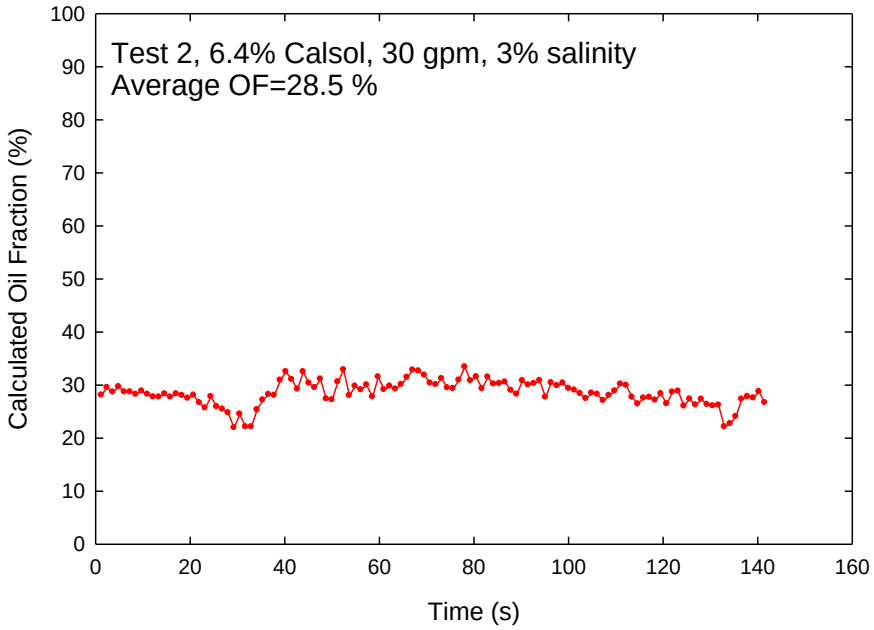

Figure 27: Test 2 (July 12, 2023) measured oil fraction as a function of time.

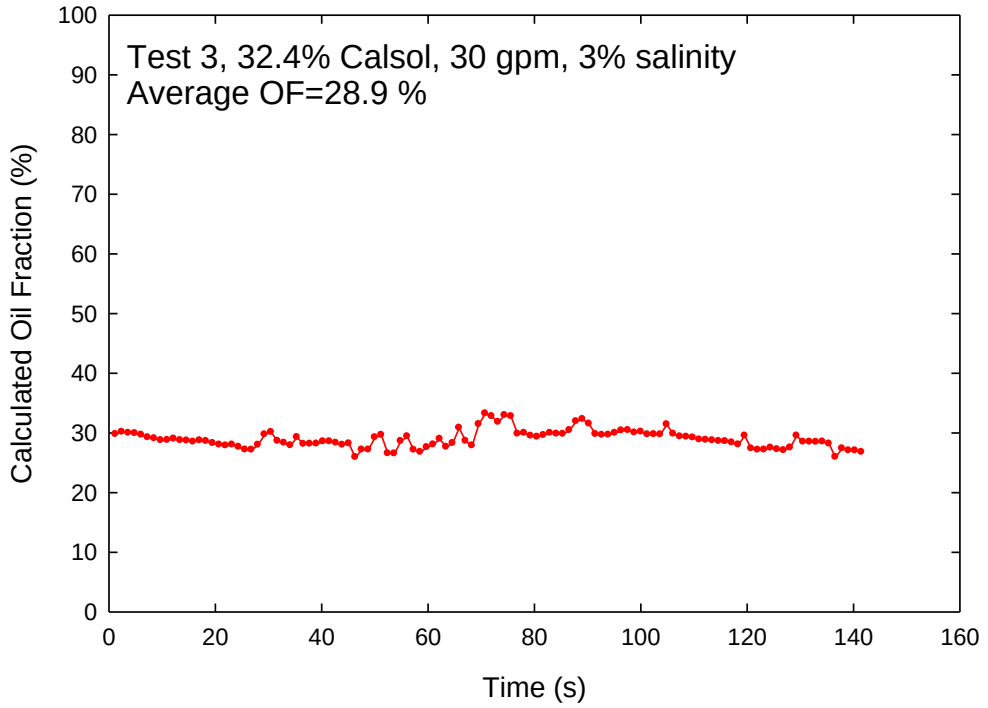

Figure 28: Test 3 (July 12, 2023) measured oil fraction as a function of time.

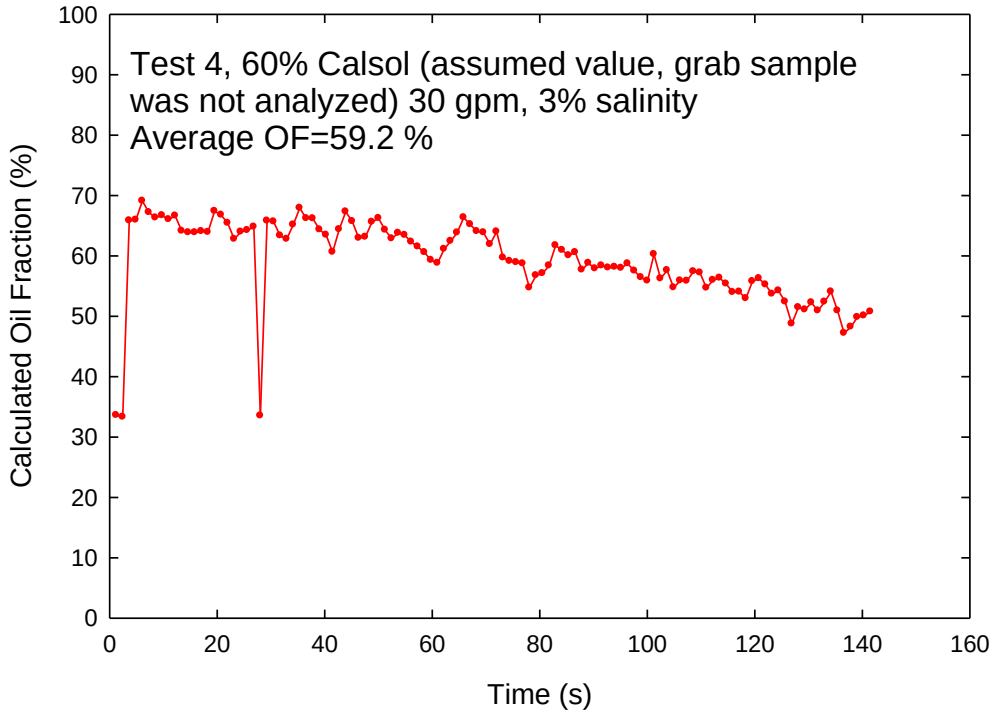

Figure 29: Test 4 (July 12, 2023) measured oil fraction as a function of time.

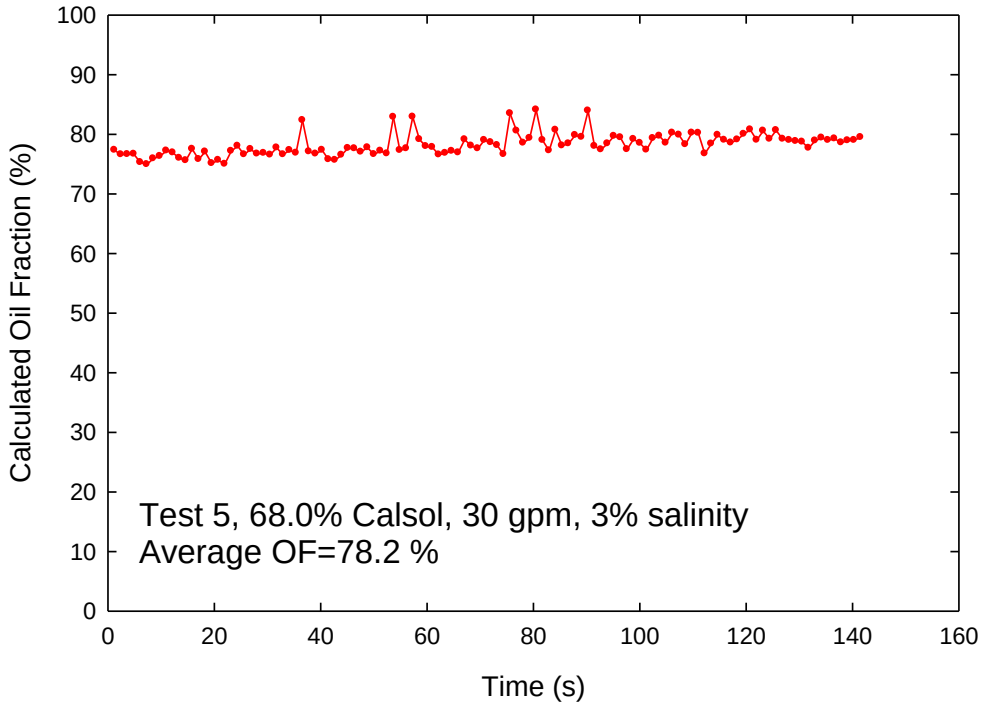

Figure 30: Test 5 (July 12, 2023) measured oil fraction as a function of time.

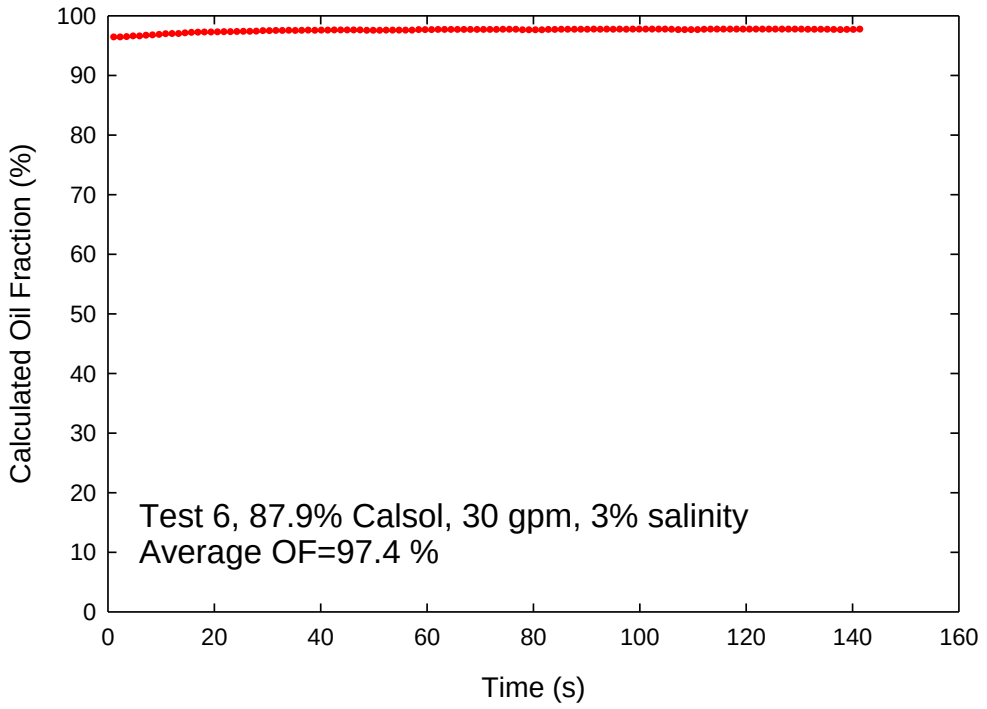

Figure 31: Test 6 (July 13, 2023) measured oil fraction as a function of time.

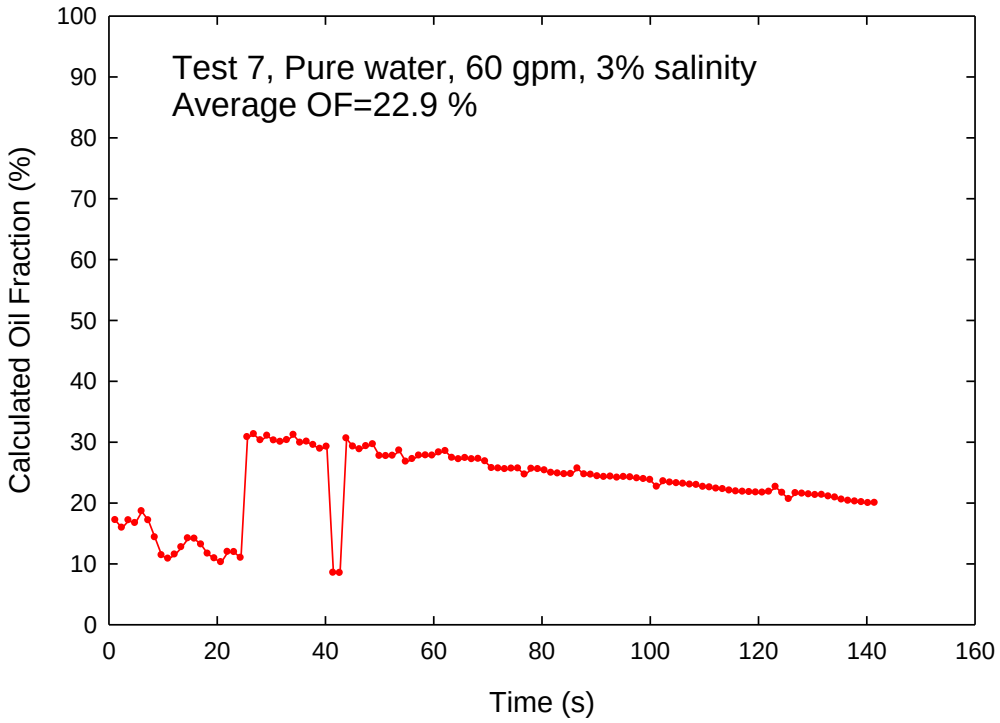

Figure 32: Test 7 (July 13, 2023) measured oil fraction as a function of time.

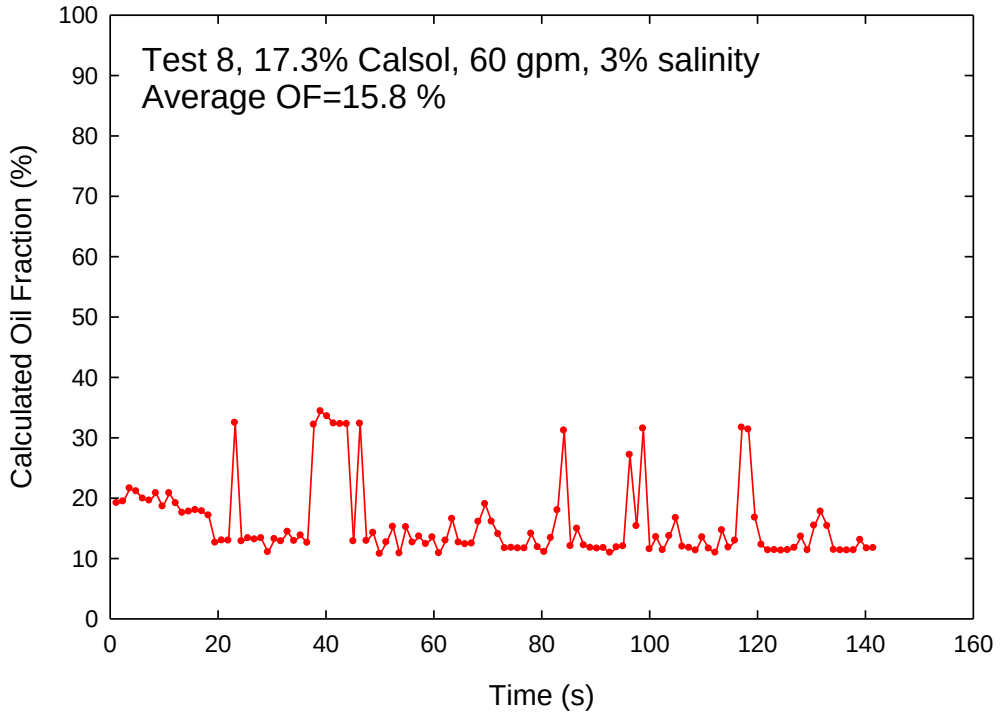

Figure 33: Test 8 (July 13, 2023) measured oil fraction as a function of time.

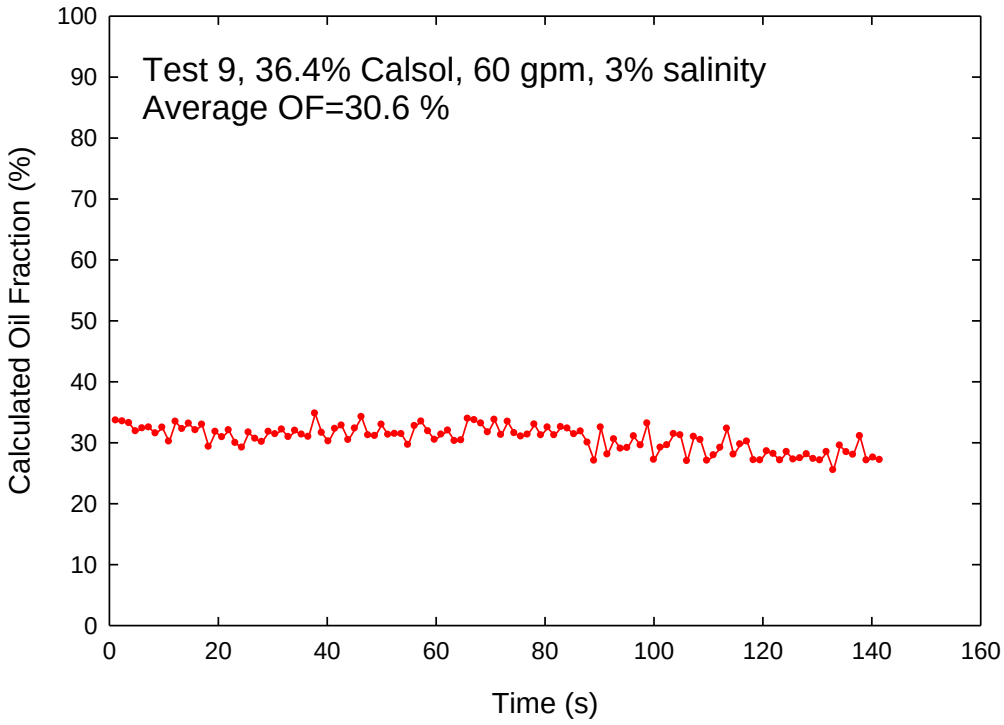

Figure 34: Test 9 (July 13, 2023) measured oil fraction as a function of time.

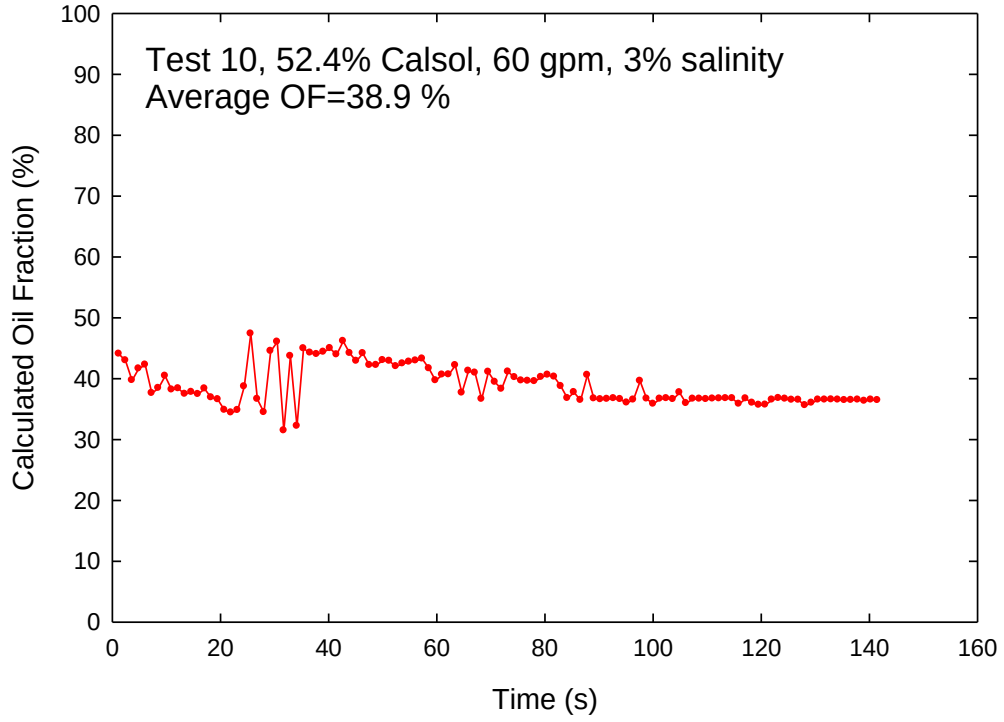

Figure 35: Test 10 (July 13, 2023) measured oil fraction as a function of time.

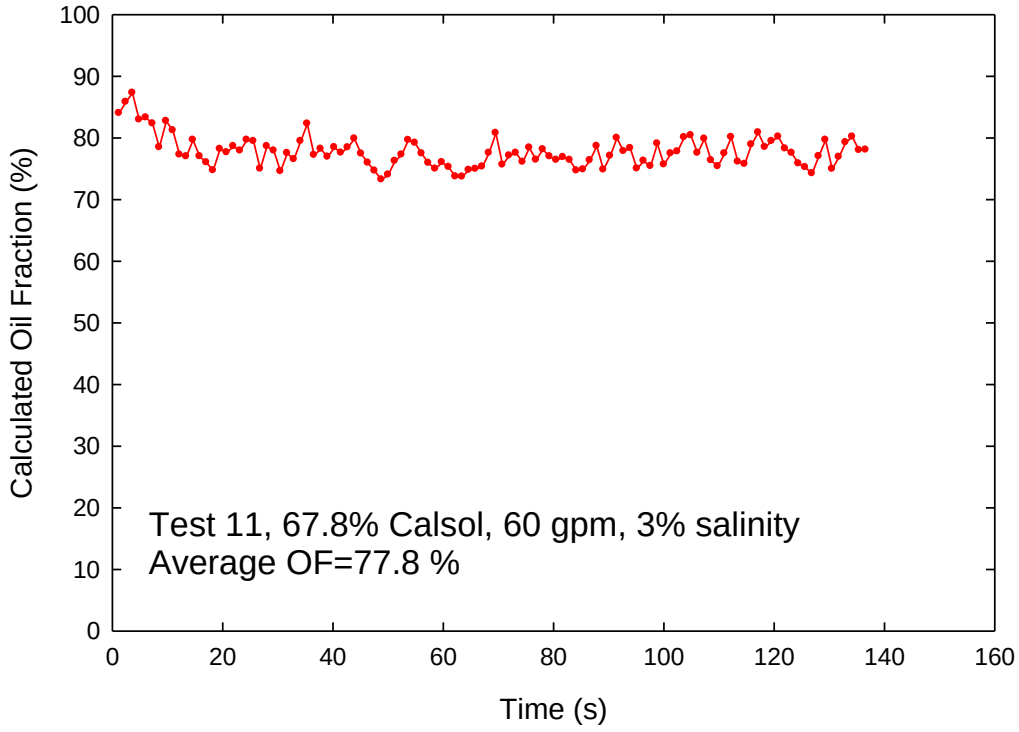

Figure 36: Test 11 (July 13, 2023) measured oil fraction as a function of time.

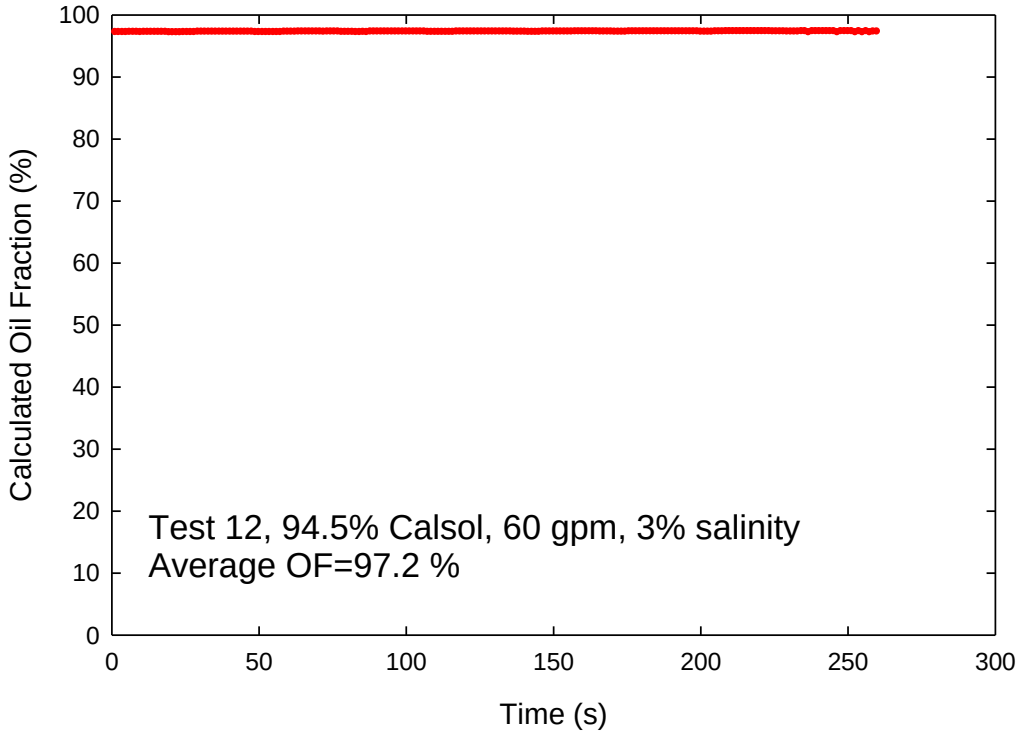

Figure 37: Test 12 (July 13, 2023) measured oil fraction as a function of time.

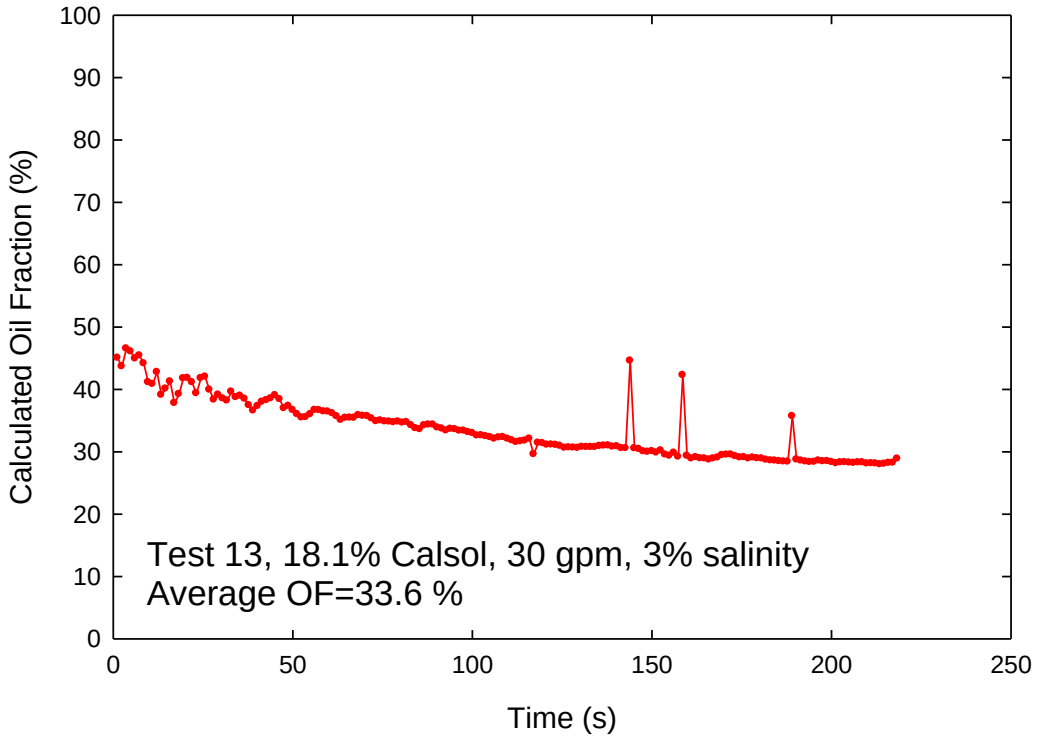

Figure 38: Test 13 (July 13, 2023) measured oil fraction as a function of time.

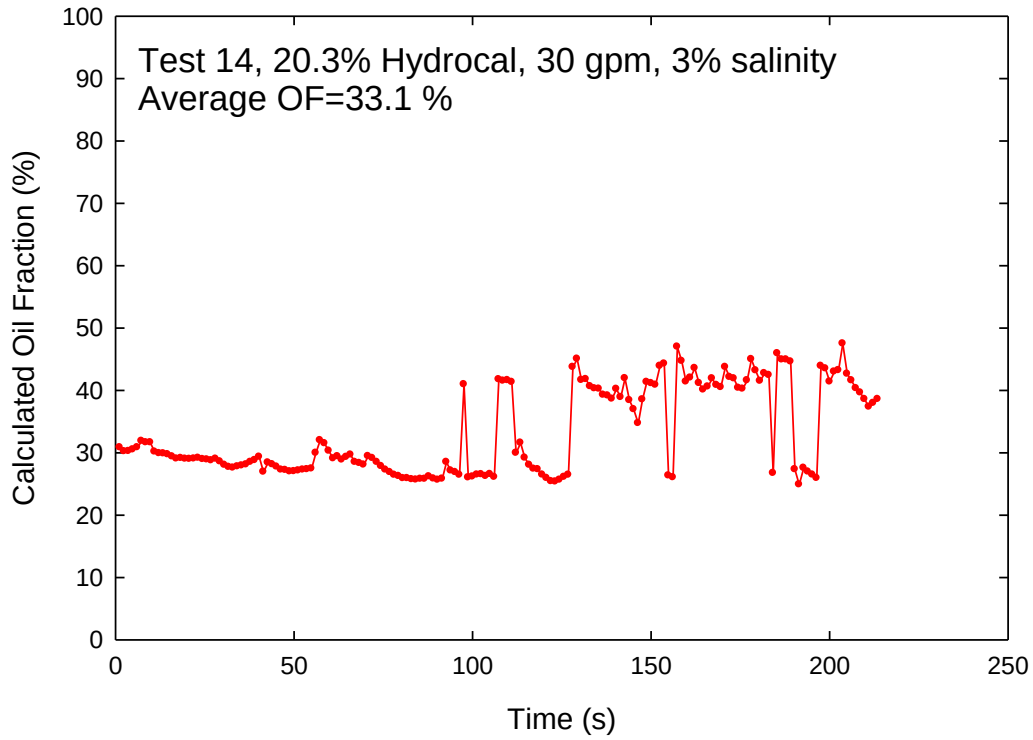

Figure 39: Test 14 (July 14, 2023) measured oil fraction as a function of time.

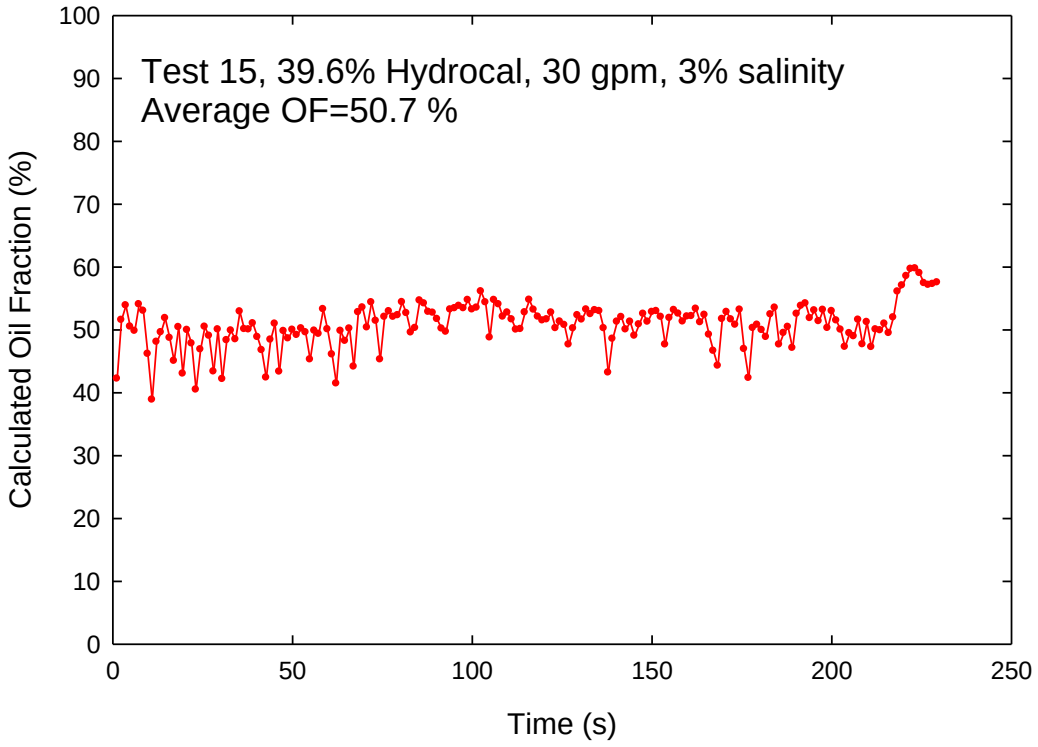

Figure 40: Test 15 (July 14, 2023) measured oil fraction as a function of time.

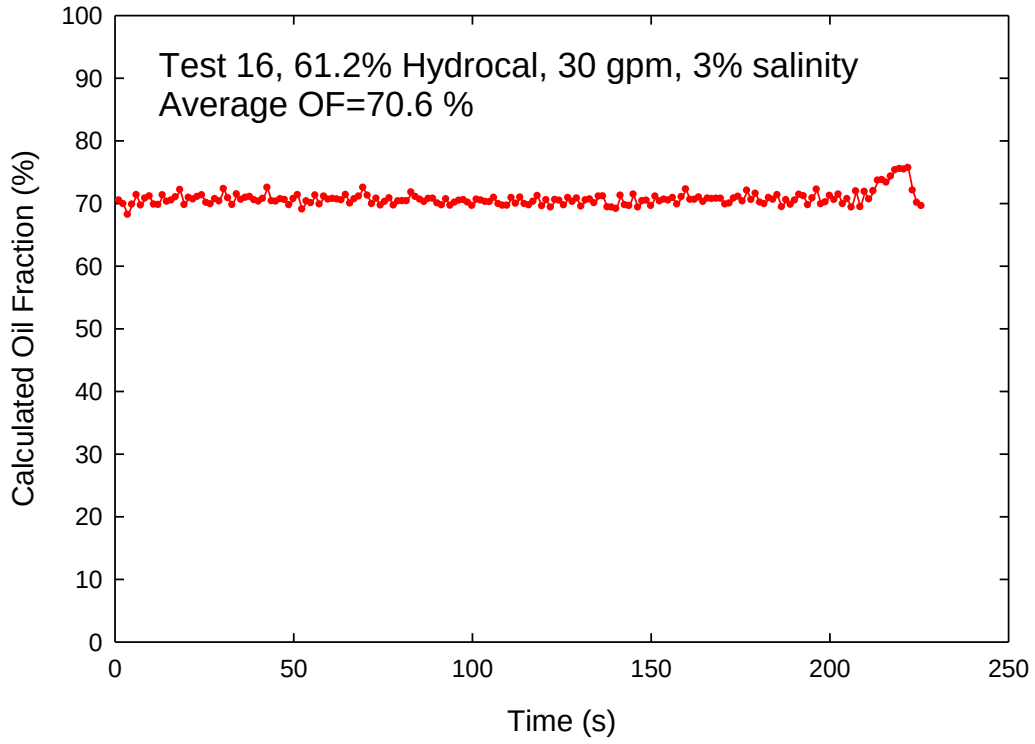

Figure 41: Test 16 (July 14, 2023) measured oil fraction as a function of time.

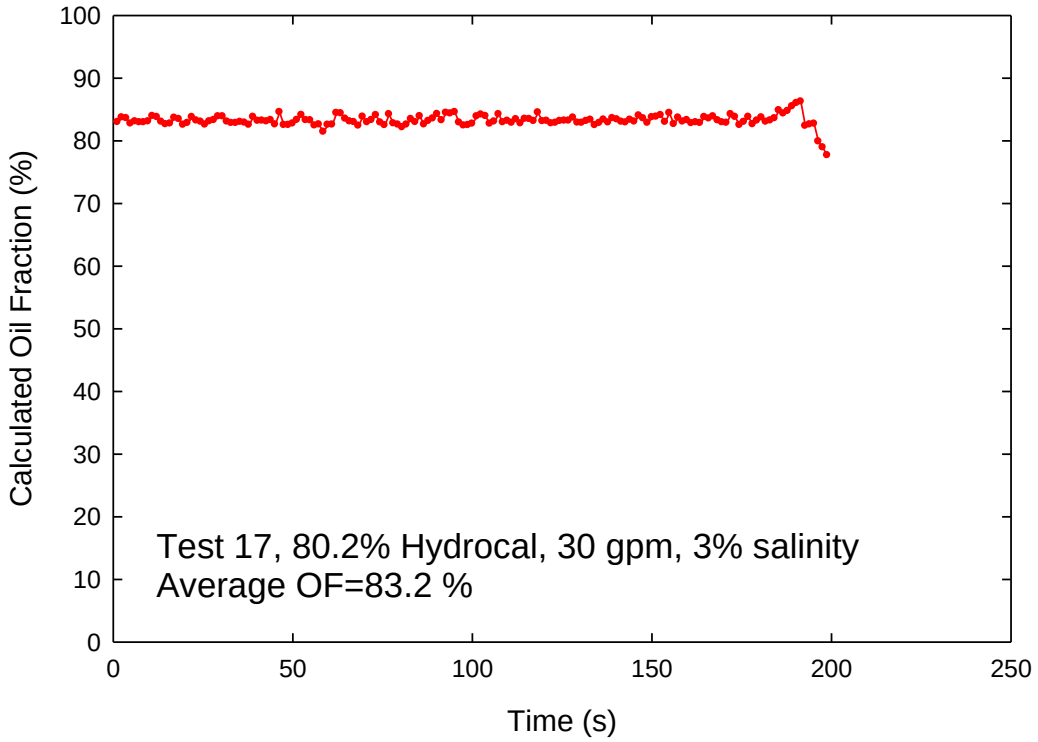

Figure 42: Test 17 (July 14, 2023) measured oil fraction as a function of time.

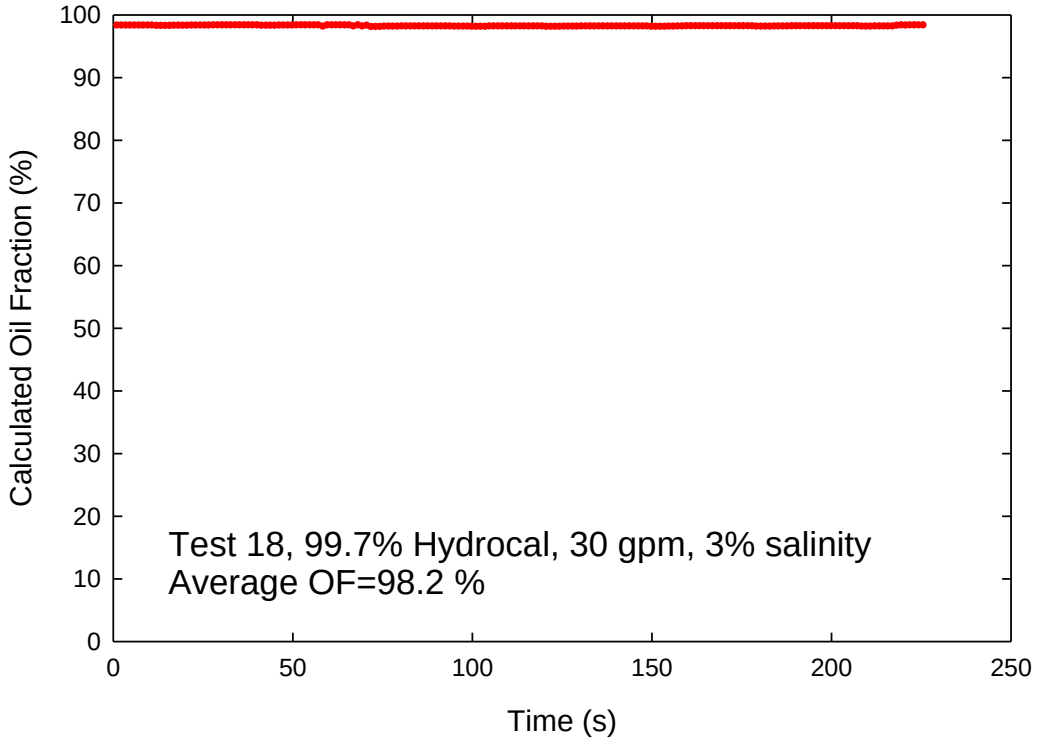

Figure 43: Test 18 (July 14, 2023) measured oil fraction as a function of time.

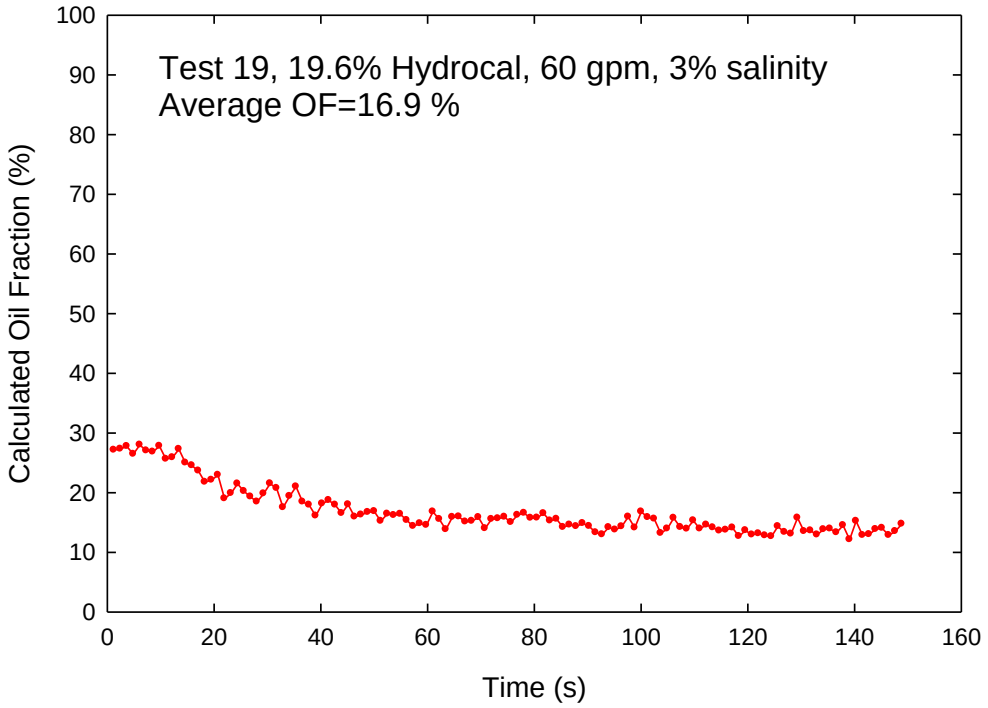

Figure 44: Test 19 (July 14, 2023) measured oil fraction as a function of time.

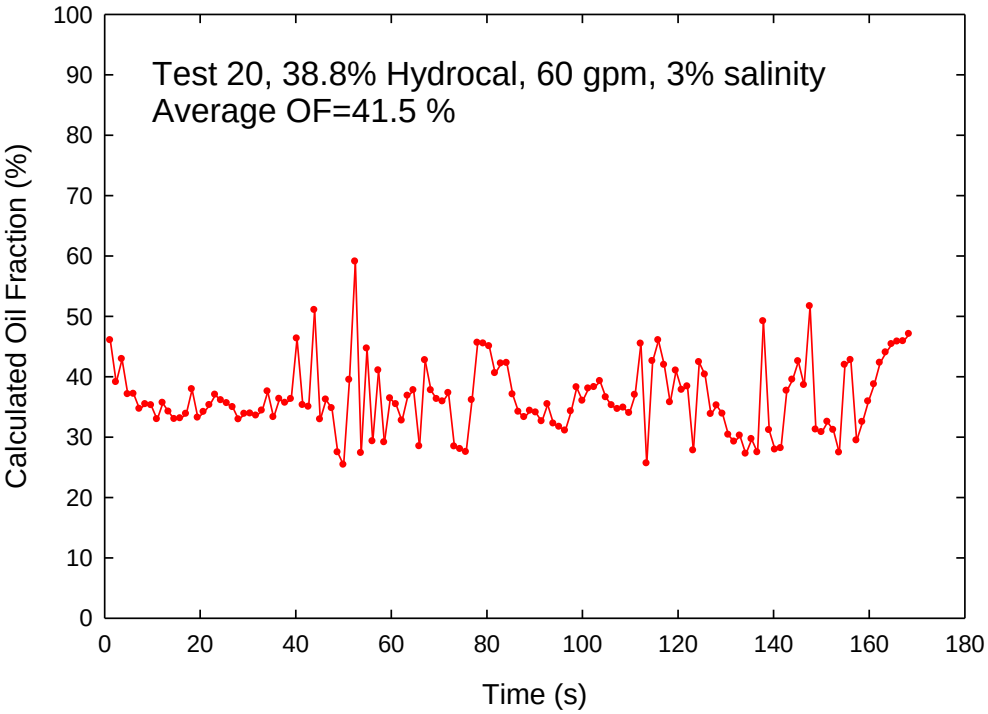

Figure 45: Test 20 (July 17, 2023) measured oil fraction as a function of time.

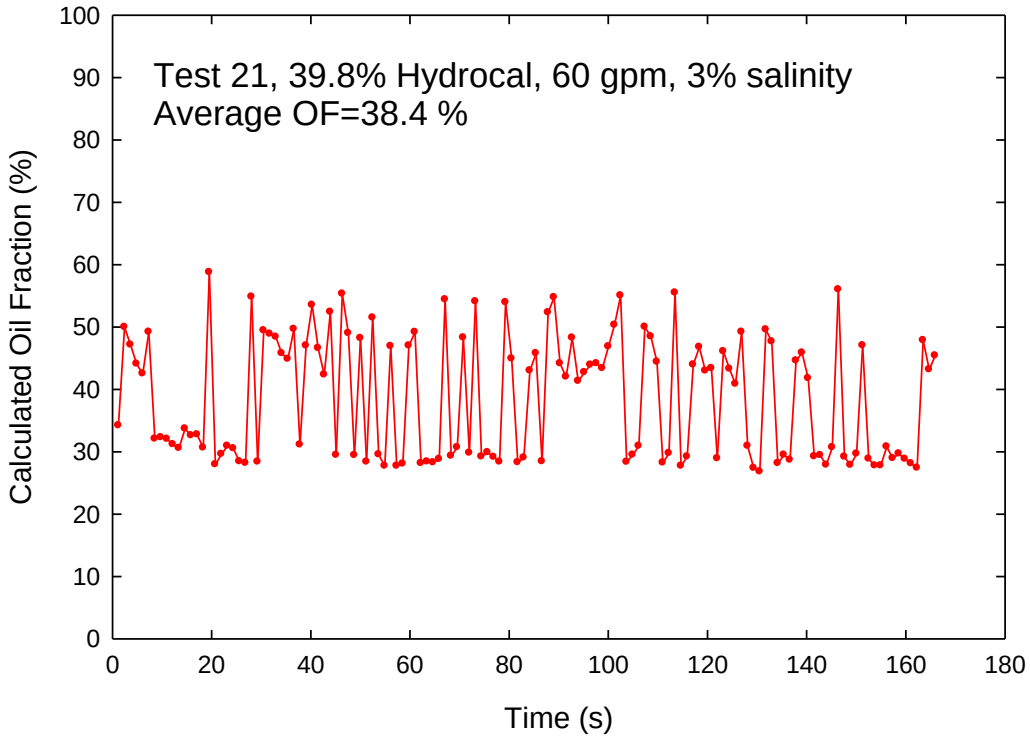

Figure 46: Test 21 (July 17, 2023) measured oil fraction as a function of time.

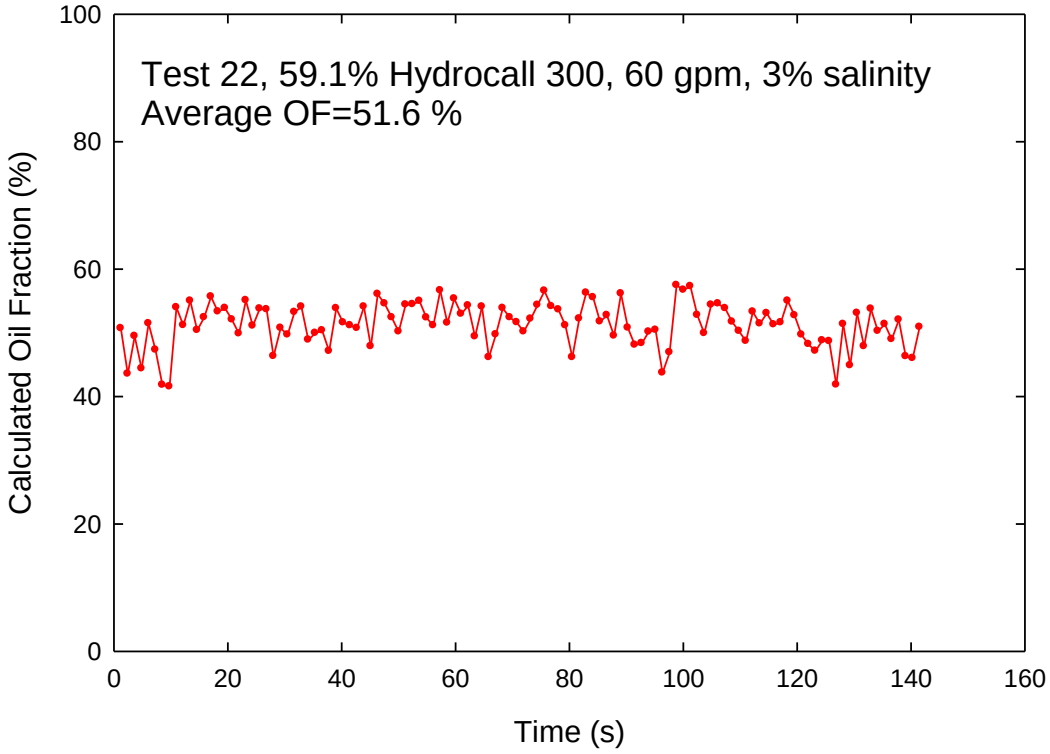

Figure 47: Test 22 (July 17, 2023) measured oil fraction as a function of time.

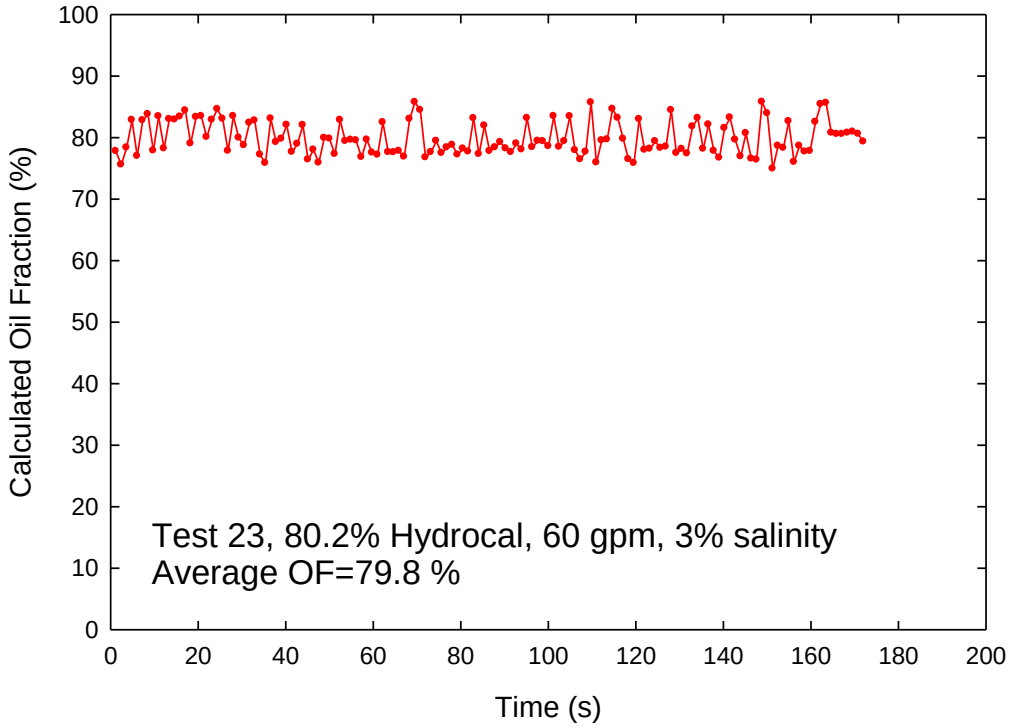

Figure 48: Test 23 (July 18, 2023) measured oil fraction as a function of time.

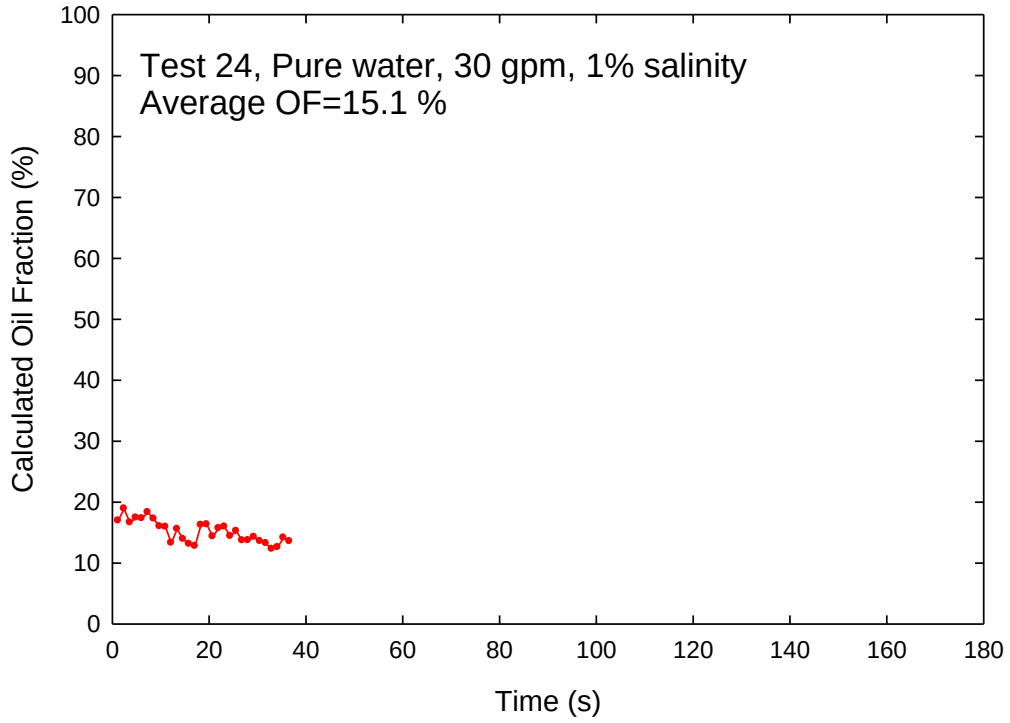

Figure 49: Test 24 (July 18, 2023) measured oil fraction as a function of time.

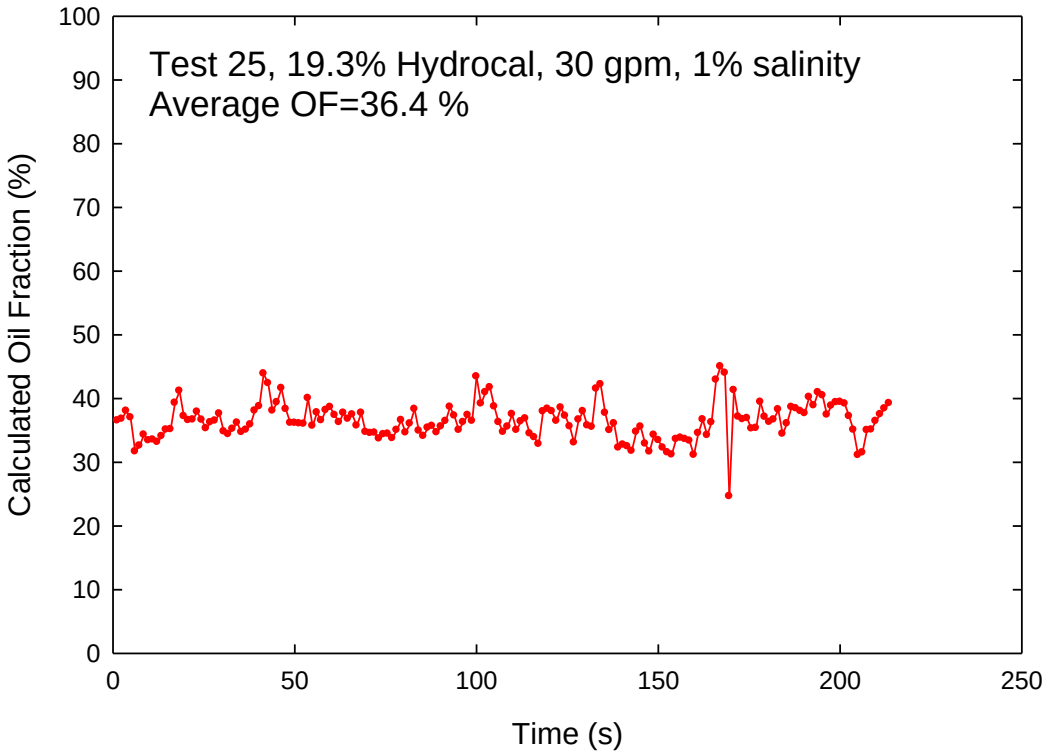

Figure 50: Test 25 (July 18, 2023) measured oil fraction as a function of time.

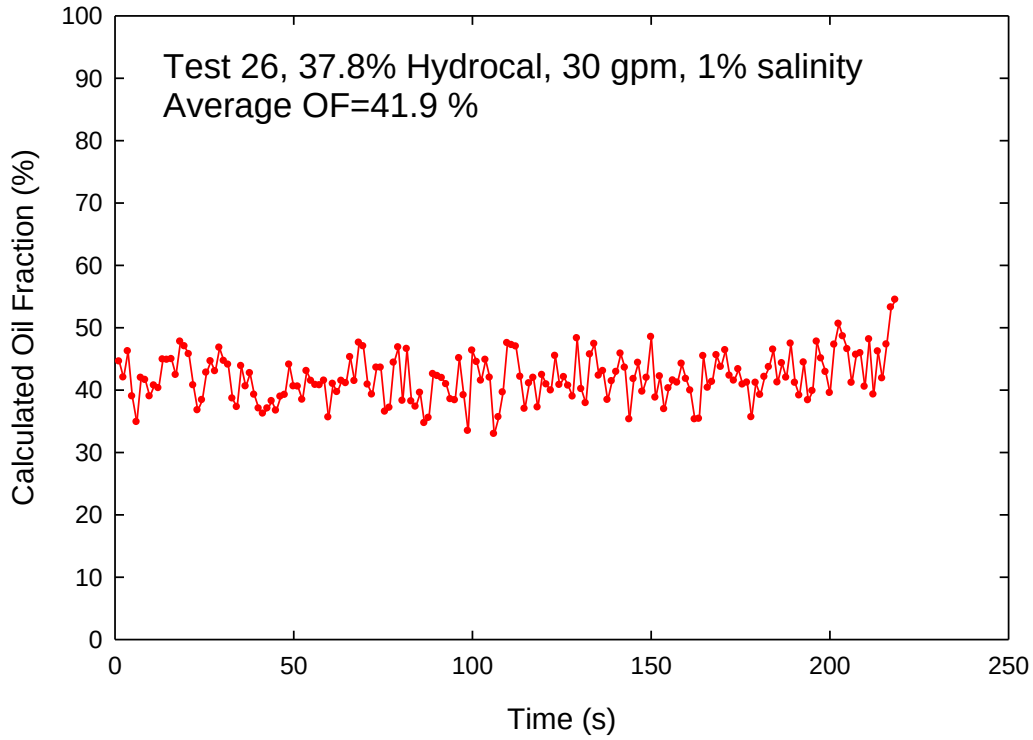

Figure 51: Test 26 (July 18, 2023) measured oil fraction as a function of time.

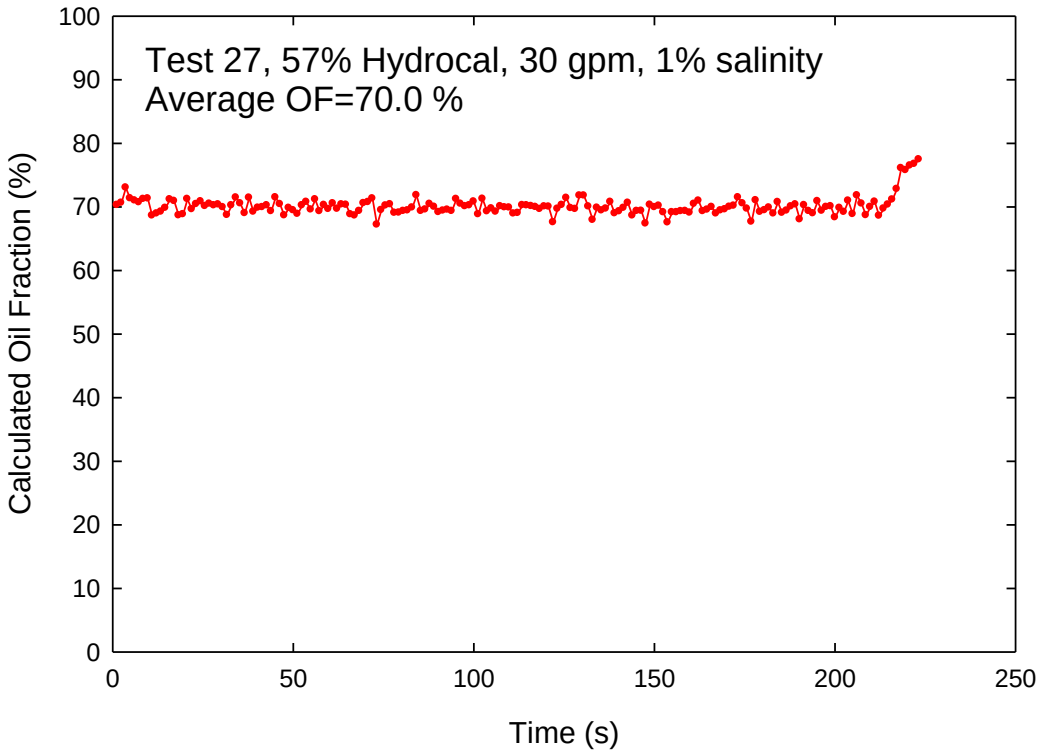

Figure 52: Test 27 (July 19, 2023) measured oil fraction as a function of time.

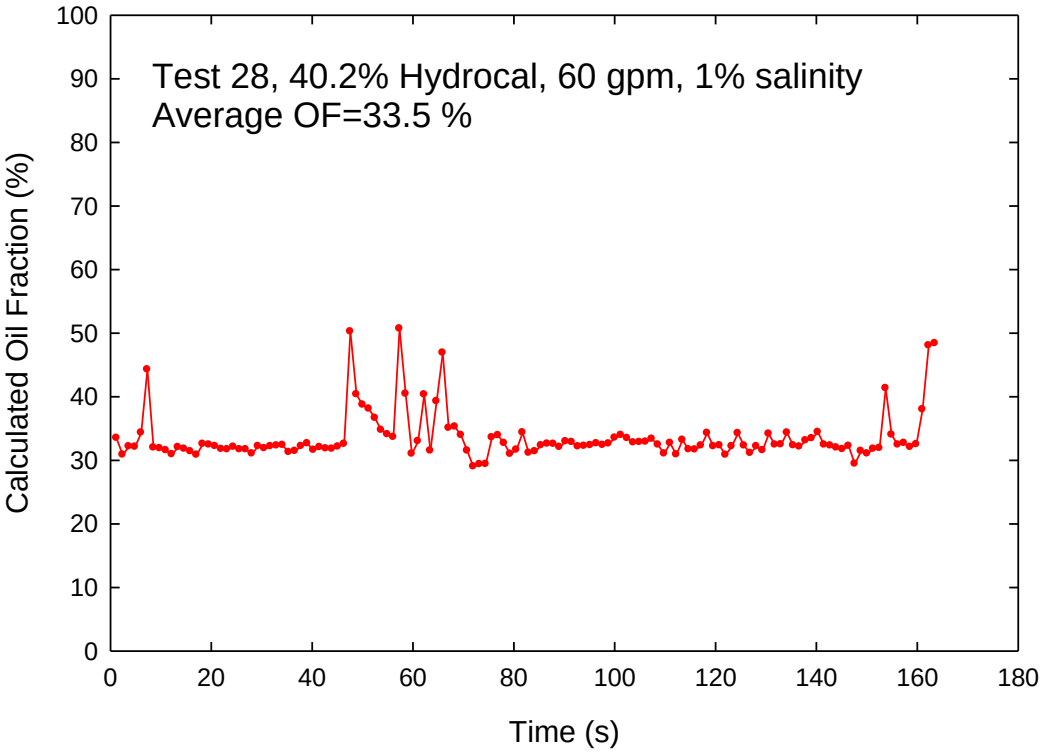

Figure 53: Test 28 (July 19, 2023) measured oil fraction as a function of time.

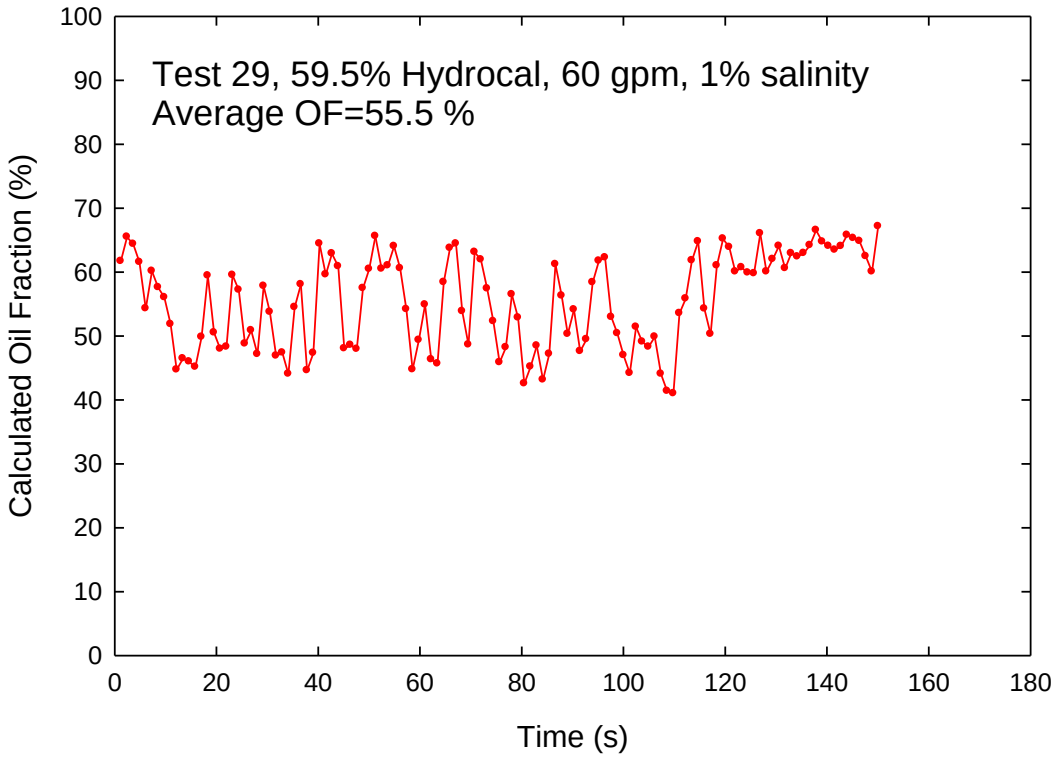

Figure 54: Test 29 (July 19, 2023) measured oil fraction as a function of time.

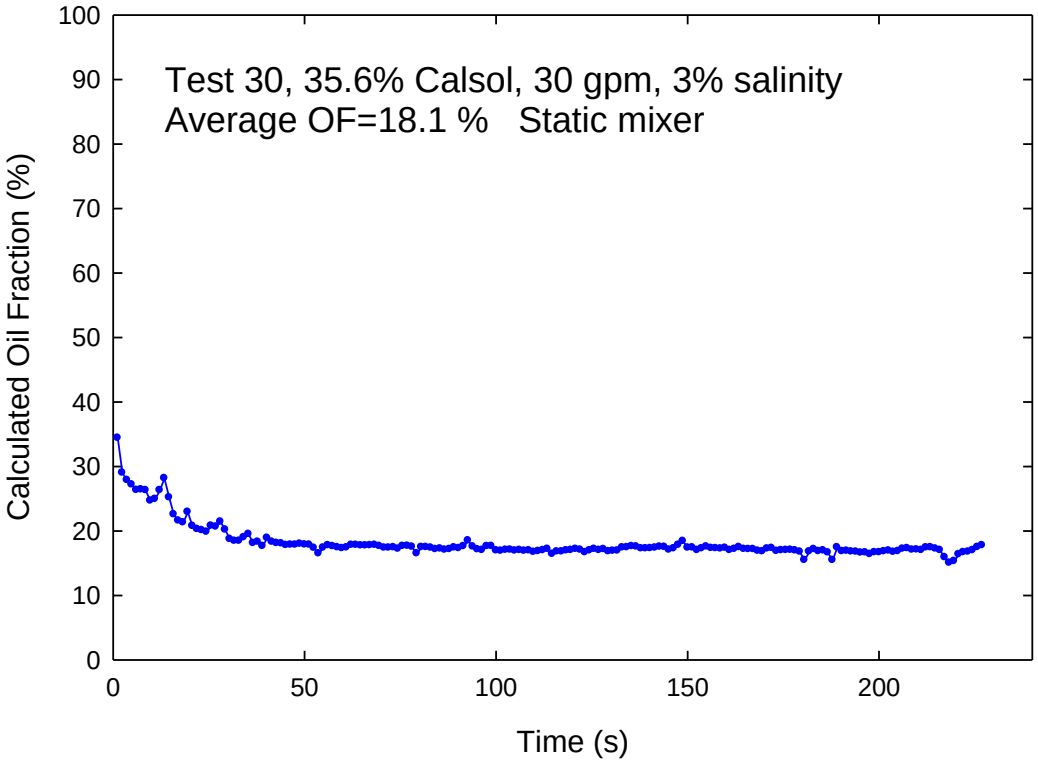

Figure 55: Test 30 (July 19, 2023) measured oil fraction as a function of time.

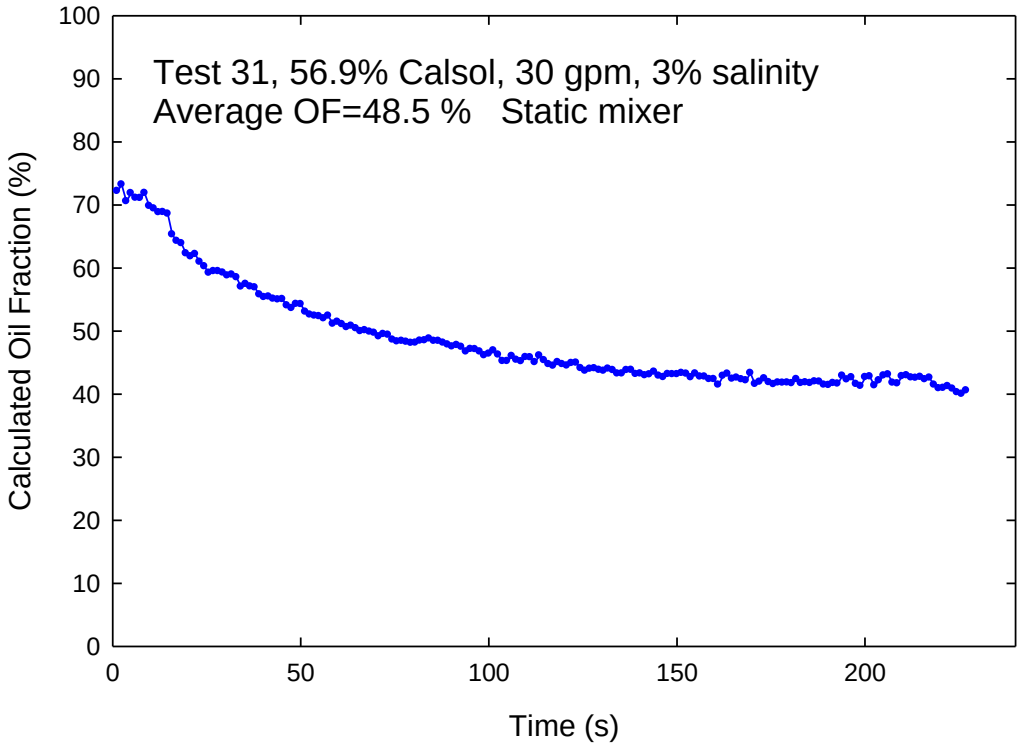

Figure 56: Test 31 (July 19, 2023) measured oil fraction as a function of time.

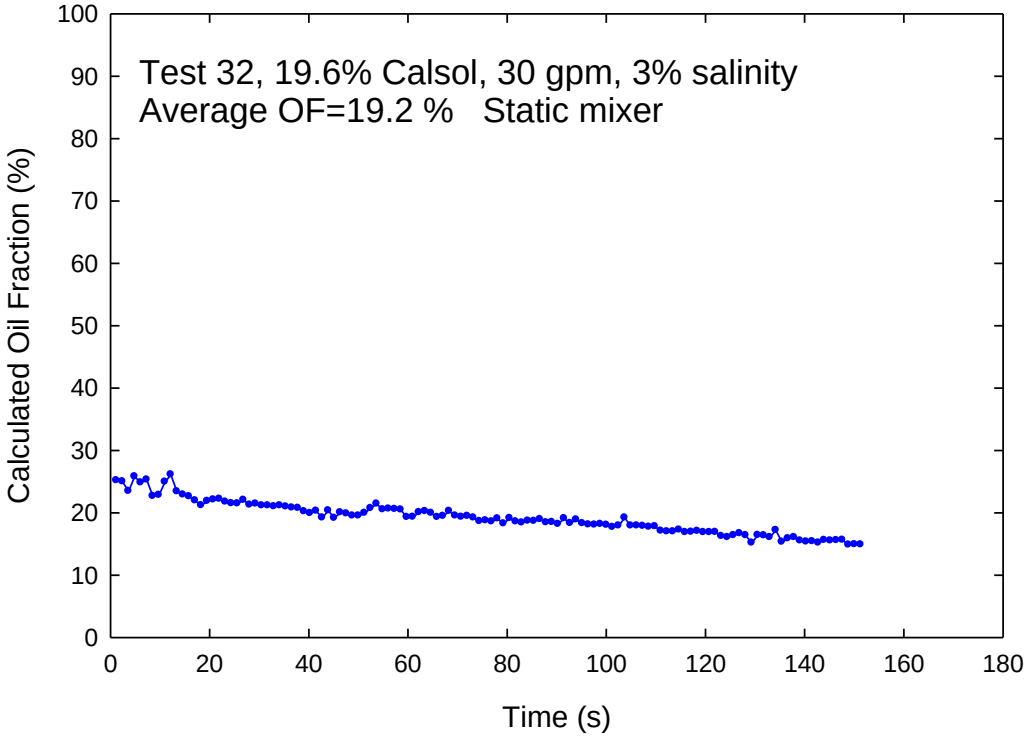

Figure 57: Test 32 (July 19, 2023) measured oil fraction as a function of time.

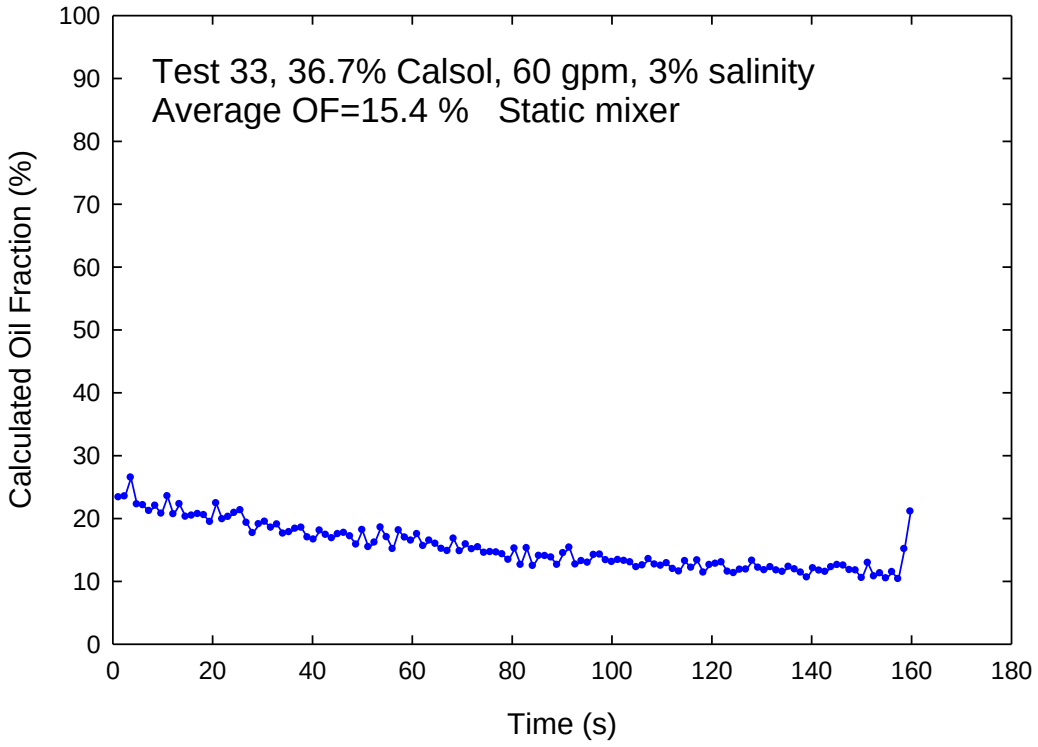

Figure 58: Test 33 (July 19, 2023) measured oil fraction as a function of time.

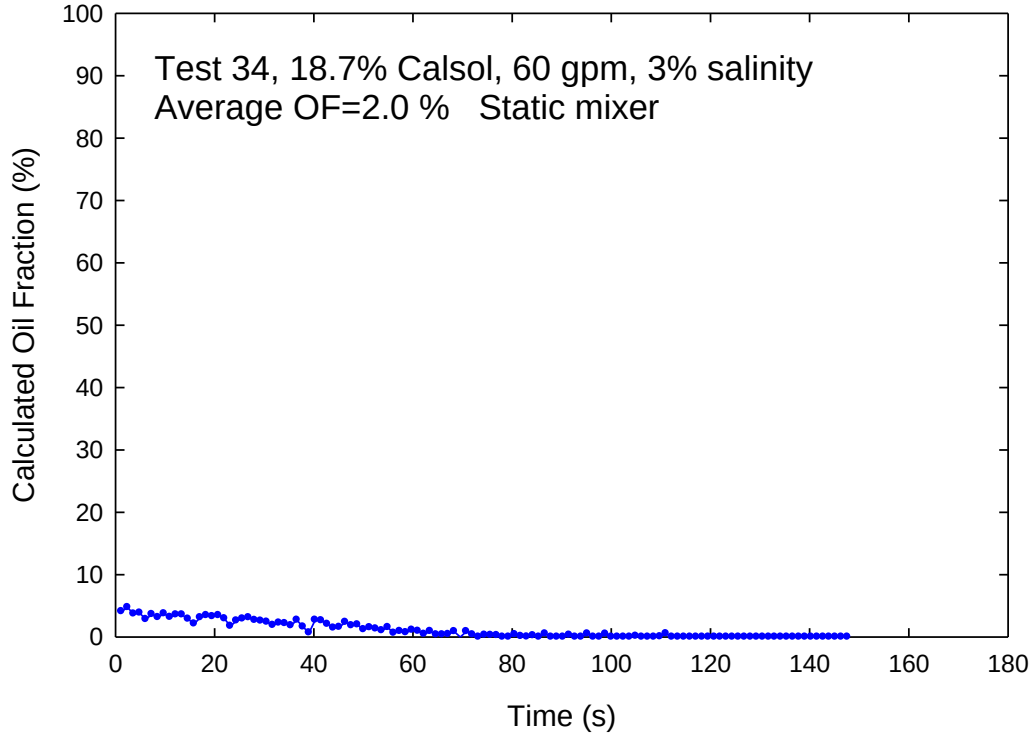

Figure 59: Test 34 (July 19, 2023) measured oil fraction as a function of time.

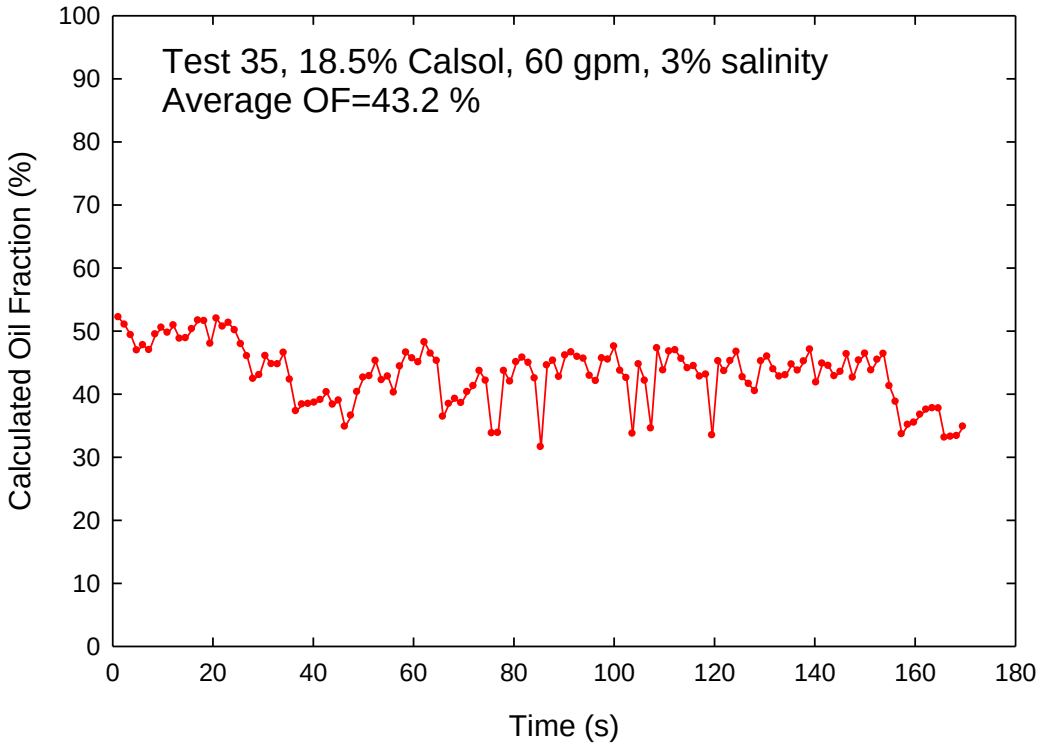

Figure 60: Test 35 (July 20, 2023) measured oil fraction as a function of time.

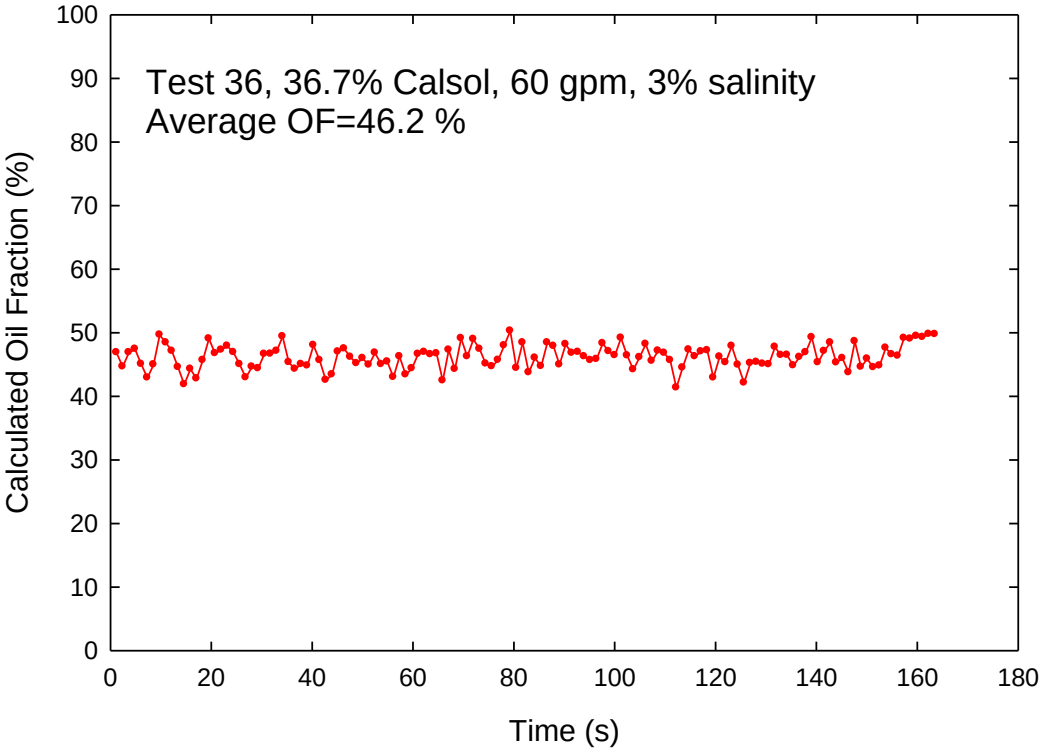

Figure 61: Test 36 (July 20, 2023) measured oil fraction as a function of time.

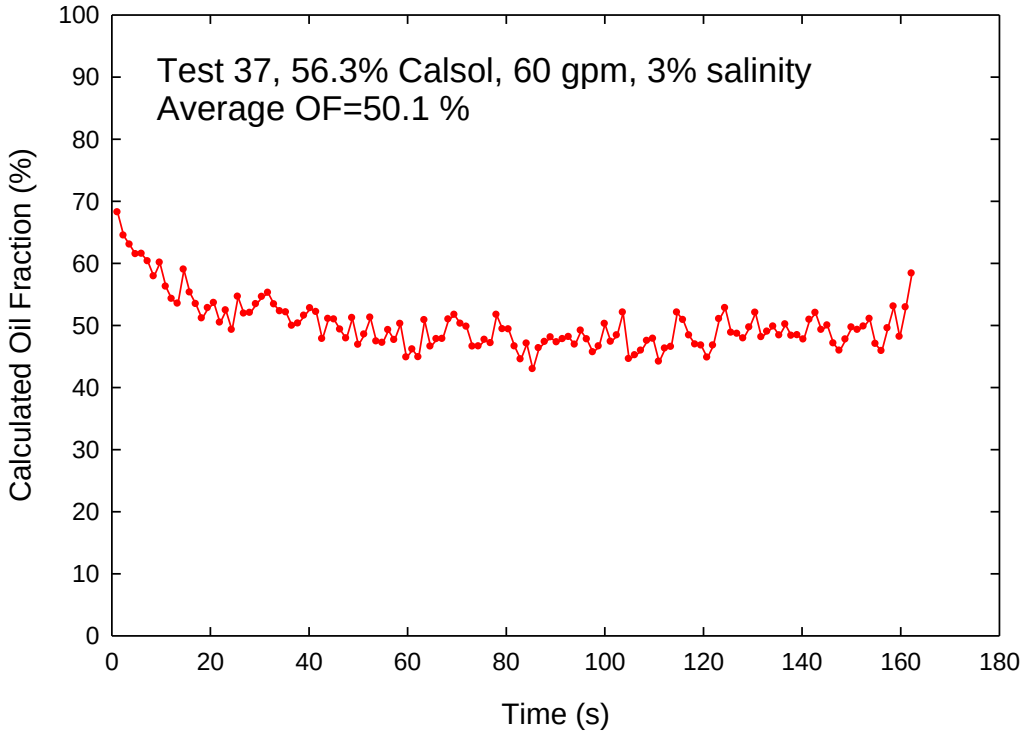

Figure 62: Test 37 (July 20, 2023) measured oil fraction as a function of time.

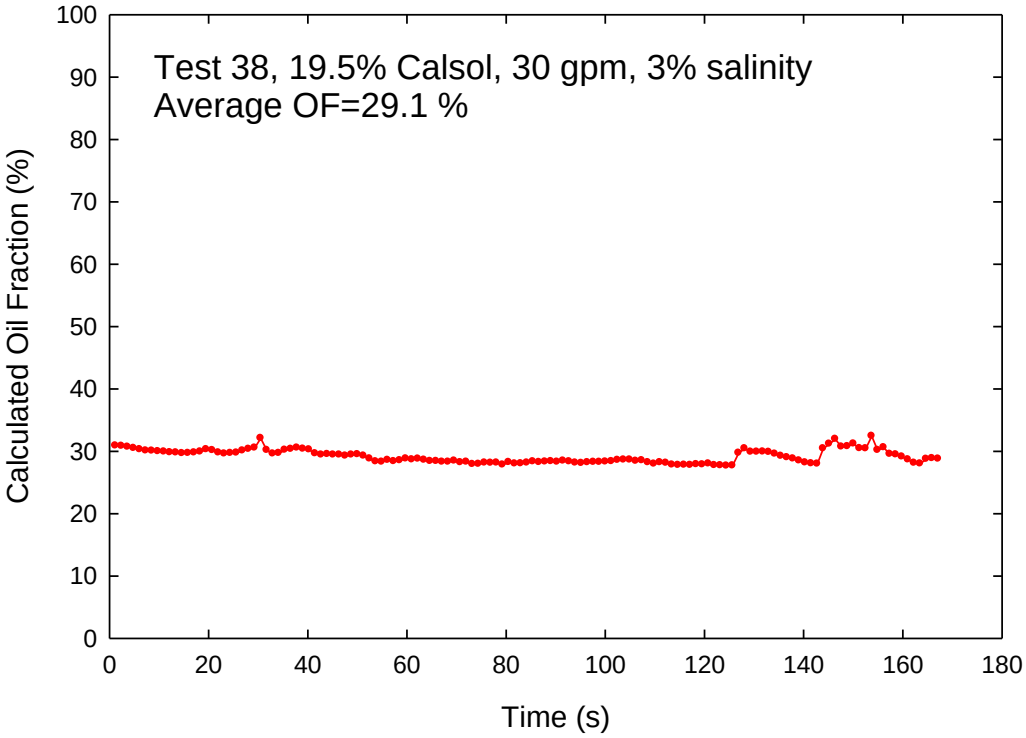

Figure 63: Test 38 (July 20, 2023) measured oil fraction as a function of time.

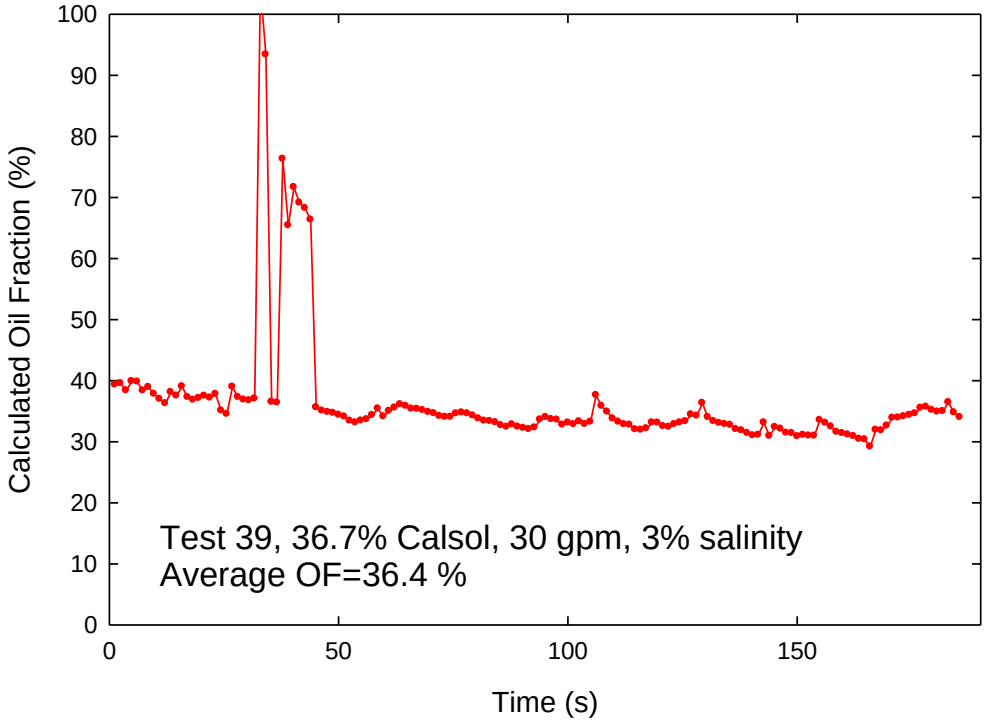

Figure 64: Test 39 (July 20, 2023) measured oil fraction as a function of time.

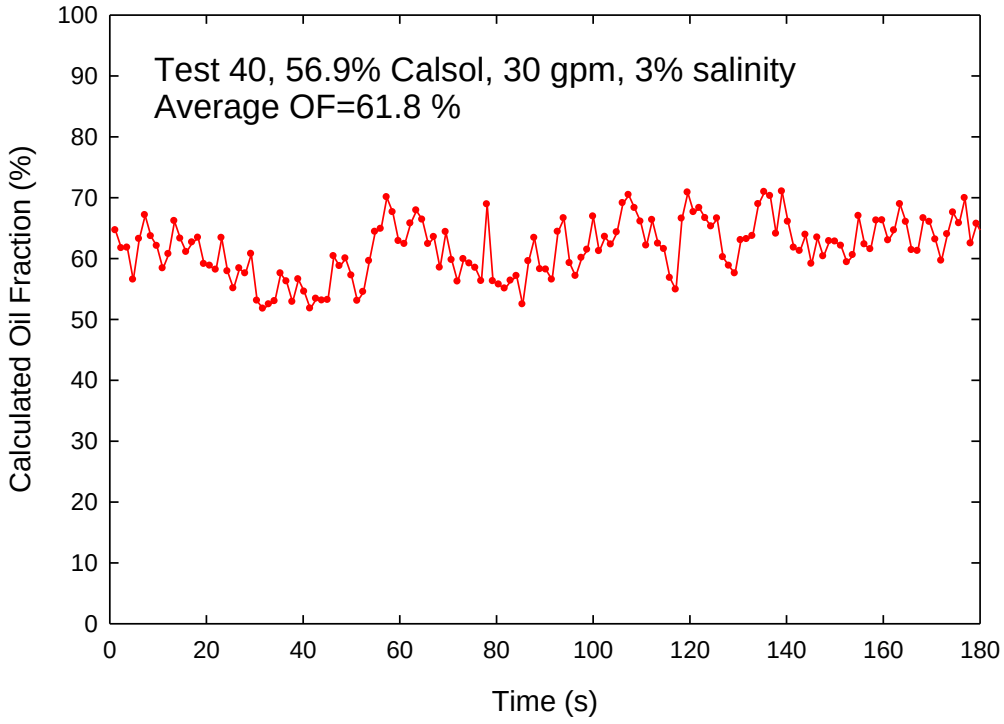

Figure 65: Test 40 (July 20, 2023) measured oil fraction as a function of time.

Ohmsett 2022 campaign

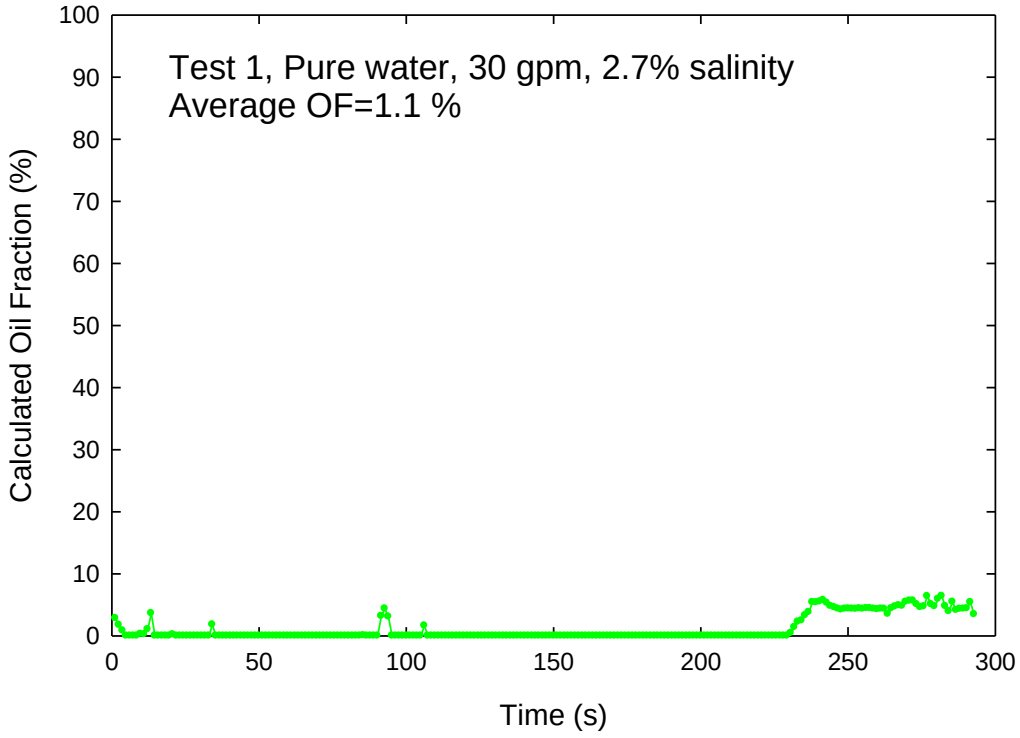

Figure 66: Test 1 (June 28, 2022) measured oil fraction as a function of time.

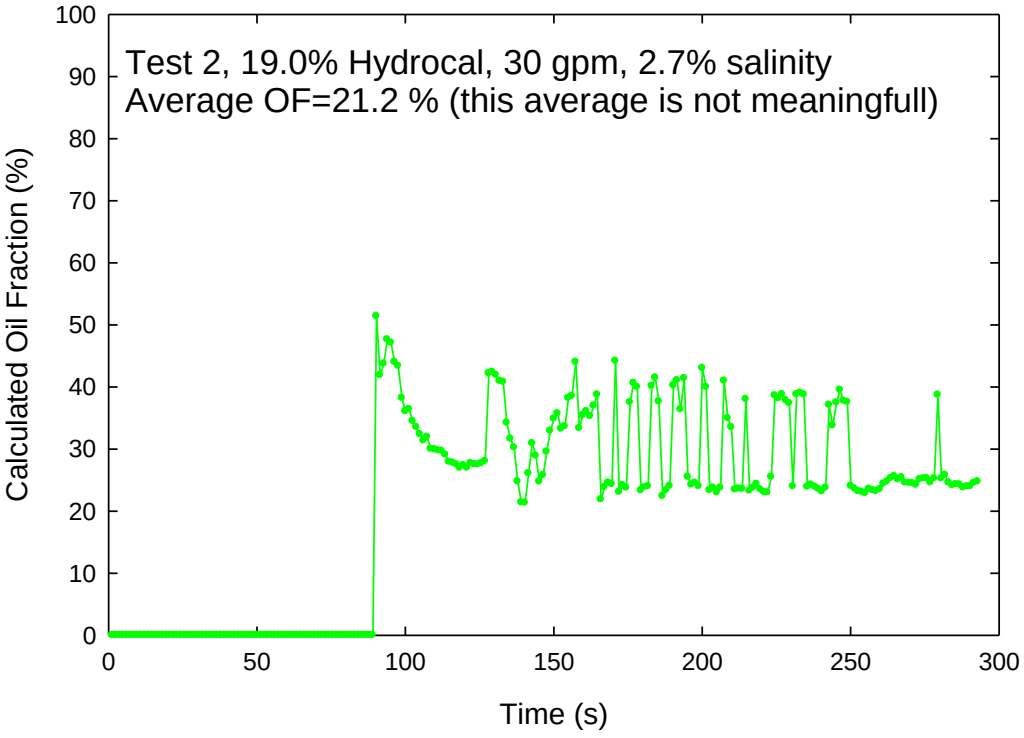

Figure 67: Test 2 (June 28, 2022) measured oil fraction as a function of time.

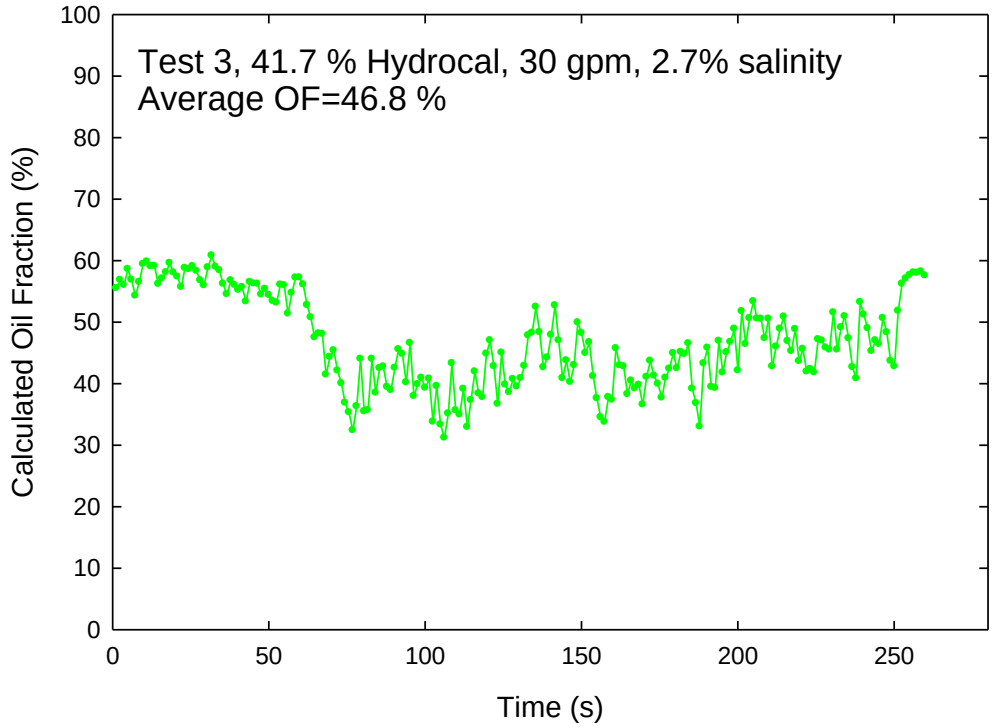

Figure 68: Test 3 (June 28, 2022) measured oil fraction as a function of time.

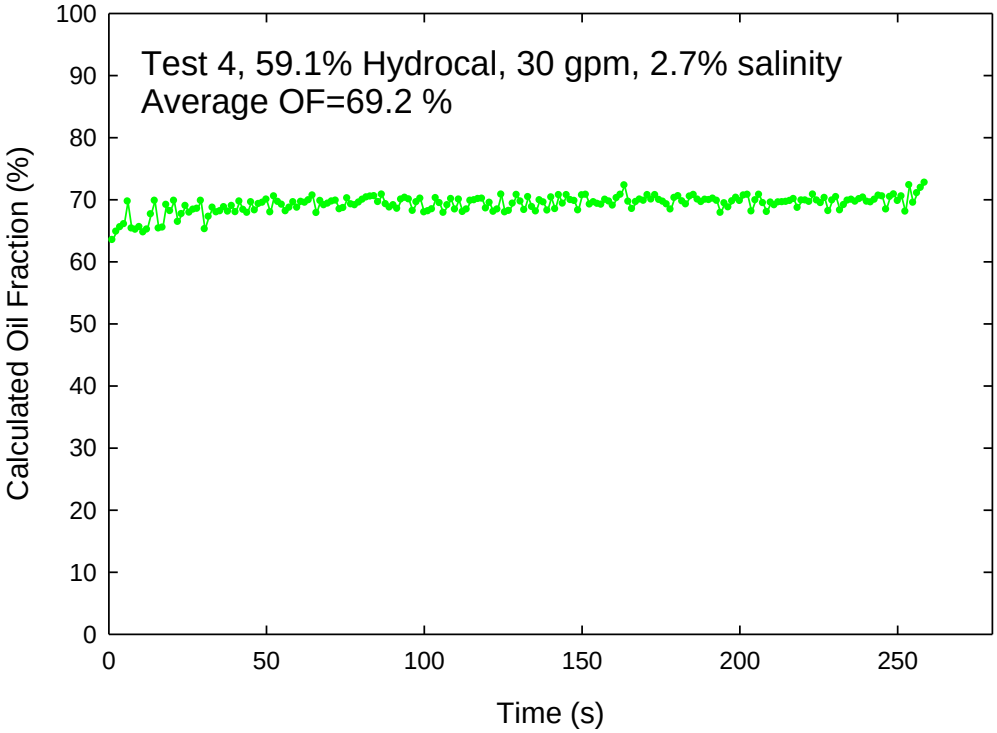

Figure 69: Test 4 (June 28, 2022) measured oil fraction as a function of time.

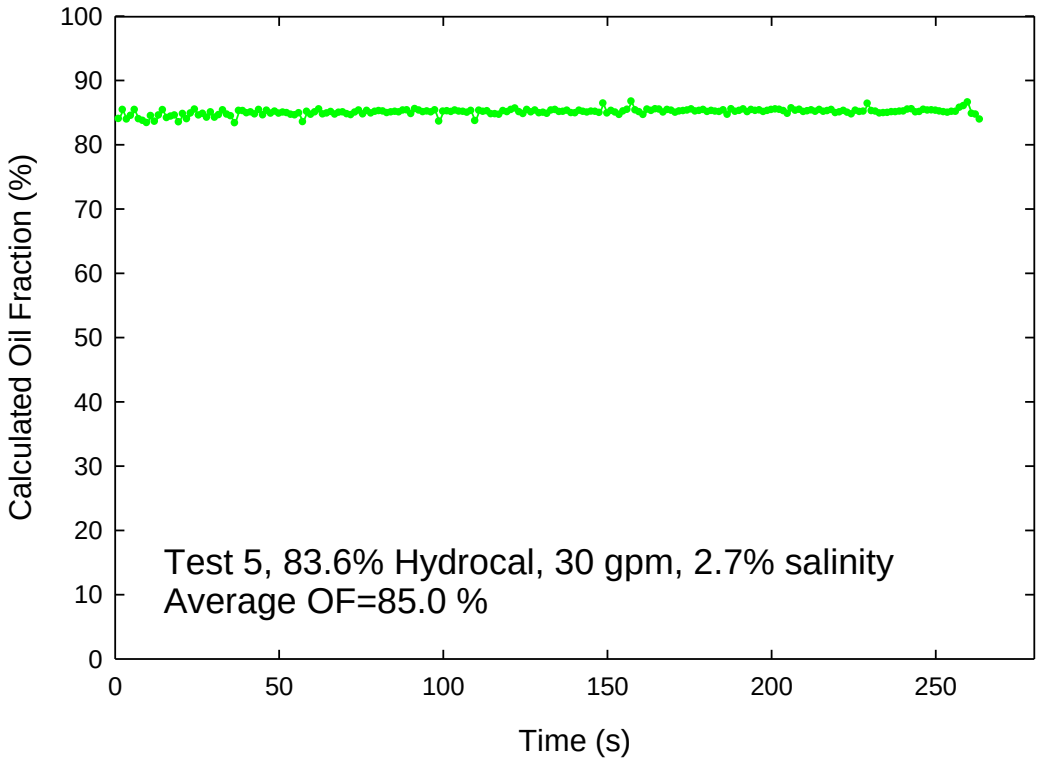

Figure 70: Test 5 (June 28, 2022) measured oil fraction as a function of time.

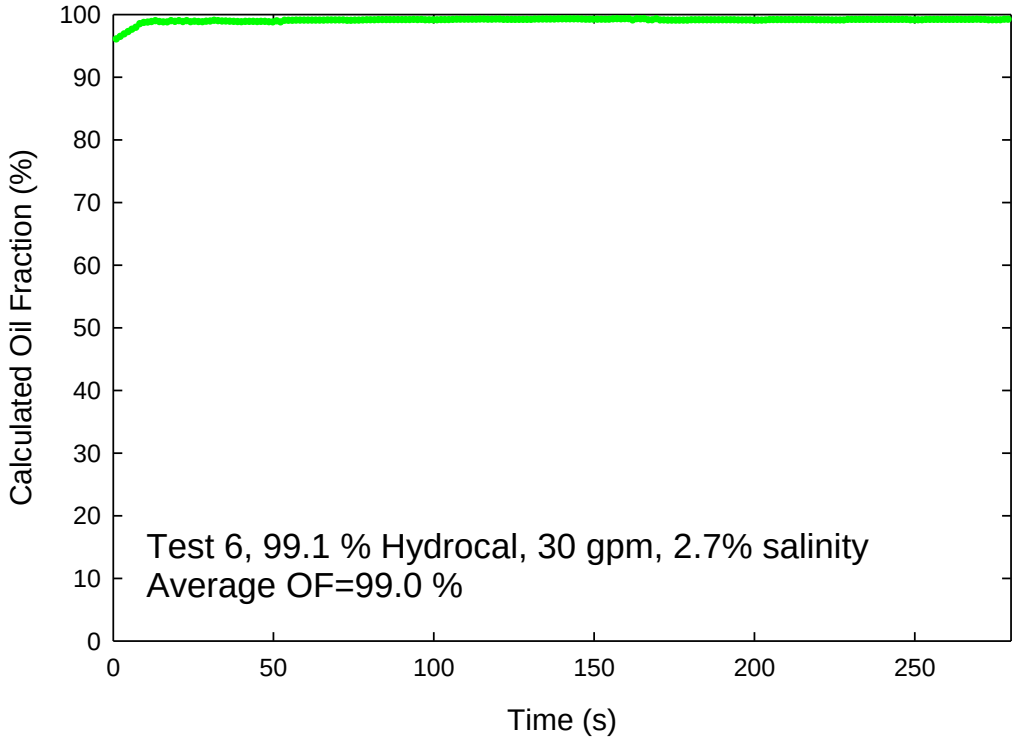

Figure 71: Test 6 (June 28, 2022) measured oil fraction as a function of time.

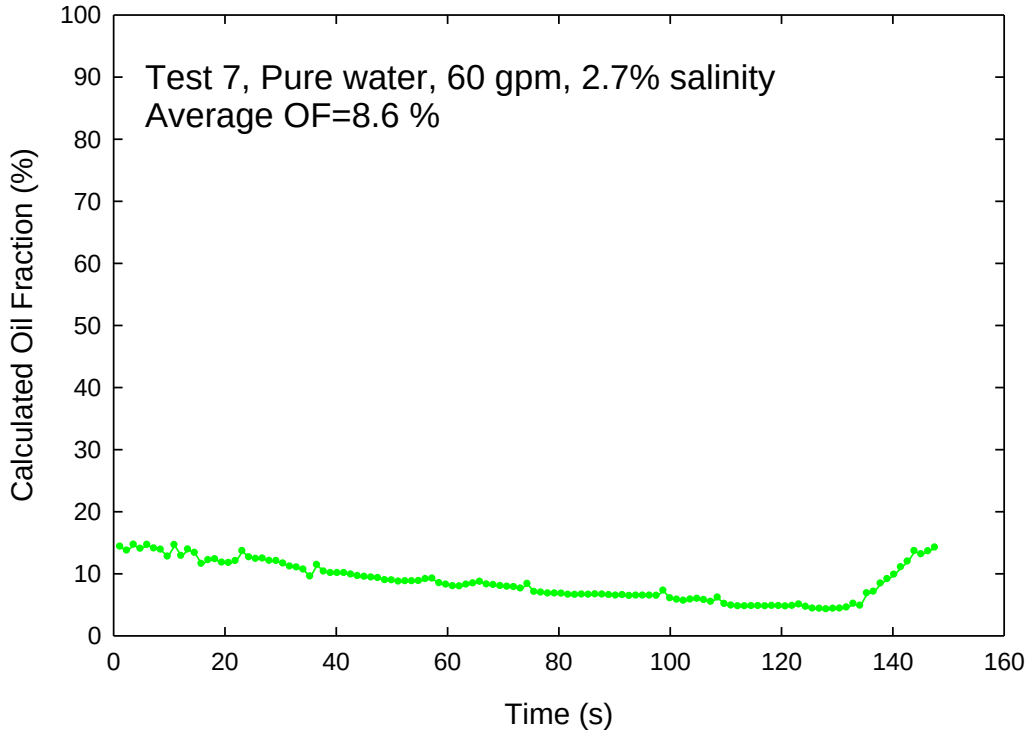

Figure 72: Test 7 (June 28, 2022) measured oil fraction as a function of time.

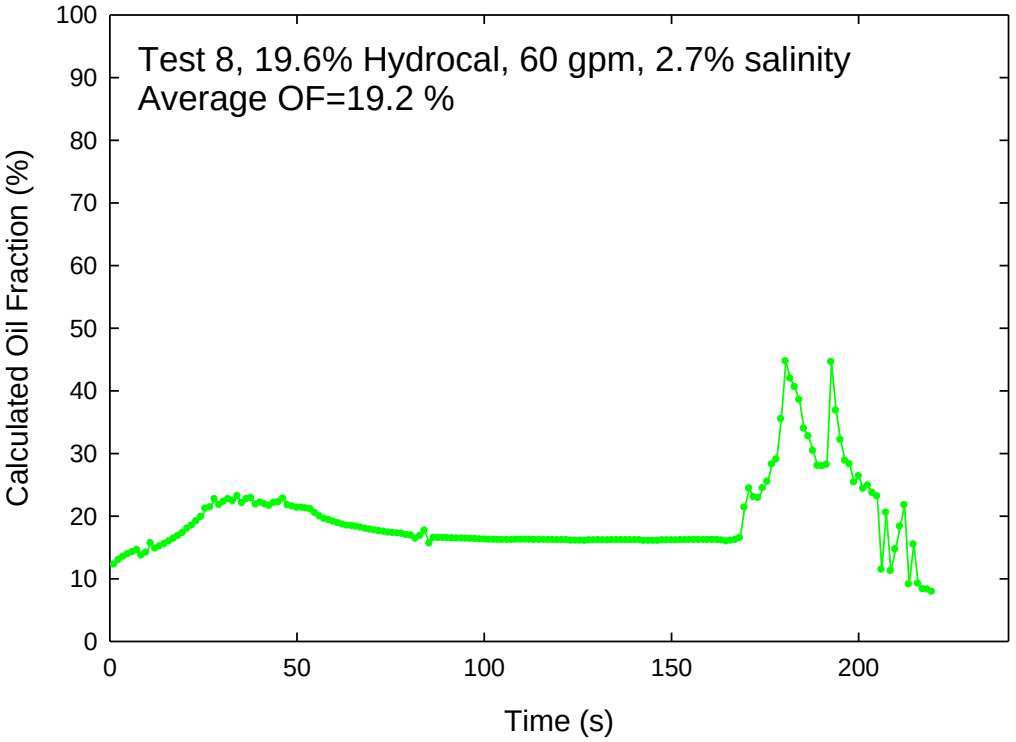

Figure 73: Test 8 (June 28, 2022) measured oil fraction as a function of time.

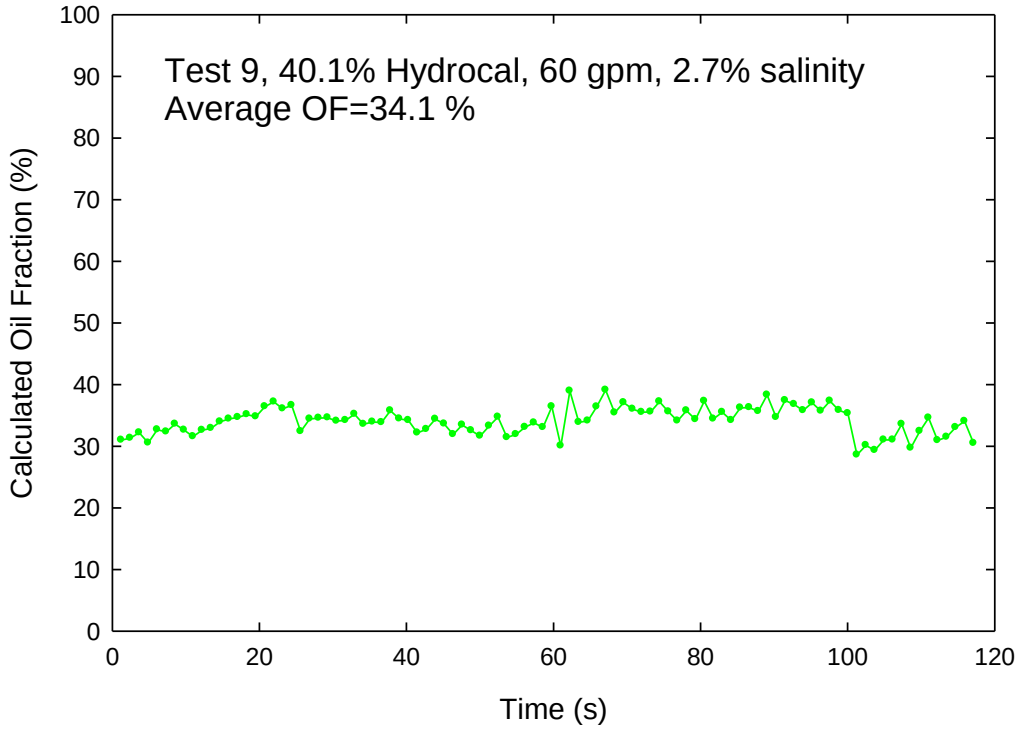

Figure 74: Test 9 (June 28, 2022) measured oil fraction as a function of time.

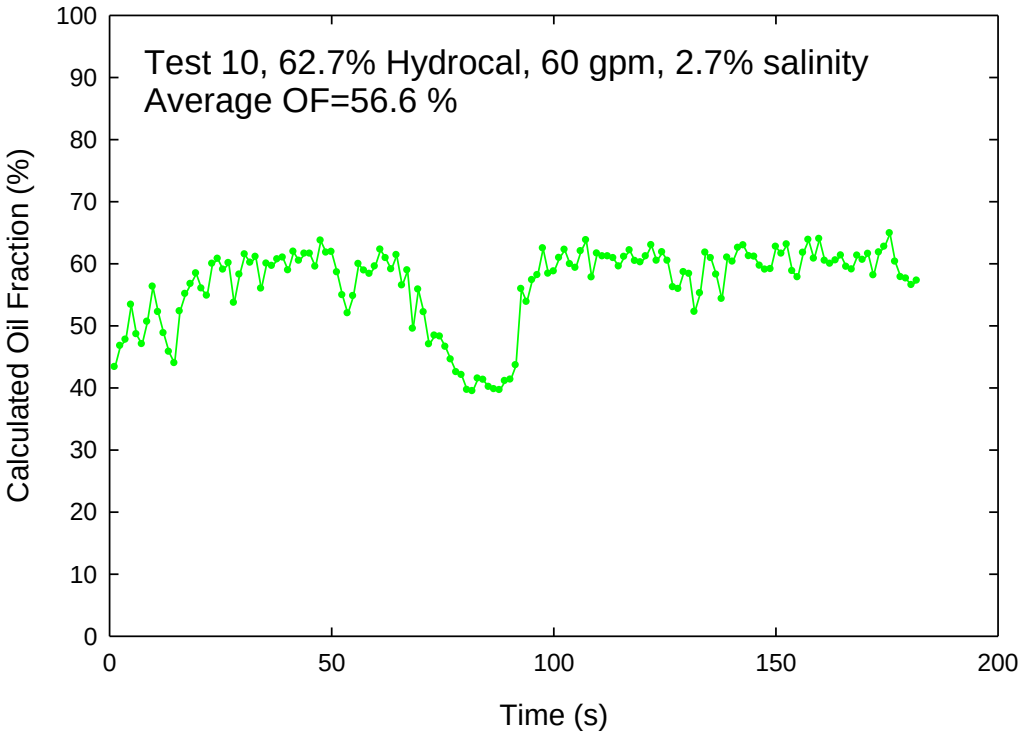

Figure 75: Test 10 (June 28, 2022) measured oil fraction as a function of time.

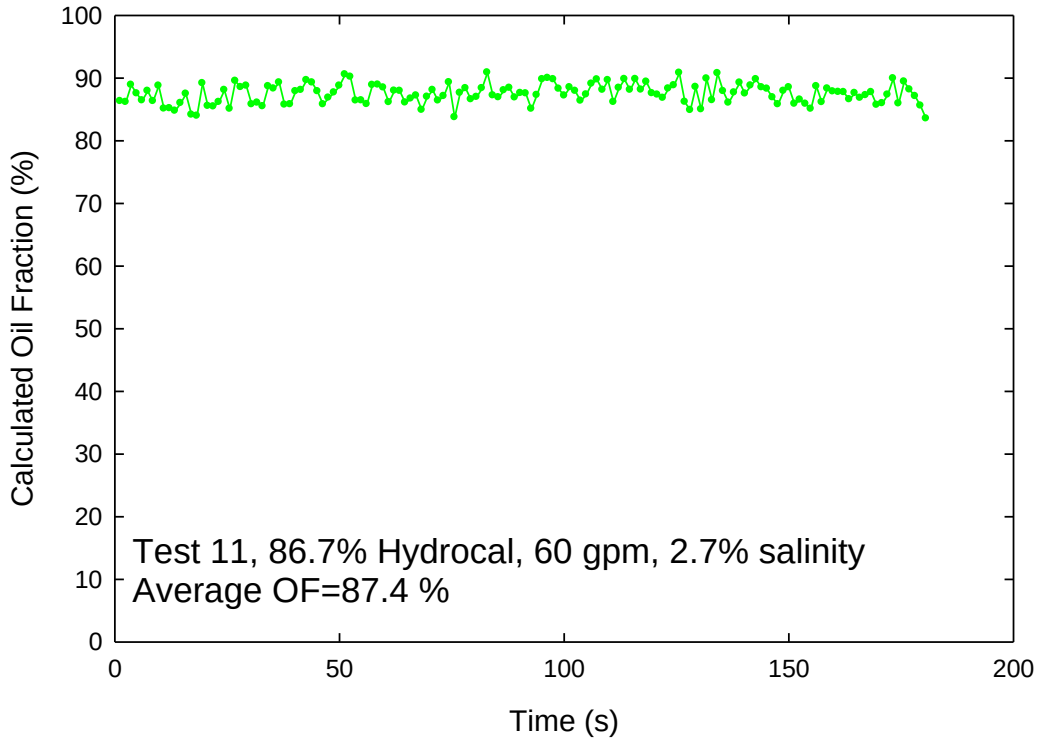

Figure 76: Test 11 (June 29, 2022) measured oil fraction as a function of time.

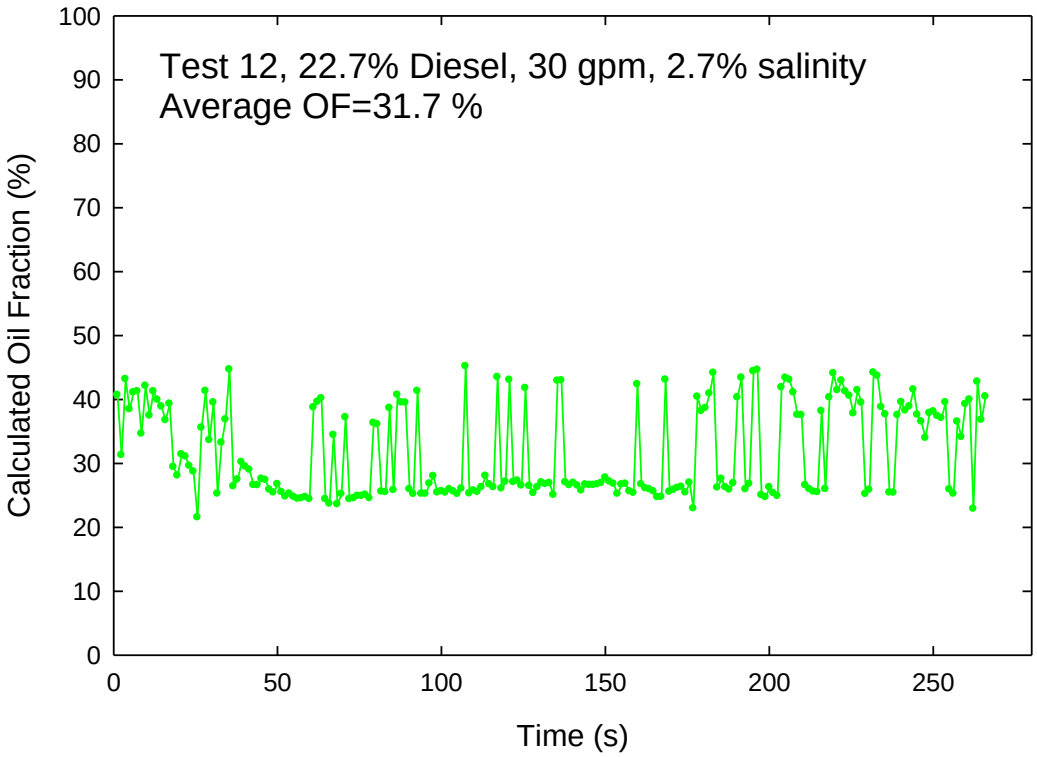

Figure 77: Test 12 (June 29, 2022) measured oil fraction as a function of time.

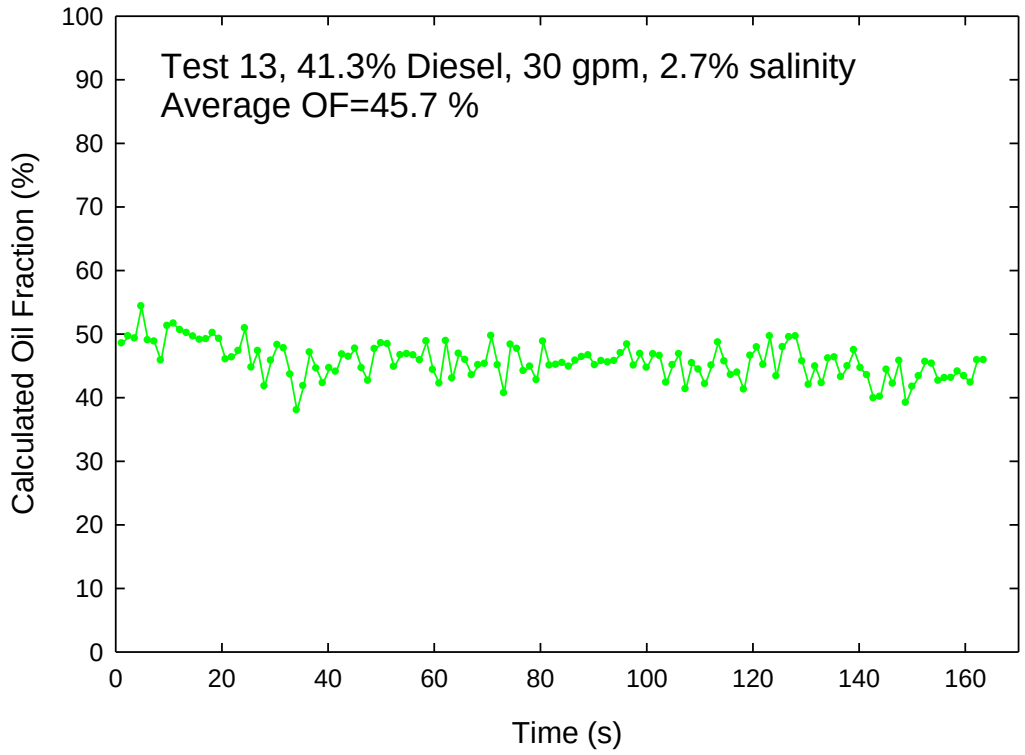

Figure 78: Test 13 (June 29, 2022) measured oil fraction as a function of time.

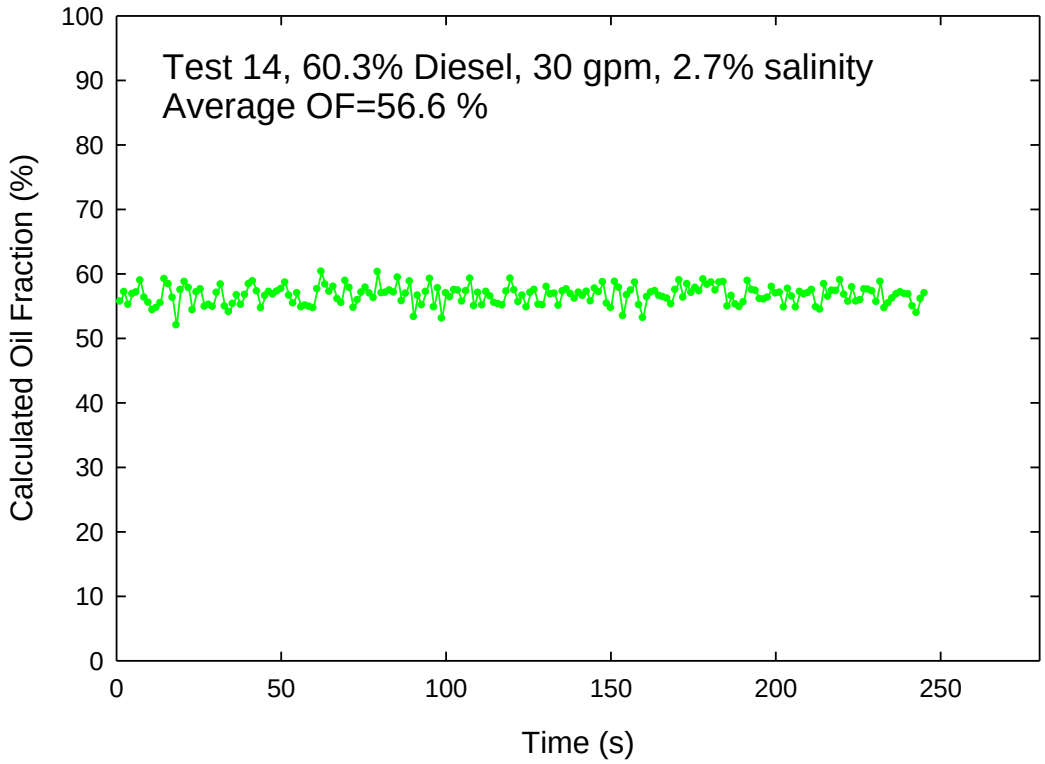

Figure 79: Test 14 (June 29, 2022) measured oil fraction as a function of time.

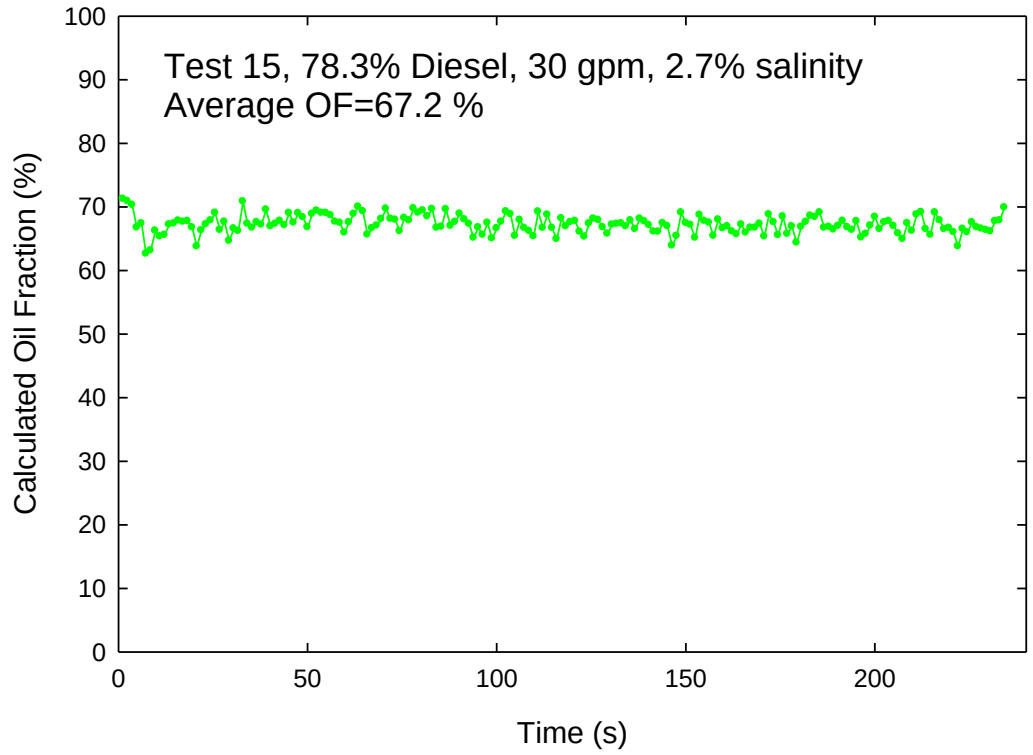

Figure 80: Test 15 (June 29, 2022) measured oil fraction as a function of time.

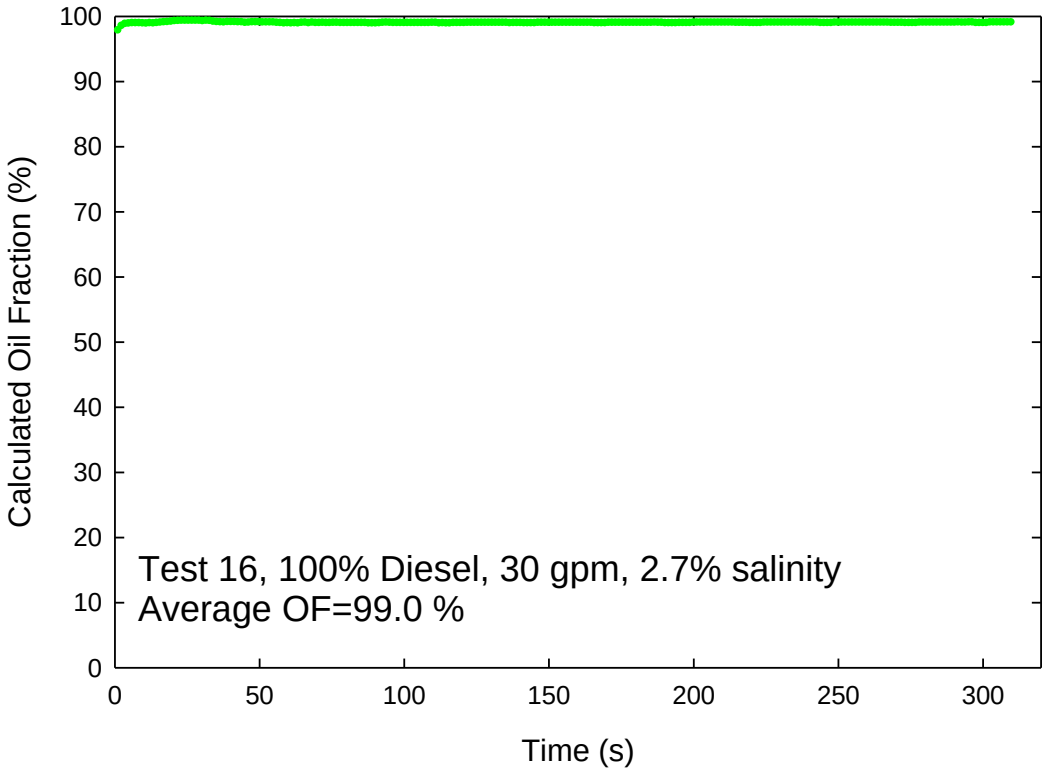

Figure 81: Test 16 (June 29, 2022) measured oil fraction as a function of time.

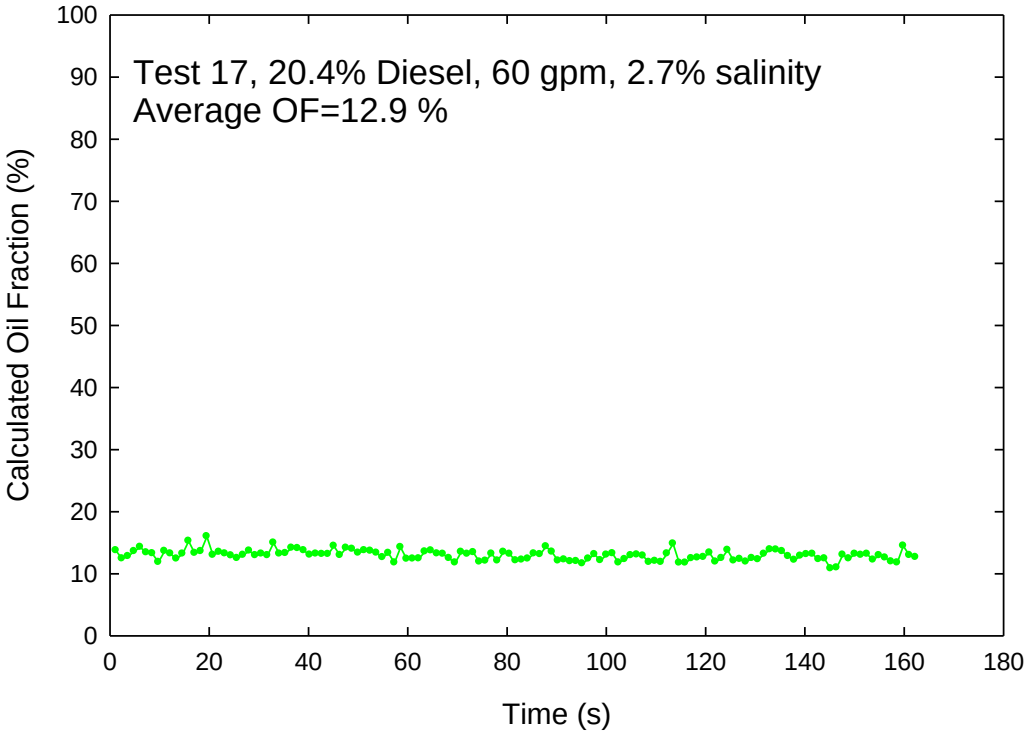

Figure 82: Test 17 (June 29, 2022) measured oil fraction as a function of time.

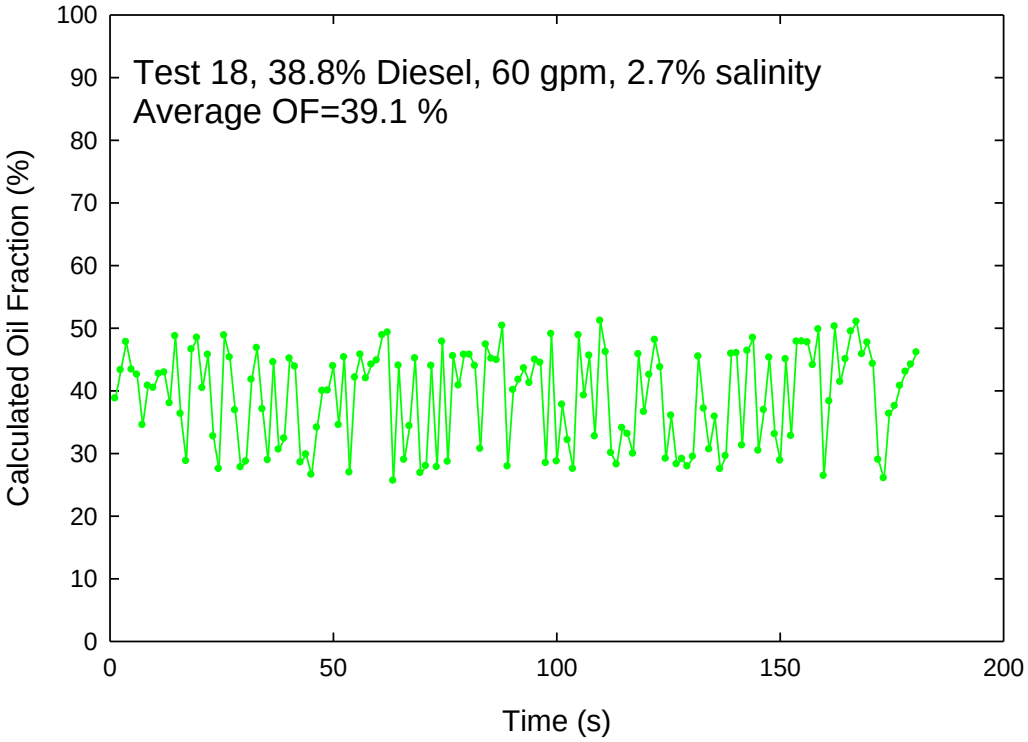

Figure 83: Test 18 (June 29, 2022) measured oil fraction as a function of time.

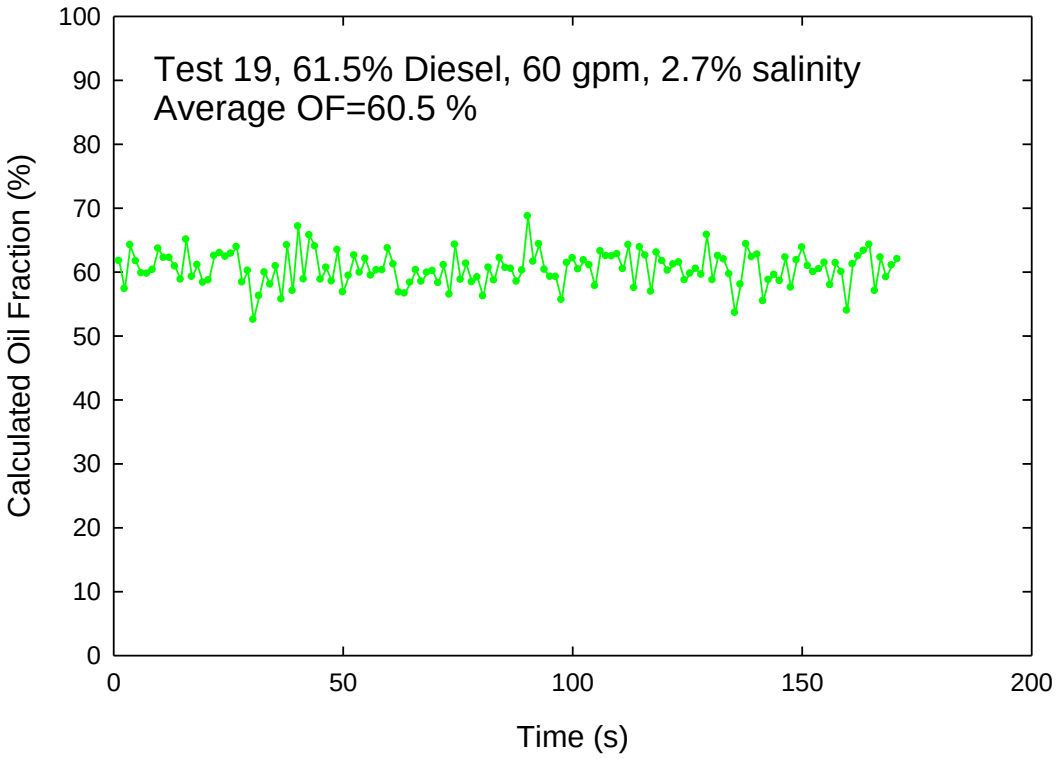

Figure 84: Test 19 (June 30, 2022) measured oil fraction as a function of time.

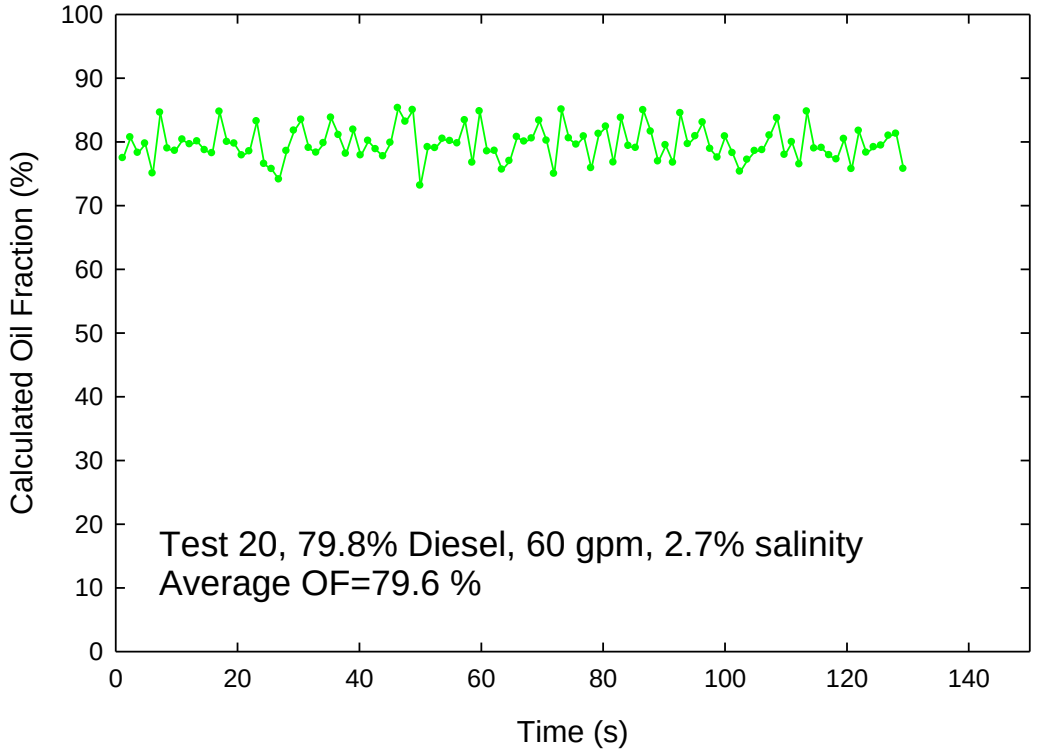

Figure 85: Test 20 (June 30, 2022) measured oil fraction as a function of time.

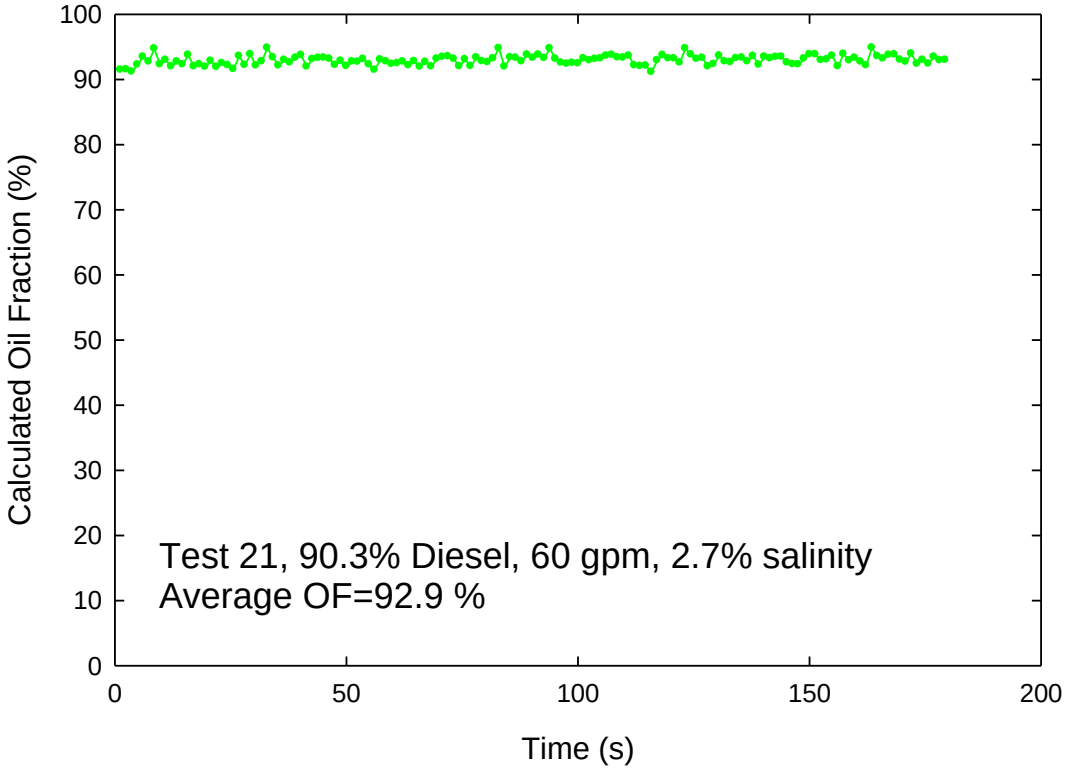

Figure 86: Test 21 (June 30, 2022) measured oil fraction as a function of time.

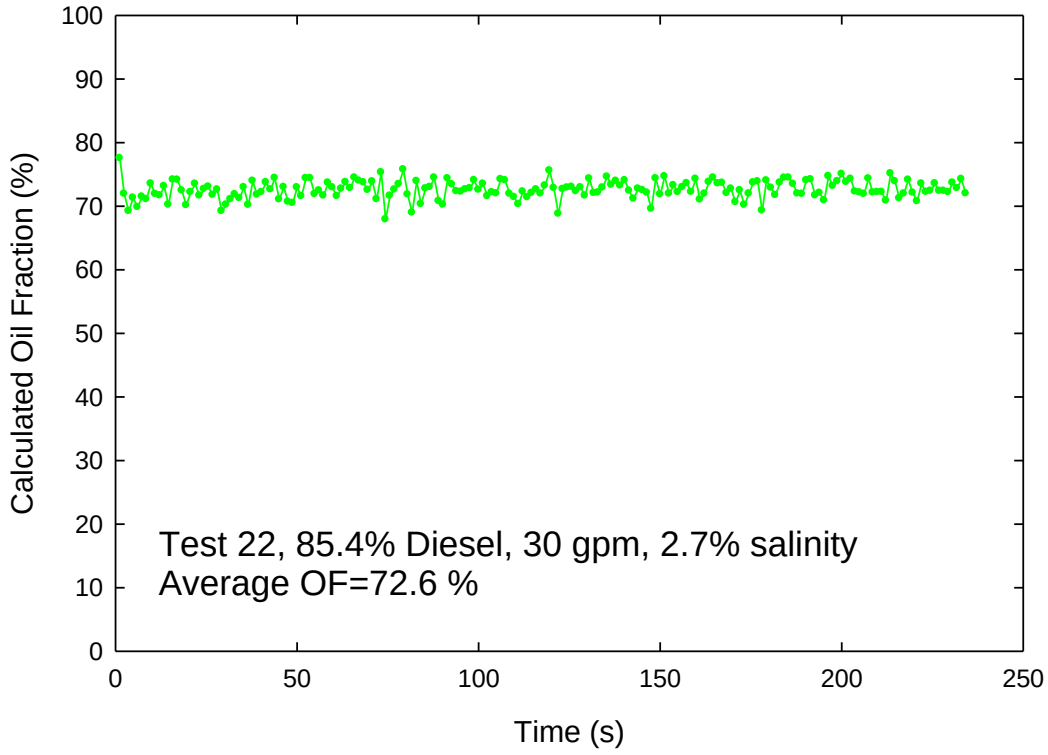

Figure 87: Test 22 (June 30, 2022) measured oil fraction as a function of time.

References

[1] S. Winecki, J.H. Fought, M.H. Yugulis, D. Argumedo, R. Stonebraker, W. Gibbs “Oil recovery sensor” U.S. Patent 10,620,161 (2020)
[2] S. Winecki, R.J. Davis, M.V. Melnik “Oil content sensor” U.S. Patent 10,591,441 (2020)
[3] S. Winecki, J.H. Fought, M.H. Yugulis, D. Argumedo, R. Stonebraker, W. Gibbs “Oil recovery sensor” U.S. Patent 10,481,129 (2019)
[4] Delahay, P. *New Instrumental Methods in Electrochemistry,* Interscience Publishers Inc, 1954.
[5] https://www.bsee.gov/sites/bsee.gov/files/osrr-oil-spill-response-research//1042aa.pdf

BATTELLE

It can be done